UNIVERSIDADE ESTADUAL PAULISTA
"JÚLIO DE MESQUITA FILHO"
Câmpus de São José do Rio Preto

Mírian Luisa Faria Freitas

Preparo e caracterização de emulsões e microcápsulas de óleo de buriti *(Mauritia flexuosa)* utilizando isolado proteico de soja e pectina de alta metoxilação como estabilizantes

São José do Rio Preto
2018

Mírian Luisa Faria Freitas

Preparo e caracterização de emulsões e microcápsulas de óleo de buriti *(Mauritia flexuosa)* utilizando isolado proteico de soja e pectina de alta metoxilação como estabilizantes

Tese apresentada como parte dos requisitos para obtenção do título de Doutor em Engenharia e Ciência de Alimentos, junto ao Programa de Pós-Graduação em Engenharia e Ciência de Alimentos, do Instituto de Biociências, Letras e Ciências Exatas da Universidade Estadual Paulista "Júlio de Mesquita Filho", Câmpus de São José do Rio Preto.

Financiadoras:
FAPESP – Proc. 2014/08520-6
CAPES – Proc. 88881.132893/2016-01

Orientadora: Profª. Drª. Vânia Regina Nicoletti

Co-orientadora no Brasil: Profª. Drª. Ana Paula Badan Ribeiro

Co-orientador no Exterior: Prof. Dr. Yrjö Henrik Roos

São José do Rio Preto
2018

Freitas, Mírian Luisa Faria.
Preparo e caracterização de emulsões e microcápsulas de óleo de buriti (Mauritia flexuosa) utilizando isolado proteico de soja e pectina de alta metoxilação como estabilizantes / Mírian Luisa Faria Freitas. -- São José do Rio Preto, 2018
177 f. : il., tabs.

Orientador: Vânia Regina Nicoletti
Coorientador: Ana Paula Badan Ribeiro
Coorientador: Yrjö Henrik Roos
Tese (doutorado) – Universidade Estadual Paulista “Júlio de Mesquita Filho”, Instituto de Biociências, Letras e Ciências Exatas

1. Tecnologia de alimentos. 2. Óleos vegetais. 3. Buriti. 4. Emulsões 5. Microencapsulação. 6. Compostos bioativos. 7. Agentes estabilizantes. I. Universidade Estadual Paulista "Júlio de Mesquita Filho". Instituto de Biociências, Letras e Ciências Exatas. II. Título.

CDU – 664.34

Ficha catalográfica elaborada pela Biblioteca do IBILCE
UNESP - Câmpus de São José do Rio Preto

Mírian Luisa Faria Freitas

Preparo e caracterização de emulsões e microcápsulas de óleo de buriti *(Mauritia flexuosa)* utilizando isolado proteico de soja e pectina de alta metoxilação como estabilizantes

Tese apresentada como parte dos requisitos para obtenção do título de Doutor em Engenharia e Ciência de Alimentos, junto ao Programa de Pós-Graduação em Engenharia e Ciência de Alimentos, do Instituto de Biociências, Letras e Ciências Exatas da Universidade Estadual Paulista "Júlio de Mesquita Filho", Câmpus de São José do Rio Preto.

Financiadoras:
FAPESP – Proc. 2014/08520-6
CAPES – Proc. 88881.132893/2016-01

Comissão Examinadora

Profª. Drª. Vânia Regina Nicoletti
UNESP – Câmpus de São José do Rio Preto
Orientadora

Prof. Dr. Fábio Yamashita
Universidade Estadual de Londrina

Prof. Dr. Wanderley Pereira de Oliveira
Universidade de São Paulo – Câmpus de Ribeirão Preto

Profª. Drª. Maria Aparecida Mauro
UNESP – Câmpus de São José do Rio Preto

Prof. Dr. Márcio José Tiera
UNESP – Câmpus de São José do Rio Preto

São José do Rio Preto
23 de março de 2018

AGRADECIMENTOS

Agradeço a Deus por iluminar meu caminho e guiar meus passos, todos os dias.

À minha orientadora, Profa. Dra. Vânia Regina Nicoletti, agradeço todo o conhecimento compartilhado, orientação, paciência, carinho e amizade.

Aos meus co-orientadores, Profa. Dra. Ana Paula Badan Ribeiro e Prof. Dr. Yrjö Henrik Roos, agradeço toda colaboração, conhecimentos compartilhados e disponibilidade para me receber nos laboratórios de pesquisa em suas instituições.

A meus pais e meus irmãos, peço desculpas por tantos momentos em que estive ausente e agradeço por todo amor, carinho, apoio e incentivo. Vocês foram essenciais nessa caminhada!

Ao Ademir, agradeço o carinho, o apoio, longas conversas e bons momentos de descontração.

Ao Grupo de Oração Kairós, agradeço os momentos de orações, fortalecimento na fé, a amizade e o carinho.

Agradeço à Universidade Estadual Paulista “Júlio de Mesquita Filho”, Instituto de Biociências, Letras e Ciências Exatas por proporcionar a realização de um sonho.

Agradeço aos professores da Comissão Examinadora, Prof. Dr. Fábio Yamashita, Prof. Dr. Wanderley Pereira de Oliveira, Profa. Dra. Maria Aparecida Mauro e Prof. Dr. Márcio José Tiera, pela disponibilidade em colaborar e enriquecer o trabalho realizado durante o doutorado.

Aos professores da Pós-graduação em Engenharia e Ciência de Alimentos do Ibilce meus agradecimentos pelo conhecimento compartilhado, grande auxílio em minha formação.

Agradeço ao Prof. Dr. Eloi da Silva Feitosa e Monique Lemos pela colaboração com a análise de cargas dos biopolímeros realizada no

Laboratório de Física de Sistemas Coloidais no Departamento de Física do Ibilce.

À Marcella Aparecida Stahl agradeço a ajuda e paciência com as análises de caracterização do óleo de buriti e microscopia eletrônica de varredura das emulsões realizadas no Laboratório de Óleos e Gorduras do Departamento de Tecnologia de Alimentos da FEA/Unicamp.

Agradeço ao Prof. Dr. Renan Campos Chisté do Instituto de Tecnologia da Faculdade de Engenharia de Alimentos da Universidade Federal do Pará pelo auxílio no desenvolvimento do método para determinação do teor de β-caroteno e carotenoides totais do óleo de buriti por cromatografia líquida de alta eficiência (HPLC).

À Dra. Juliana Campos Hashimoto agradeço a colaboração no desenvolvimento dos métodos e nas análises de cargas e de tamanho de gotas das emulsões realizadas no Laboratório de Análise Instrumental do Departamento de Tecnologia de Alimentos da FEA/Unicamp.

Agradeço ao Luiz Roberto Falleiros Júnior, à Profa. Dra. Patrícia Simone Leite Villamaior e ao Prof. Dr. Sebastião Roberto Taboga pelo auxílio na realização da análise de microscopia confocal de varredura a laser das emulsões realizada no Laboratório de Microscopia e Microanálise do Departamento de Biologia do Ibilce.

À Dra. Izabela Dutra Alvim agradeço o auxílio na realização da análise de tamanho de partículas das microcápsulas realizada no Centro de Tecnologia de Cereais e Chocolates, CEREAL CHOCOTEC, no Instituto de Tecnologia de Alimentos, ITAL, em Campinas, SP.

Ao Laboratório de Caracterização Estrutural do Departamento de Engenharia de Materiais da Universidade Federal de São Carlos agradeço o auxílio na análise de microscopia eletrônica de varredura das microcápsulas.

Aos técnicos do Departamento de Engenharia e Tecnologia de Alimentos do Ibilce e da Faculdade de Ciência de Alimentos e Nutrição da

University College Cork agradeço a ajuda com os equipamentos e material do laboratório.

Aos amigos do Laboratório da Medidas Físicas do Ibilce, do Laboratório de Pesquisa em Ciência de Materiais da UCC, agradeço imensamente a amizade, companhia, auxílio com os equipamentos e conhecimentos compartilhados. Vocês são amigos muito especiais!

Às amigas Tati e Natália agradeço imensamente a companhia, conversas, carinho e atenção, tão necessários e reconfortantes.

Agradeço à Tovani Benzaqen Igredientes pela doação do isolado proteico de soja e à CP Kelco pela doação da pectina de alta metoxilação.

À Fundação de Amparo à Pesquisa do Estado de São Paulo, FAPESP, agradeço pela concessão da bolsa de doutorado, processo nº 2014/08520-6.

Agradeço à Coordenação de Aperfeiçoamento de Pessoal de Nível Superior, Capes, pela concessão de bolsa de doutorado e bolsa de estágio sanduíche no exterior, processo nº 88881.132893/2016-01.

Recebam meus agradecimentos e minha gratidão! Esse trabalho tem um pouco de cada um vocês!

“*Tudo é do Pai*
Toda honra e toda glória
É Dele a vitória
Alcançada em minha vida”
Frederico Cruz

RESUMO

A proposta desse trabalho foi a produção e caracterização de emulsões e microcápsulas de óleo de buriti utilizando isolado proteico de soja e pectina de alta metoxilação como estabilizantes. Os biopolímeros foram caracterizados, individualmente, por meio de análises de solubilização, carga, turbidimetria e microscopia ótica. O complexo isolado proteico de soja-pectina de alta metoxilação foi caracterizado por ensaios de turbidimetria e microscopia ótica. Para caracterizar o óleo de buriti realizaram-se determinações de propriedades físico-químicas e termofísicas, matéria insaponificável, composição em ácidos graxos, classes acilglicerólicas, composição triacilglicerólica, classes triacilglicerólicas e comportamento térmico. As emulsões de óleo de buriti foram caracterizadas por análises de estabilidade, tamanho das gotas, condutividade elétrica, intensidade de cargas, microscopia ótica, microscopia confocal de varredura a laser e microscopia eletrônica de varredura. O comportamento reológico das emulsões foi analisado através de ensaios em cisalhamento constante e cisalhamento oscilatório. Microcápsulas de óleo de buriti foram obtidas por meio da secagem por spray dryer da emulsão de óleo de buriti otimizada e adicionou-se maltodextrina como adjuvante de secagem. As microcápsulas, por sua vez, foram caracterizadas por meio das análises de cor, umidade, rendimento, tamanho de partículas, eficiência de encapsulação e retenção de carotenoides, eficiência de encapsulação e retenção de óleo, sorção de água, plastificação pela água e relaxação mecânica. A morfologia das microcápsulas foi observada por microscopia ótica e microscopia eletrônica de varredura. Através dos ensaios de caracterização dos biopolímeros, pôde-se notar que a pectina de alta metoxilação apresentou alta solubilização, independente do pH, e as cargas negativas aumentaram com o aumento do pH até estabilizarem. O isolado proteico de soja apresentou

baixa solubilização perto do ponto isoelétrico, aumentando com o pH em soluções alcalinas, até chegar a 100% no pH 11. Esse biopolímero apresentou cargas positivas em pH abaixo do ponto isoelétrico e cargas negativas em pH acima do ponto isoelétrico. Em pH abaixo do ponto isoelétrico foi verificada a interação atrativa do isolado proteico de soja e pectina de alta metoxilação por meio da observação de complexos formados, definindo-se o pH de 3,5 para produção das emulsões. A caracterização do óleo de buriti atestou sua alta qualidade, revelando altos teores de carotenoides, tocoferóis e ácidos graxos monoinsaturados. O planejamento experimental DCCR levou à obtenção de uma emulsão em condições otimizadas rica em óleo, estável por pelo menos 7 dias, com tamanho de gotas reduzido, baixa condutividade elétrica e alto módulo de cargas negativas. Esse material foi caracterizado como pseudoplástico e apresentou comportamento viscoelástico com módulo de armazenamento maior que o módulo de dissipação. Por meio das análises microscópicas foi possível observar a interação do isolado proteico de soja com o óleo de buriti formando as gotículas e a interação da pectina de alta metoxilação com o isolado proteico de soja formando a dupla camada da emulsão. O excesso de pectina foi observado disperso na fase contínua, contribuindo para a estabilidade do sistema. As diferentes amostras de microcápsulas apresentaram diferença significativa ($p \leq 0,05$) entre si com relação à cor, rendimento, eficiência de encapsulação e retenção de carotenoides e eficiência de encapsulação e retenção de óleo. A amostra contendo maior teor de maltodextrina apresentou coloração menos intensa, porém, maior rendimento, eficiência de encapsulação e retenção dos compostos bioativos. As temperaturas de transição vítrea e de relaxação das microcápsulas se mostraram dependentes da umidade relativa a que foram expostas, sendo que quanto maior a umidade relativa, menor a temperatura de transição vítrea e de relaxação.

Palavras-chave: carotenoides, tocoferóis, reologia, morfologia, spray drying, retenção de compostos bioativos, temperatura de transição vítrea, temperatura de relaxação.

ABSTRACT

The aim of this study was the preparation and characterization of buriti oil emulsions and microcapsules using soy protein isolate and high-methoxyl pectin as stabilizers. The biopolymers were characterized individually by analysis of solubilization, charge, turbidity and optical miscrocopy. The soy protein isolate-high-methoxyl pectin complexes were characterized by turbidity and optical microscopy analyses. Characterization of the buriti oil was performed by analyses of physicochemical and thermophysical properties, unsaponifiable matter, fatty acid composition, acylglycerol classes, triacylglycerol composition, triacylglycerol classes, and thermal behavior. The buriti oil emulsions were characterized by analyses of stability, particle size, electric conductivity, zeta potencial, optical microscopy, confocal laser scanning microscopy, and scanning electron microscopy. The rheological behavior of the emulsions was analyzed by constant shear and oscillatory shear tests. The buriti oil microcapsules were produced by spray drying of the optimized conditions for elaborating buriti oil emulsion added with maltodextrin as a drying aid. The microcapsules, in turn, were evaluated by analyses of colour, moisture content, encapsulation yield, particle size distribution, encapsulation efficiency and retention of carotenoids, encapsulation efficiency and retention of oil, water sorption, water plasticization and mechanical relaxation. The microcapsules morphology was analysed by optical and scanning electron microscopy. Through the biopolymer characterization, it could be noted that the high-methoxyl pectin showed high solubilization, independent of the pH, and the negative charges increased with increasing pH until stabilization. The soy protein isolate had low solubilization near the isoelectric point and it increased with increasing pH in alkaline solutions, up to reach 100% at pH 11. This biopolymer presented positive charges in pH below the isoelectric point and negative charges at pH above the isoelectric point. At pH lower

than the isoelectric point there was attractive interaction between soy protein isolate and high-methoxyl pectin, leading to definition of the pH 3.5 for preparation of the emulsions. The characterization of buriti oil confirmed its high quality, showing high levels of carotenes, tocols and monounsaturated fatty acids. The CCRD experimental design was adequate for the study of buriti oil emulsions, leading to definition of an optimized conditions for producing emulsion rich in oil, stable for at least 7 days, with reduced droplet size, low electric conductivity and high modulus of negative charges. This material was characterized as pseudoplastic and showed viscoelastic behavior with storage modulus greater than the loss modulus. Moreover, through microscopic analysis it was possible to observe the interaction of soy protein isolate with buriti oil forming oil droplets and the interaction of high-methoxyl pectin with soy protein isolate forming the double layer of the emulsion. The excess pectin was observed dispersed in the continuous phase, contributing to system stability. The different samples of microcapsules presented significant differences ($p \leq 0.05$) with respect to color parameters, encapsulation yield, encapsulation efficiency and retention of carotenoid, and encapsulation efficiency and retention of buriti oil. The sample with the highest maltodextrin content presented less intense coloration, in contrast, presented the highest encapsulation yield, encapsulation efficiency and retention of bioactive compounds. The glass transition and relaxation temperatures of the microcapsules were dependent on the ambient relative humidity, and the higher the relative humidity, the lower the glass transition temperature and the relaxation temperature.

Keywords: carotenoids, tocopherols, rheology, morphology, spray drying, bioactive compounds retention, glass transition temperature, relaxation temperature.

SUMÁRIO

INTRODUÇÃO GERAL

Palmeiras nativas pertencentes à família *Arecaceae* estão entre os recursos vegetais mais importantes da Amazônia. Os frutos dessas palmeiras são não apenas alimentos alternativos para a população local, mas também uma fonte de óleos vegetais de alta qualidade (SANTOS et al., 2013). O valor nutricional do óleo de buriti (*Mauritia flexuosa*) é devido ao alto conteúdo de carotenoides e tocoferóis, conferindo-lhe propriedades de pró-vitamina A e antioxidantes (SILVA et al., 2009), mas perdas podem acontecer pela exposição à luz, oxigênio e altas temperaturas.

A tecnologia de emulsões apresenta-se como uma forma adequada de encapsular, proteger e liberar compostos lipídicos bioativos para uso nas indústrias de alimentos e farmacêutica (McCLEMENTS; DECKER; WEISS, 2007). Os estabilizantes são importantes para controle das propriedades como textura e viscosidade e a estabilidade de emulsões pode ser aumentada através da formação de complexos proteína-polissacarídeos atuando como estabilizantes (LAM et al., 2007; PERRECHIL; CUNHA, 2013).

A utilização dos efeitos sinérgicos resultantes das interações de proteínas e polissacarídeos na formação e estabilização de sistemas como emulsões e espumas tem sido de grande interesse (SERFERT et al., 2013). O tipo de interação entre proteínas e polissacarídeos afetam as características reológicas interfaciais tanto do ar com a água como do óleo com a água (RODRÍGUEZ PATINO; PILOSOF, 2011).

Proteínas e polissacarídeos podem ser neutros ou carregados, dependendo do pH da solução em relação a seus pontos isoelétricos (McCLEMENTS, 1999). Segundo Lam et al. (2007), estudando as interações entre o isolado proteico de soja e pectina em pH baixo é possível otimizar a estabilidade da proteína de soja em dispersões ácidas, bem como controlar a formação de complexos e o limite de desestabilização. Assim, é possível supor que em pH abaixo do ponto isoelétrico das

proteínas, as pectinas e proteínas são naturalmente atraídas, pois as pectinas estarão carregadas negativamente e as proteínas de soja estarão, em geral, carregadas positivamente.

A microencapsulação pode ser uma alternativa para aumentar a estabilidade dos componentes lipofílicos e tem sido usada com sucesso na indústria de alimentos para proteger substâncias sensíveis a temperatura, luz, oxigênio e umidade por reduzir a taxa de transferência do núcleo com o meio em que o produto se encontra, e por modificar as características físicas do material, facilitando o manuseio (ROCHA; FÁVARO-TRINDADE; GROSSO, 2012; DESAI; PARK, 2005).

Secagem por atomização ou spray drying refere-se à remoção de umidade de um material fluido, como emulsão, através da divisão em pequenas gotas na presença de ar quente para obter um pó seco. Nesse processo de secagem, o fluido é bombeado e atomizado na câmara de secagem (AL-ASHEH et al., 2003; RÉ, 1998). Essa técnica de microencapsulação tem sido a mais utilizada na indústria de alimentos em diversos processos industriais para obtenção de materiais desidratados na forma de pós finos (JACKSON; LEE, 1991; RÉ, 1998; JAFARI et al., 2008).

Carboidratos, tais como amidos, maltodextrinas e xarope de milho são geralmente utilizados na microencapsulação de ingredientes alimentícios. Estes materiais são considerados como bons agentes de encapsulação porque apresentam baixas viscosidades com elevados teores de sólidos e boa solubilização, mas a maioria deles não possui as propriedades interfaciais necessárias para uma elevada eficiência de microencapsulação e geralmente está associada a outros materiais encapsulantes, como proteínas ou gomas (GHARSALLAOUI et al., 2007).

Diante desse cenário, a proposta deste trabalho foi a produção e caracterização de emulsões e microcápsulas de óleo de buriti utilizando isolado proteico de soja e pectina de alta metoxilação como estabilizantes.

Essa tese está organizada em capítulos e no Capítulo 1, *Revisão Bibliográfica Geral*, são apresentados os conceitos teóricos que serviram de base para o desenvolvimento do projeto.

O Capítulo 2, *Caracterização dos Biopolímeros e do Complexo Isolado Proteico de Soja-Pectina de Alta Metoxilação*, refere-se à primeira parte do trabalho, na qual análises físico-químicas e microscópicas foram realizadas para melhor compreensão dos estabilizantes a serem utilizados no preparo das emulsões e microcápsulas de óleo de buriti. O conteúdo desse capítulo está publicado como artigo científico-tecnológico no periódico Polímeros: Ciência e Tecnologia, v. 21, n. 1, p. 62-67, 2017.

O Capítulo 3, *Características de Qualidade e Comportamento Térmico do Óleo de Buriti* (*Mauritia flexuosa*), trata da caracterização do óleo utilizado como fonte de carotenoides, tocoferóis e ácidos graxos monoinsaturados para a produção das emulsões e microcápsulas ricas em compostos bioativos. O estudo do óleo de buriti está publicado como artigo original no periódico Grasas y Aceites, v. 68, n. 4, p. 220-228, 2017.

O Capítulo 4, *Estabilidade, Microestrutura e Reologia de Emulsões de Óleo de Buriti (Mauritia flexuosa) Afetadas pela Proporção de Isolado Proteico de Soja/Pectina de Alta Metoxilação, Teor de Óleo e Pressão de Homogeneização*, apresenta o estudo da produção de emulsões segundo um delineamento composto central rotacional 2^3 para avaliação das diferentes variáveis do processo bem como a caracterização das amostras obtidas. Esse capítulo será submetido como artigo científico para possível publicação.

O Capítulo 5, *Efeito da Adição de Maltodextrina em Emulsões Óleo em Água para Produção de Microcápsulas de Óleo de Buriti (Mauritia flexuosa) por Secagem por Atomização*, refere-se à produção das microcápsulas com diferentes proporções de material de parede, além dos resultados de caracterização dessas amostras. Esse estudo será submetido como artigo científico para possível publicação.

* As referências bibliográficas utilizadas na *Introdução* estão apresentadas juntamente com as referências bibliográficas do Capítulo 1 – *Revisão Bibliográfica Geral*.

OBJETIVOS GERAIS

O objetivo geral deste trabalho foi estudar as etapas de produção e correspondente caracterização de emulsões de óleo de buriti estabilizadas por isolado proteico de soja e pectina de alta metoxilação em diferentes formulações. Posteriormente, realizar a secagem em spray dryer e caracterizar as microcápsulas produzidas, visando maior estabilidade dos compostos bioativos do óleo e ampliação das possibilidades de aplicação na indústria de alimentos. Além de colaborar para o conhecimento das propriedades do óleo de buriti e do comportamento interativo do par de biopolímeros utilizado como estabilizante nas emulsões e microcápsulas.

Para isso, os objetivos específicos foram:

- Caracterizar o comportamento em solução aquosa do isolado proteico de soja e da pectina de alta metoxilação, individualmente, em função do pH, por análises de solubilização, cargas, turbidimetria e microscopia ótica.

- Caracterizar os complexos formados por esses biopolímeros, em diferentes proporções e valores de pH, por meio de turbidimetria e microscopia ótica.

- Caracterizar o óleo de buriti por meio de análises de acidez livre, índice de peróxidos, índice de iodo, índice de saponificação, índice de refração, comportamento reológico, densidade, carotenos totais, teor de β-caroteno, composição tocoferólica, composição em ácidos graxos, classes acilglicerólicas, composição em triacilgliceróis, classes triacilglicerólicas e análises de cristalização e fusão.

- Produzir emulsões com diferentes teores de óleo de buriti, proporções proteína/polissacarídeo e pressões aplicadas em homogeneizador a alta pressão.

- Caracterizar as emulsões por meio de análises de estabilidade, tamanho das gotas, condutividade elétrica, intensidade de cargas, microscopia ótica, microscopia eletrônica de varredura, microscopia confocal de varredura a laser e comportamento reológico.

- Produzir microcápsulas de óleo de buriti por meio da secagem em spray dryer da emulsão otimizada com adição de maltodextrina em diferentes teores.

- Caracterizar as microcápsulas por meio de análises de cor, umidade, rendimento de encapsulação, tamanho de partículas, eficiência de encapsulação e retenção de carotenoides, eficiência de encapsulação e retenção de óleo, sorção de água, plastificação pela água, relaxação mecânica, microscopia ótica e microscopia eletrônica de varredura.

CAPÍTULO 1

Revisão bibliográfica geral

O conteúdo deste capítulo apresenta os conceitos teóricos que serviram de base para o desenvolvimento do trabalho.

1. Óleo de buriti

Buriti (*Mauritia flexuosa*) é uma palmeira nativa do Brasil que normalmente cresce em áreas permanente ou periodicamente alagadas ao longo de rios, florestas e savanas (centro-norte do Brasil e Venezuela). Sua fruta possui uma casca vermelha, dura e com escamas que cobre uma polpa macia e oleosa, podendo sua cor variar entre amarelo escuro a avermelhado após completa maturação. É possível extrair até 45 kg de óleo de buriti de 1000 kg de frutos maduros (ALBUQUERQUE et al., 2005; SILVA et al., 2009).

O óleo de buriti apresenta alta concentração de ácidos graxos monoinsaturados, com valores mais elevados que aqueles encontrados em azeitonas ou castanha do Pará, alimentos conhecidos por possuir óleos de elevada qualidade nutricional devido às propriedades de reduzir o colesterol sanguíneo (FRANÇA et al., 1999; SILVA et al., 2009). O óleo de buriti contém, ainda, outros compostos químicos que lhe dão especial valor nutritivo, com valores para β-caroteno mais altos que vários alimentos muito consumidos pelos brasileiros, como cenoura, goiaba, pitanga, mamão, maracujá e outros frutos da Amazônia, como dendê, pupunha e tucumã (RODRIGUEZ-AMAYA, 1996; DE ROSSO; MERCADANTE, 2007), além de apresentar altos teores de tocoferóis.

Os carotenoides são um grupo diversificado de componentes lipofílicos, sendo que o β-caroteno é uma pró-vitamina A, com 100% de atividade (RODRIGUEZ-AMAYA, 1996; McCLEMENTS; DECKER; WEISS, 2007). Entre os efeitos benéficos à saúde atribuídos aos carotenoides, podem ser citados a prevenção de câncer, doenças cardíacas e degeneração macular devido à atividade antioxidante dessas substâncias (ALQUEZAR; RODRIGO; ZACARÍAS, 2008; MELÉNDEZ-MARTÍNEZ; VICARIO; HEREDIA, 2007). Os tocoferóis são importantes antioxidantes e também apresentam atividade de vitamina E, especialmente o α-tocoferol (DE GREYT; KELLENS, 2005).

Quando usados como aditivos em alimentos, os carotenoides e tocoferóis são relativamente instáveis por serem sensíveis a luz, oxigênio, temperatura e auto-oxidação (clivagem não enzimática), o que provoca sua rápida degradação (XIANQUAN et al., 2005; HEINONEN et al., 1997; RIBEIRO; AX; SCHUBERT, 2003; GUINAZI et al., 2009). A microencapsulação é uma tecnologia que tem permitido o desenvolvimento de ingredientes que podem aumentar a qualidade nutricional dos alimentos e se apresenta como uma possibilidade para a incorporação de carotenoides e tocoferóis em alimentos, sem afetar suas propriedades (AUGUSTIN; HEMAR, 2009).

2. Complexo isolado proteico de soja-pectina de alta metoxilação

A soja tem sido o principal material usado para produção industrial de concentrados e isolados proteicos, o que se deve, principalmente, a seu alto teor de proteínas e ao bom desempenho tecnológico dos produtos, além de representar uma alternativa de origem vegetal às proteínas de origem láctica (TOMOSKOZI et al., 2001).

O isolado proteico de soja (SPI) contém pelo menos 90% de proteínas, sendo livre de lipídios e carboidratos. Os principais componentes dessas proteínas são as frações β-conglicinina (7S) e glicinina (11S) representando mais que 85% do total de proteínas do grão (LAM; PAULSEN; CORREDIG, 2008). Essas duas frações possuem ação emulsificante, apresentando a capacidade de estabilizar emulsões por formar uma camada adsorvida na interface óleo/água (SINGH; MOHAMED, 2007).

O uso da proteína de soja como ingrediente em formulações alimentícias é atrativo pela sua funcionalidade e valor nutritivo, porém a funcionalidade e solubilização das frações proteicas são alteradas pelo pH e pela força iônica (LAKEMOND et al., 2000; ROUDSARI et al., 2006).

Para a maioria das proteínas a menor solubilização é observada no ponto isoelétrico, onde a carga líquida é zero e a interação com a água é

mínima, ocorrendo assim, agregação e precipitação. Longe do ponto isoelétrico as proteínas se encontram carregadas e podem interagir com a água, contribuindo para a solubilização (DAMODARAN; PARAF, 1997). O ponto isoelétrico da proteína de soja é observado em pH entre 4,0 e 5,0 e uma alta solubilização é relatada em pH acima de 10,0 (JARAMILLO; ROBERTS; COUPLAND, 2011; RENKEMA; GRUPPEN; VAN VLIET, 2002; KUMAR et al., 2002).

A pectina é uma macromolécula natural complexa sendo o estabilizante mais comumente utilizado em bebidas ácidas a base de proteína, contribuindo positivamente para o sabor, estabilidade e textura do produto final, inclusive quando adicionada em pequenas quantidades (TROMP et al., 2004; CANTERI et al., 2012; SANTOS et al., 2010).

Apesar de a pectina fazer parte do tecido da maioria das plantas, o número de fontes comerciais usadas é bastante limitado (SANTOS et al., 2010). O polissacarídeo mais utilizado é derivado principalmente de frutas cítricas, sendo classificado, com relação ao grau de esterificação, em pectinas de alta metoxilação, quando metade ou mais dos grupos carboxilas estão esterificados, e pectinas de baixa metoxilação, quando menos da metade dos grupos carboxilas estão esterificados (LAM et al., 2007).

A pectina de alta metoxilação é geralmente utilizada como espessante em produtos alimentares e é reconhecida como potencial estabilizante de emulsões devido ao fato de sua estrutura ser um polieletrólito aniônico linear. O pKa desse biopolímero é observado em pH próximo a 3,5 e em soluções ligeiramente ácidas a pectina tem carga negativa devido à presença de grupos carboxílicos ionizados ao longo da cadeia (ABERKANE; ROUDAUT; SAUREL, 2014; THAKUR et al., 1997).

A formação de complexos entre proteínas e polissacarídeos de cargas opostas é um fenômeno coloidal envolvido na estruturação de muitos sistemas biológicos. Percebe-se um considerável interesse em complexos formados por esses biopolímeros nos últimos anos devido a

suas potenciais aplicações na indústria de alimentos, sendo utilizados como estabilizantes de bebidas lácteas, emulsificantes, estabilizantes de espuma, substituição de gorduras, encapsulação, imobilização e recuperação de enzimas e processos de separação de proteínas, conforme apresentado por Dong et al. (2015).

Em um estudo conduzido por Lam et al. (2007) sobre estabilidade de pectinas em soluções ácidas de proteínas, utilizando isolado proteico de soja, foi demonstrado que a pectina de alta metoxilação apresentou maior estabilidade que a pectina de baixa metoxilação. Jaramillo, Roberts e Coupland (2011) observaram que em pH próximo ao ponto isoelétrico do isolado proteico de soja (próximo a pH 4,0), a adição de pectina aumentou a solubilização da proteína, evitando sua agregação através da interação eletrostática. Verificaram, ainda, que os complexos proteína-polissacarídeo formados foram capazes de suportar o tratamento térmico, apesar de algumas modificações em suas propriedades.

Os valores de pH nos quais ocorre solubilização ou formação de complexos dos biopolímeros não dependem ou dependem muito pouco da concentração total destes. Por outro lado, estão fortemente relacionados com o pI da proteína, a razão entre os biopolímeros, a força iônica e massa molar dos mesmos (MATTISON; BRITTAIN; DUBIN, 1995; MATTISON et al., 1999; MARFIL, 2014).

Tratando-se do emprego desse par em emulsões, foi observado que os polissacarídeos aumentam a estabilidade física da emulsão através de efeitos eletrostáticos e/ou estéricos, por modificar as propriedades reológicas da interface e aumentar a viscosidade da emulsão (SERFERT et al., 2013).

3. Produção de emulsões

Um sistema que consiste de gotículas de óleo dispersas em fase aquosa é denominado de emulsão óleo em água ou O/A, enquanto um sistema que consiste de gotículas de água dispersas em óleo é

denominado de emulsão água em óleo ou A/O (McCLEMENTS, 1999). Por meio da adição de substâncias conhecidas como estabilizantes, por exemplo, emulsificantes e modificadores de textura, torna-se possível a formação de emulsões cineticamente estáveis por um período razoável de tempo (McCLEMENTS; DECKER; WEISS, 2007).

Proteínas e polissacarídeos normalmente são usados como hidrocolóides naturais na indústria de alimentos. A combinação, no mesmo sistema, das vantagens da proteína (rápida adsorção comparada ao polissacarídeo) e dos polissacarídeos (repulsão estérica ou aumento da viscosidade) para estabilizar emulsões tem sido cada vez mais estudada (ABERKANE; ROUDAUT; SARUEL, 2014). As propriedades de emulsificante e estabilizante das proteínas e polissacarídeos contribuem para a produção de emulsões com melhores características de estabilidade e funcionalidade (BOUYER et al., 2012).

Considerando o par isolado proteico de soja-pectina de alta metoxilação em emulsões óleo em água, o isolado proteico de soja é usado como emulsificante devido às propriedades constitutivas de suas proteínas (7S e 11S). Essas proteínas diminuem a tensão interfacial entre a água e o óleo, ajudando a estabilizar emulsões por formar uma barreira física na interface óleo/água (ROUDSARI et al., 2006). No entanto, fatores ambientais como pH, força iônica ou presença de outros ingredientes podem afetar o comportamento estabilizante dessa proteína em emulsões alimentícias (DIFTIS; KIOSSEOGLOU, 2004; PUPPO et al., 2005). Em baixo pH a estabilidade das emulsões pode ser melhorada pela formação de dupla camada ao redor das gotas de óleo. A pectina de alta metoxilação carregada negativamente interage com as cargas positivas da proteína para formar a dupla camada, prevenindo a coalescência (GU; DECKER; McCLEMENTS, 2007; GANCZ; ALEXANDER; CORREDIG, 2005).

Em um estudo de emulsões utilizando proteína do soro de leite e pectina de alta metoxilação foi observado que abaixo da concentração crítica da pectina as moléculas se ligaram a mais de uma gotícula de óleo,

causando a floculação (GANCZ; ALEXANDER; CORREDIG, 2005). A concentração crítica de pectina é a concentração mínima do polissacarídeo capaz de promover a cobertura das gotículas de óleo individualmente, de modo a dificultar a floculação.

Todas as emulsões são instáveis termodinamicamente e tendem a romper e desfazer-se com o tempo, resultando em duas fases líquidas separadas. Existem diversos mecanismos de desestabilização, sendo os principais a separação gravitacional (cremeação ou sedimentação), floculação e coalescência, coalescência parcial, Ostwald ripening e inversão de fases (DICKINSON, 1992) (Figura 1).

Figura 1. Representação esquemática dos mecanismos de desestabilização das emulsões.

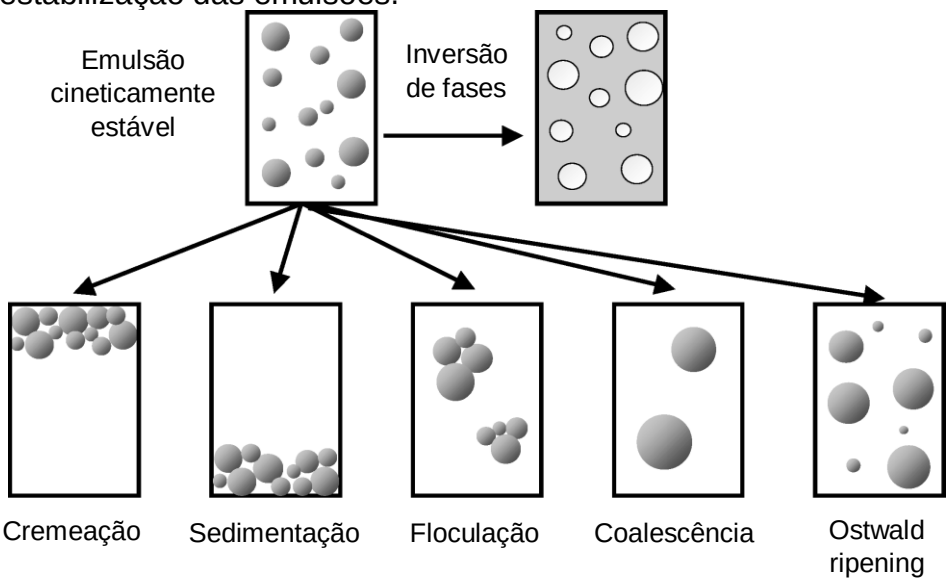

Fonte: McCLEMENTS (2007).

Separação gravitacional é o processo em que as gotículas se movem para cima (cremeação) porque elas possuem densidade menor que a fase contínua, ou para baixo (sedimentação) porque elas possuem densidade maior que a fase contínua. Floculação é o processo em que as gotas se associam para formar flocos, mas cada uma das gotas matém sua integridade. Coalescência é a união de duas ou mais gotas para formar

uma única gota maior. Coalescência parcial é a união de duas ou mais gotas parcialmente cristalinas (no estado sólido) formando um único agregado de forma irregular devido à penetração de cristais sólidos de uma gota na região fluida da outra gota. Ostwald ripening é o processo em que as gotas maiores crescem às custas das menores devido ao transporte de massa do material da fase dispersa através da fase contínua. Inversão de fase é o processo em que uma emulsão óleo em água se transforma em uma emulsão água em óleo, ou vice-versa. É importante notar que vários desses mecanismos físico-químicos de instabilidade estão normalmente inter-relacionados (McCLEMENTS, 2007).

A etapa de homogeneização no processamento de emulsões é muito importante para proporcionar algumas propriedades fisico-químicas e sensoriais, tais como, textura, sabor, aparência e estabilidade (McCLEMENTS, 1999). Os sistemas de homogeneização de alta pressão são eficazes na redução do tamanho de gotas de emulsões pré-existentes. Nesses equipamentos o fluido a ser homogeneizado é bombeado através de um pequeno orifício ajustável, localizado entre a válvula e seu suporte, gerando uma combinação de intenso cisalhamento e cavitação em regime turbulento, que promovem a redução do tamanho das gotas. A diminuição do orifício da válvula de homogeneização leva à formação de gotas menores e alguns equipamentos têm o dispositivo de alta pressão em dois estágios, em que a emulsão passa através de duas válvulas dentro do mesmo equipamento. Nesse caso, a primeira válvula é regulada em alta pressão e é responsável pela redução do tamanho das gotas, enquanto a segunda válvula, que é fixada em menor pressão, é a principal responsável pela ruptura de flocos formados no primeiro estágio (PERRECHIL; PICONE; CUNHA, 2016).

Conforme relatado por Kaltsa et al. (2013), comparando diferentes técnicas foi possível observar que emulsões preparadas em homogeneizadores a alta pressão apresentaram gotículas de menor diâmetro. Bons resultados quanto à estabilidade foram relatados para

emulsões estabilizadas com o par proteína-polissacarídeo aplicando-se a técnica de alta pressão (PERRECHIL; CUNHA, 2013).

A olho nu, podem ser observados objetos relativamente grandes, enquanto muitas estruturas de interesse em emulsões são microscópicas, como por exemplo, gotas individuais, flocos, cristais de gordura, bolhas de ar e cristais de gelo (AGUILERA; STANLEY; BARBOSA-CÁNOVAS, 1999; RUSS, 2004). As técnicas de microscopia fornecem informações sobre sistemas estruturalmente complexos na forma de imagens que podem ser de compreensão relativamente fácil. Cada técnica de microscopia trabalha com um princípio físico-químico diferente e pode ser usado para examinar diferentes níveis e tipos de organização estrutural (McCLEMENTS, 2007).

Um importante avanço em técnicas de microscopia foi a ampla disponibilidade da microscopia confocal de varredura a laser. Essa técnica permite a obtenção de imagens tridimensionais a partir de uma série de cortes bidimensionais na direção vertical, sem a necessidade física de secção da estrutura (PLUCKNETT et al., 2001). Essas imagens tridimensionais podem ser usadas para determinar a localização espacial das gotas na emulsão e assim, é possível obter informações detalhadas sobre a microestrutura dos flocos. Essa técnica de microscopia também é importante para examinar a localização e transporte de componentes específicos na emulsão devido à possibilidade de usar corantes fluorescentes para marcar moléculas específicas (LOREN; LANGTON; HERMANSSON, 2007).

A condutividade elétrica é a medida da facilidade com a qual o meio permite a passagem de uma corrente elétrica. Esta propriedade está associada à presença de íons carregados na emulsão, como por exemplo, a presença de sais ou polímeros carregados (LAMBA; SATHISH; SABIKHI, 2015). Desta forma, podem ser estudados os efeitos dos biopolímeros de cargas opostas na estabilidade das gotas e, como consequência, na formação de um campo eletrostático nas emulsões (LEVIC et al., 2015). Em emulsões que utilizam sais como estabilizantes, o aumento da

condutividade elétrica com o tempo sugere uma desestabilização do sistema devido à liberação destes sais para a fase contínua (LAMBA; SATHISH; SABIKHI, 2015). Por outro lado, a aproximação das gotículas de óleo na fase creme pode ser acompanhada pela diminuição da condutividade elétrica (McCLEMENTS, 2007; ANVISA, 2004). Isso se deve ao fato de que quanto mais rico em óleo, menor a condutividade do sistema e quanto mais rico em água, maior a condutividade do sistema, pois a constante dielétrica da água é superior à do óleo (BRUTTEL, 2004).

Em emulsões de dupla camada, cada biopolímero disperso deve possuir uma carga superficial para ser capaz de atrair o biopolímero de carga oposta e formar a dupla camada. Potencial zeta é uma propriedade superficial que fornece a medida do potencial elétrico no limite nominal da camada difusa da superfície da gota (LAMBA; SATHISH; SABIKHI, 2015). Emulsões com potencial zeta maiores que 25 mV em valor absoluto normalmente são consideradas estáveis. Valores abaixo desse, mostram fortes atrações de van der Waals, o que causa agregação e consequentemente desestabilização da emulsão (NANOCOMPOSIX, 2012). Quanto maior o potencial zeta das emulsões, maior será a estabilidade contra a floculação devido a maior prevalência de cargas repulsivas nas superfícies das gotas (LAMBA; SATHISH; SABIKHI, 2015). A estabilidade das emulsões de dupla camada pode ser afetada por qualquer modificação na superfície e/ou alteração nas etapas de processo. Assim, a utilização do potencial zeta para avaliar estabilidade torna-se importante porque a estabilidade é dependente da polaridade das superfícies e da presença de estruturas iônicas (LAMBA; SATHISH; SABIKHI, 2015).

Conhecer as propriedades reológicas de emulsões é importante por diversos motivos, uma vez que a viscosidade dos componentes individuais, por exemplo, influencia a ruptura das gotas em um homogeneizador e a vida de prateleira de emulsões alimentícias. Informações sobre o comportamento do produto são utilizadas pelos engenheiros de alimentos

para o dimensionamento de operações como escoamento através de tubulações, agitação, passagem através de trocadores de calor e envasamento (McKENNA; LYNG, 2003). Atributos sensoriais relacionados à textura também estão relacionados com as propriedades reológicas. Além disso, tais propriedades podem fornecer informações fundamentais sobre a organização estrutural e interações entre os componentes das emulsões (McCLEMENTS, 1999).

As emulsões alimentícias exibem diferentes comportamentos reológicos, podendo ser caracterizados como fluidos de baixa viscosidade (leite), géis viscoelásticos (iogurtes) ou sólidos bastante duros (manteiga sob refrigeração). Apesar dessa diversidade de comportamentos, é possível caracterizá-los utilizando modelos simples, sendo definidos como sólidos, líquidos e plásticos, enquanto que os sistemas muito complexos podem ser descritos pela combinação de dois ou mais desses modelos simples (RAO, 1999; McCLEMENTS, 1999). Os líquidos Newtonianos ideais devem ser incompressíveis, homogêneos e isotrópicos (suas propriedades são as mesmas em todas as direções), porém, muitos alimentos líquidos não se encaixam nesses critérios. O comportamento reológico não-ideal se apresenta de diversas maneiras, assim, a viscosidade dos sistemas pode depender da taxa de deformação ou do tempo de aplicação da tensão de cisalhamento (MACOSKO, 1994).

Nos sistemas em que a viscosidade aumenta ou diminui com o aumento da taxa de deformação, a viscosidade é chamada de viscosidade aparente (WALSTRA, 2003). Os fluidos cuja viscosidade aparente diminui com o aumento da taxa de deformação são os fluidos pseudoplásticos, e os fluidos dilatantes são aqueles cuja viscosidade aparente aumenta com o aumento da taxa de deformação (McCLEMENTS, 1999). Os fluidos dependentes do tempo, por sua vez, podem ser classificados como tixotrópicos ou reopéticos. No comportamento tixotrópico, a viscosidade aparente do fluido diminui com o tempo de cisalhamento em uma taxa de

deformação constante, e no comportamento reopético observa-se o oposto (McCLEMENTS, 1999).

No entanto, muitas emulsões alimentícias não são líquidos puros e nem sólidos puros, exibindo propriedades reológicas que são parcialmente elásticas e parcialmente viscosas (WALSTRA, 2003). Os materiais plásticos apresentam comportamento elástico abaixo do valor de tensão inicial e comportamento viscoso acima desse valor, porém os fluidos viscoelásticos apresentam ambos os comportamentos simultaneamente. Os sólidos ideais armazenam toda a energia mecânica na deformação de suas ligações e retornam às suas formas originais quando a força é removida, enquanto que em um líquido ideal toda a energia mecânica aplicada ao material é dissipada devido ao atrito, convertida para a forma de calor. Nos materiais viscoelásticos, por sua vez, parte da energia é estocada no material e parte é dissipada na forma de calor. Dessa maneira, quando uma força é aplicada ao material viscoelástico, ele não se deforma instantaneamente e nem retorna à sua forma original quando a força é retirada. Assim, as propriedades reológicas de um material viscoelástico são compostas por uma contribuição elástica e uma viscosa (McCLEMENTS, 1999).

As propriedades reológicas das emulsões são influenciadas por diversos fatores, como a fração volumétrica da fase dispersa, o tamanho das gotas, interações coloidais, entre outros. A viscosidade de uma emulsão não floculada aumenta com a fração volumétrica da fase dispersa porque a presença das gotículas aumenta a dissipação de energia associada ao fluxo do fluido (MEWIS; MACOSKO, 1994). Com baixas concentrações de gotículas, a viscosidade aumenta linearmente com fração volumétrica da fase dispersa, mas em maiores concentrações de gotículas o aumento de viscosidade é mais pronunciado. Acima de uma fração volumétrica de fase dispersa crítica, as gotículas são arranjadas tão próximas que não podem fluir facilmente. Acima desta concentração de gotículas, a viscosidade da emulsão aumenta acentuadamente e a emulsão

ganha propriedades semelhantes a gel, por exemplo, elasticidade, viscoelasticidade e plasticidade (McCLEMENTS, 1999).

A influência do tamanho das gotículas e da distribuição do tamanho das gotículas na reologia da emulsão depende da fração volumétrica da fase dispersa e da natureza das interações coloidais. Na ausência de interações coloidais consideráveis, o tamanho das gotículas altera a reologia da emulsão devido à sua influência no movimento browniano e no efeito da tensão de cisalhamento (MEWIS; MACOSKO, 1994). Esse efeito só é apreciável em emulsões com concentrações de gotículas relativamente altas, ou seja, fração volumétrica da fase dispersa acima de 0,45 (DICKINSON, 1992). O tamanho médio das gotículas e o grau de polidispersidade têm uma influência particularmente significativa na reologia de emulsões altamente concentradas, próximo ou acima do parâmetro efetivo de aglomeração (PAL, 1996). Em emulsões contendo gotículas não floculadas, o parâmetro de aglomeração máximo depende da polidispersão. As gotículas são capazes de aglomerar de forma mais eficiente quando são polidispersas e, portanto, a viscosidade de uma emulsão polidispersa concentrada é menor que a de uma emulsão monodispersa com a mesma fração volumétrica de gotículas (McCLEMENTS, 1999).

A natureza das interações coloidais entre as gotículas em uma emulsão é um dos fatores mais importantes na determinação do seu comportamento reológico. As propriedades reológicas dependem da magnitude e da amplitude relativa das interações atrativas (principalmente van der Waals, hidrofóbicas e depleção) e repulsivas (principalmente eletrostática, estérica e flutuação térmica) entre as gotículas. Quando as interações são de longo alcance e repulsivas, a fração volumétrica efetiva da fase dispersa pode ser significativamente maior do que a fração volumétrica real e, assim, a viscosidade da emulsão aumenta. Quando as interações entre as gotículas são suficientemente atrativas, a fração volumétrica efetiva da fase dispersa é aumentada devido à floculação, o

que também resulta em um aumento na viscosidade da emulsão. A manipulação das interações coloidais entre as gotículas pode, portanto, ser usada para controlar as propriedades reológicas das emulsões (McCLEMENTS, 1999).

4. Produção de microcápsulas por secagem em spray dryer

A microcápsula consiste de uma camada de material encapsulante que age como um filme protetor, isolando a substância ativa e impedindo os efeitos da exposição a condições inapropriadas, como a presença de luz, oxigênio ou pH extremos, estabilizando e aumentando a vida útil dos compostos encapsulados, além de permitir sua liberação em locais e quantidades específicos (JIZOMOTO et al., 1993; RÉ, 2006). Assim, a microencapsulação na indústria de alimentos apresenta potencial de aplicação para diversos materiais como óleos poli-insaturados, enzimas, micro-organismos, vitaminas, sais, aminoácidos, óleos essenciais, corantes, entre outros (DESAI; JIN, 2005).

As características de morfologia, disposição do núcleo (único ou múltiplo) e tamanho das partículas obtidas é dependente dos materiais de parede e da técnica de encapsulação empregados. As partículas com tamanho entre 1 e 1000 µm são classificadas como micropartículas enquanto para nanopartículas o tamanho varia entre 10 a 1000 nm (SILVA et al., 2003). Esse parâmetro é considerado importante para a indústria de alimentos, pois interefe diretamente nas propriedades sensoriais (VAN DEN BERG et al., 2008).

Diversas técnicas podem ser utilizadas para encapsulação de substâncias ativas como a coacervação simples ou complexa, gelificação iônica, separação por fase orgânica, envolvimento lipossômico, *spray drying* (atomização), *spray coating*, *spray chilling*, extrusão, liofilização, polimerização interfacial e inclusão molecular (JACKSON; LEE, 1991). O processo de secagem por spray dryer é a técnica mais comum utilizada para encapsular ingredientes da indústria de alimentos devido a alta

eficiência, baixo custo e disponibilidade de equipamentos, razões pelas quais tem sido utilizada há décadas para encapsulação de aromas, lipídeos e carotenoides (GOUIN, 2004).

Segundo Gharsallaoui et al. (2007) antes de ser considerada uma ciência, a microencapsulação por spray drying deveria ser considerada uma arte devido aos muitos fatores para otimizar e à complexidade dos fenômenos de transferência de calor e massa que ocorrem durante a formação da microcápsula. Durante esse processo, a evaporação do solvente, água na maioria das vezes, é rápida e o aprisionamento dos compostos de interesse ocorre quase instantaneamente. Essa característica do processo exige o rigoroso cuidado na escolha dos materiais encapsulantes, além da otimização das condições de operação.

Em geral, lipídeos apresentam dificuldades para se dispersarem em produtos alimentícios e, além disso, especialmente os ácidos graxos poli-insaturados são susceptíveis à oxidação, resultando em aromas desagradáveis e formação de compostos tóxicos. Matsuno e Adachi (1993) enumeraram cinco vantagens da encapsulação de lipídeos: retardar a oxidação, aumentar a estabilidade, controlar a liberação dos aromas lipossolúveis, mascarar o sabor amargo de substâncias lipossolúveis e proteger subtâncias dissolvidas de hidrólise enzimática. Se o composto a ser encapsulado for de natureza hidrofóbica, a estabilidade da emulsão de alimentação também deve ser considerada.

A preservação da estrutura interfacial é de extrema importância para garantir alta eficiência de microencapsulação e manter a funcionalidade desejada. Assim sendo, a secagem de emulsões requer a utilização de um material de parede capaz de formar uma matriz contínua para recobrir as gotículas de óleo no material seco (SERFERT et al., 2013). A funcionalidade química, a solubilização e a difusão do material encapsulado pela matriz determinam o grau de retenção do núcleo durante a produção das microcápsulas por atomização, de modo que a estabilidade das

microcápsulas, durante o armazenamento, é altamente dependente da composição do material de parede (GHARSALLAOUI et al., 2007).

As maltodextrinas proporcionam boa estabilidade oxidativa ao óleo encapsulado, mas apresentam fraca capacidade emulsionante, proporcionando baixa estabilidade da emulsão e baixa retenção de óleo (KENYON, 1995). Em contraste, as proteínas possuem carácter anfifílico e oferecem propriedades físico-químicas e funcionais necessárias para encapsular materiais hidrofóbicos. A pectina, por sua vez, é um polímero capaz de auxiliar na produção de emulsões estáveis a baixa concentração (GHARSALLAOUI et al., 2007).

A técnica de secagem por atomização foi utilizada com sucesso por Serfert et al. (2013) ao estudarem a secagem por spray dryer de emulsão de óleo de peixe estabilizada por β-lactoglobulina e pectina com adição de xarope de glicose, atingindo eficiência de microencapsulação acima de 95%. Aberkane, Roudaut e Saruel (2014) observaram a maximização da eficiência de encapsulação e a minimização da oxidação lipídica nas microcápsulas ao adicionar maltodextrina às emulsões de óleo rico em ácidos graxos ômega-3 estabilizadas por proteína de ervilha e pectina antes da secagem por spray-dryer. Botrel et al. (2014) mostraram que a inulina pode ser um material de parede alternativo para a produção de microcápsulas de óleo de peixe por secagem em spray dryer, uma vez que o uso desse carreador foi responsável por diminuir o óleo superficial nas microcápsulas. Huynh et al. (2008) reportaram a produção de microcápsulas de óleo de *Backhousia citriodora* utilizando spray dryer. Utilizaram dois sistemas para material de parede, um composto por amido modificado e maltodextrina e o outro composto por concentrado proteico de soro de leite e maltodextrina e concluíram que ambos podem auxiliar na produção de microcápsulas com características satisfatórias quanto à retenção de óleo e teor de óleo superficial.

Um estudo para avaliar o potencial da combinação de maltodextrina com diferentes materiais de parede na encapsulação de óleo de linhaça por

spray dryer foi conduzido por Carneiro et al. (2013). Estudando os sistemas compostos por maltodextrina com goma arábica, com concentrado proteico de soro de leite e com dois tipos de amidos modificados (Hi-Cap e Capsul), os autores obtiveram melhor resultado para eficiência de encapsulação quando o material de parede foi composto por maltodextrina e amido modificado Hi-Cap. Avaliando a proteção contra oxidação lipídica, o material de parede mais eficiente foi o composto por maltodextrina e concentrado proteico de soro de leite.

Em alimentos com baixo teor de água, como os alimentos desidratados, os sólidos amorfos não-cristalinos formam estruturas vítreas em estado de não-equilíbrio. O estado vítreo desses sólidos é atingido durante o processamento dos alimentos por meio de uma transição vítrea reversível causada pela rápida remoção de água ou rápido resfriamento. O sucesso da liofilização, spray drying e extrusão, bem como a estabilidade dos alimentos desidratados em relação ao colapso e à recristalização é baseado no controle do estado vítreo dos componentes durante o processo de desidratação e armazenamento. Os processos de encapsulação geralmente usam materiais com capacidade para formar estruturas vítreas para proteger os compostos de interesse (ROOS, 2010).

A sorção de água e a plastificação pela água são propriedades físicas importantes dos alimentos secos. Essas propriedades estão relacionadas à estabilidade dos materiais durante o processamento e armazenamento (ROOS, 1995; RAHMAN, 2009). A sorção de água relaciona o conteúdo de água e a atividade de água do material, enquanto a plastificação pela água está relacionada com o teor de água e a temperatura de transição vítrea de uma fase amorfa. A correlação entre a sorção de água e a plastificação pela água é frequentemente utilizada para determinar a umidade crítica e a atividade de água crítica para a estabilidade do material nas temperaturas de interesse (ROOS, 1995; NURHADI; ROOS; MAIDANNYK, 2016). A plastificação das estruturas não cristalinas devido ao aumento da temperatura ou da umidade reduz

exponencialmente o tempo de relaxação acima da temperatura de transição vítrea, resultando em uma rápida deterioração do produto, ou seja, os materiais com umidade inferior à respectiva umidade crítica, apresentam maior estabilidade, especialmente em termos de estabilidade física (ROOS, 1995; ROOS, 2010).

As relaxações estruturais correspondem aos rearranjos moleculares cinéticos impedidos e relacionam-se às mudanças dependentes do tempo de propriedades termodinâmicas, mecânicas ou dielétricas, após uma perturbação como mudança de temperatura ou pressão (FAN; ROOS, 2016). O tempo de relaxação é o tempo necessário para a recuperação de perturbações (LE MESTE et al., 2002). As relaxações estruturais e o tempo de relaxação podem estar relacionados à estrutura das partículas, viscosidade e propriedades mecânicas que controlam a qualidade e estabilidade dos materiais alimentares, particularmente em temperaturas próximas e acima da transição vítrea (FAN; ROOS, 2016). As variações na mobilidade molecular, como a deformação molecular, a migração molecular e a difusão molecular, podem estar relacionadas à estabilidade dos alimentos durante o armazenamento (ROUDAUT et al., 2004). Nas estruturas em estado vítreo, a mobilidade molecular (vibrações de átomos ou reorientação de pequenos grupos de átomos) é principalmente local e não envolve os átomos ou moléculas circundantes. Um aumento de temperatura acima da Tg resulta em um aumento rápido da mobilidade molecular, resultando na diminuição da viscosidade do material (HANCOCK; SHAMBLIN; ZOGRAFI, 1995; FAN; ROOS, 2016). A relaxação, dependente da frequência de perturbação, de polímeros amorfos é regida pela umidade, atividade de água e temperatura (ROOS; KAREL, 1991). A análise dinâmina-mecânica (DMA) pode ser usada em estudos de relaxações estruturais próximas à transição vítrea e fornecer a temperatura de relaxação (FAN; ROOS, 2016).

5. Referências bibliográficas

ABERKANE, L.; ROUDAUT, G.; SAUREL, R. Encapsulation and oxidative stability of PUFA-rich oil microencapsulated by spray drying using pea protein and pectin. **Food and Bioprocess Technology**, v. 7, p. 1505-1517, 2014.

AGUILERA, J. M.; STANLEY, D. W.; BARBOSA-CÁNOVAS, G. V. **Microstructural Principles of Food Processing Engineering.** Gaithersburg, USA: Aspen Puslishers, 1999.

AL-ASHEH, S.; JUMAH, R.; BANAT, F.; HAMMAD, S. The use of experimental factorial design for analysing the effect of spray dryer operating variables on the production of tomato powder. **Food and Bioproducts Processing**, v. 81, n. 2, p. 81–88, 2003.

ALBUQUERQUE, M. L. S.; GUEDES, I.; ALCANTARA JR, P.; MOREIRA, S. G. C.; BARBOSA NETO, N. M.; CORREA, D. S.; ZILIO, S. Characterization of buriti (*Mauritia flexuosa* L.) oil by absorption and emission spectroscopies. **Journal of the Brazilian Chemical Society**, v. 16, n. 6A, p. 1113-1117, 2005.

ALQUEZAR, B.; RODRIGO, M. J.; ZACARÍAS, L. Regulation of carotenoid biosynthesis during fruit maturation in the red-fleshed orange mutant Cara Cara. **Phytochemistry**, v. 69, n. 10, p. 1997-2007, 2008.

ANVISA. Agência Nacional de Vigilância Sanitária. **Guia de Estabilidade de Produtos Cosméticos**, 1ed, Brasília, 2004.

AUGUSTIN, M. A.; HEMAR, Y. Nano- and micro-structured assemblies for encapsulation of food ingredients. **Chemical Society Reviews**, v. 38, n. 4, p. 902-912, 2009.

BOTREL, D. A.; BORGES, S. V.; FERNANDES, R. V. B.; CARMO, E. L. Optimization of fish oil spray drying using a protein:inulin system. **Drying Technology**, v. 32, p. 279-290, 2014.

BOUYER, E.; MEKHLOUFI, G.; ROSILIO, V.; GROSSIORD, J. L.; AGNELY, F. Proteins, polysaccharides, and their complexes used as stabilizers for emulsions: alternatives to synthetic surfactants in the pharmaceutical field? **International Journal of Pharmaceutics**, v. 436, p. 359–378, 2012.

BRUTTEL, P. A. **Conductometry – Conductivity Measurement**, 1ed, Switzerland, 2004.

CANTERI, M. H. H.; MORENO, L.; WOSIACKI, G.; SCHERR, A. P. Pectina: da matéria-prima ao produto final. **Polímeros**, v. 22, n. 2, p. 149-157, 2012.

CARNEIRO, H. C. F.; TONON, R. V.; GROSSO, C. R. F.; HUBINGER, M. D. Encapsulation efficiency and oxidative stability of flaxseed oil microencapsulated by spray drying using different combinations of wall materials. **Journal of Food Engineering**, v. 115, p. 443-451, 2013.

DAMODARAN, S.; PARAF, A. **Food Protein and their Aplications.** New York: Marcel Dekker, 1997.

DE GREYT, W. D.; KELLENS, M. Deodorization. In: SHAHIDI, F. **Bailey's Industrial Oil & Fat Products** 6ªed, v.5, New York, John Wiley & Son, p.341-383, 2005.

DESAI, K. G. H.; JIN, H. P. Recent developments in microencapsulation of food ingredients. **Drying Technology**, v. 23, n. 7, p. 1361-1394, 2005.

DESAI, K. G. H.; PARK, H. J. Recent developments in microencapsulation of food ingredients. **Drying Technology**, v. 23, p. 1361–1394, 2005.

DICKINSON, E. **An introduction to food hydrocolloids**, Oxford, UK: University Press, 1992.

DIFTIS N.; KIOSSEOGLOU, V. Competitive adsorption between a dry-heated soy protein-dextran mixture and surface-active materials in oil-in-water emulsions. **Food Hydrocolloids**, v. 18, p. 639-646, 2004.

DONG, D.; LI, X.; HUA, Y.; CHEN, Y; KONG, X.; ZHANG, C.; WANG, Q. Mutual titration of soy proteins and gum arabic and the complexing behavior studied by isothermal titration calorimetry, turbidity and ternary phase boundaries. **Food Hydrocolloids**, v. 46, p. 28-36, 2015.

FAN, F.; ROOS, Y. H. Structural relaxations of amorphous lactose and lactose-whey protein mixtures. **Journal of Food Engineering**, v. 173, p. 106-115, 2016.

FRANÇA, L. F.; REBER, G.;MEIRELES, M. A. A.; MACHADO, N. T.; BRUNNER, G. Supercritical extraction of carotenoids and lipids from buriti (*Mauritia flexuosa*), a fruit from the Amazon region. **The Journal of Supercritical Fluids**, v. 14, p. 247-256, 1999.

GANCZ, K.; ALEXANDER, M.; CORREDIG, M. Interactions of high methoxyl pectin with whey proteins at oil/water interfaces. **Journal of Agricultural and Food Chemistry**, v. 53, p. 2236-2241, 2005.

GHARSALLAOUI, A.; ROUDAUT, G.; CHAMBIN, O.; VOILLEY, A.; SAUREL, R. Applications of spray-drying in microencapsulation of food ingredients: an overview. **Food Research International**, v. 40, n. 9, p. 1107–1121, 2007.

GOUIN, S. Micro-encapsulation: Industrial appraisal of existing technologies and trends. **Trends in Food Science and Technology**, v. 15, p. 330–347, 2004.

GU, Y. S.; DECKER, E. A.; MCCLEMENTS, D. J. Influence of pH and β-carrageenan concentration on physicochemical properties and stability of β-lactoglobulin-stabilized oil-in-water emulsions. **Journal of Agricultural and Food Chemistry**, v. 52, p. 3626-3632, 2004.

GUINAZI, M.; MILAGRES, R. C. R. M.; PINHEIRO-SANT'ANA, H. M.; CHAVES, J. B. P. Tocoferois e tocotrienois em óleos vegetais e ovos. **Química Nova**, v. 32, n. 8, p. 2098-2103, 2009.

HANCOCK, B. C.; SHAMBLIN, S. L.; ZOGRAFI, G. Molecular mobility of amorphous pharmaceutical solids below their glass transition temperatures. **Pharmaceutical Research**, v. 12, n. 6, p. 799-806, 1995.

HEINONEN, M.; HAILA, K.; LAMPI, A. M.; PIIRONEN, V. Inhibition of oxidation in 10% oil-in-water emulsions by beta-carotene with alpha-and gamma-tocopherols. **Journal of the Brazilian Chemical Society**, v. 74, n. 9, p. 1047-1052, 1997.

HUYNH, T. V.; CAFFIN, N.; DYKES, G. A.; BHANDARI, B. Optimization of the microencapsulation of lemon myrtle oil using response surface methodology. **Drying Technology**, v. 26, p. 357-368, 2008.

JACKSON, L.S.; LEE, K.. Microencapsulation Food Industry. **Lebensmittel-Wissenschaft und -Technologie**, v. 24, n. 4, p. 289–297, 1991.

JAFARI, S. M.; ASSADPOOR, E.; HE, Y.; BHANDARI, B. Encapsulation efficiency of food flavours and oils during spray drying. **Drying Technology**, v. 27, n. 7, p. 816-835, 2008.

JARAMILLO, D. P.; ROBERTS, R. F.; COUPLAND, J. N. Effect of pH on the properties of soy protein-pectin complexes. **Food Research International**, v. 44, p. 911-916, 2011.

JIZOMOTO, H.; KANAOKA, E.; SUGITA, K..; HIRANO, K.. Gelatin-Acacia microcapsules for trapping micro oil droplets containing lipophilic drugs and ready disintegration in the gastrointestinal tract. **Pharmaceutical Research**, v. 10, n. 8, p. 115–122, 1993.

KALTSA, O.; MICHON, C.; YANNIOTIS, S.; MANDALA, I. Ultrasonic energy input influence on the production of sub-micron o/w emulsions containing whey protein and common stabilizers. **Ultrasonics Sonochemistry**, v. 20, p. 881-891, 2013.

KENYON, M. M. Modified starch, maltodextrin, and corn syrup solids as wall materials for food encapsulation. In S. J. RISCH; G. A. REINECCIUS (Eds.), **Encapsulation and Controlled Release of Food Ingredients.** Washington, DC, American Chemical Society. ACS symposium series, v. 590, p. 42–50, 1995.

KUMAR, R.; CHOUDHARY, V.; MISHRA, S.; VARMA, I. K.; MATTIASSON, B. Adhesives and plastics based on soy protein products. **Industrial Crops and Products**, v. 16, p. 155-172, 2002.

LAKEMOND, C. M. M.; DE JOUNG, H. H. J.; HESSING, M.; GRUPPEN, H.; VARAGEN, A. G. J. Soy glycinin: Influence of pH and ionic strengh on solubility and molecular structure at ambient temperatures. **Journal of Agricultural and Food Chemistry**, v. 48, n. 6, p. 1985-1990, 2000.

LAM, M.; PAULSEN, P.; CORREDIG, M. Interactions of soy protein fractions with high-methoxyl pectin. **Journal of Agricultural and Food Chemistry**, v. 56, p .4726–4735, 2008.

LAM, M.; SHEN, R.; PAULSEN, P.; CORREDIG, M. Pectin stabilization of soy protein isolates at low pH. **Food Research International**, v. 40, p. 101-110, 2007.

LAMBA, H.; SATHISH, K.; SABIKHI, L. Double emulsions: Emerging delivery system for plant bioactives. **Food and Bioprocess Technology**, v. 8, p. 709-728, 2015.

LE MESTE, M.; CHAMPION, D.; ROUDAUT, G.; BLOND, G.; SIMATOS, D. Glass transition and food technology- a critical appraisal. **Journal of Food Science**, v. 67, n. 7, p. 1365-2621, 2002.

LEVIC, S.; LIJAKOVIC, I. P.; DORDEVIC, V.; RAC, V.; RAKIC, V.; KNUDSEN, T. S.; PAVLOVIC, V.; BUGARSKI, B.; NEDOVIC, V. Characterization of sodium alginate/D-limonene emulsions and respective calcium alginate/D-limonene beads produced by electrostatic extrusion. **Food Hydrocolloids**, v. 45, p. 111-123, 2015.

LOREN, N.; LANGTON, M.; HERMANSSON, A. M. Confocal fluorescence microscopy for structure characterization. In McCLEMENTS (Ed.), **Understanding and Controlling the Microstructure of Complex Foods**, Cambridge, UK: Woodhead Publishing, 2007.

MACOSKO, C. W. **Rheology: Principles, Measurements and Applications**, New York: VCH Publishers, 1994.

MARFIL, P. H. M. **Microencapsulação de óleo de Palma por coacervação complexa em matrizes de gelatina/goma arábica e gelatina/alginato**, 135p. Tese (Doutorado em Engenharia e Ciência de Alimentos) – Universidade Estadual Paulista "Julio de Mesquita Filho", São José do Rio Preto, 2014.

MATSUNO, R.; ADACHI, S. Lipid encapsulation technology - Techniques and applications to food. **Trends in Food Science and Technology**, v. 4, p. 256–261, 1993.

MATTISON, K. W.; BRITTAIN, I. J.; DUBIN, P. L. Protein-polyelectrolyte phase boundaries. **Biotechnology Progress**, v. 11, p. 632-637, 1995.

MATTISON, K. W.; WANG, Y.; GRYMONPRE´, K.; DUBIN, P. L. Micro and macro- phase behaviour in protein-polyelectrolytes systems. **Macromolecular Symposia**, v. 140, p. 53-76, 1999.

MEWIS, J.; MACOSKO, C. W. Suspension rheology. In MACOSKO, C. W. Ed., **Rheology: Principles, Measurements and Applications**. New York: VCH Publishers, 1994.

McCLEMENTS, D. J. **Food Emulsions. Principles, Practice, and Techniques.** Boca Raton: CRC Press, 1999.

McCLEMENTS, D. J. Critical review of techniques and methodologies for characterization of emulsion stability. **Critical Reviews in Food Science and Nutrition**, v. 47, p. 611-649, 2007.

McCLEMENTS, D. J.; DECKER, E. A.; WEISS, J. Emulsion-based delivery systems for lipophilic bioactive components. **Journal of Food Science**, v. 75, n. 8, p. 109-124, 2007.

McKENNA, B. M.; LYNG, J. G. Introduction to food rheology and its measurements. In: McKENNA, B. M. (Ed.), **Texture in Food**, Volume 1: Semi-solid foods, Boca Raton: CRC Press, 2003.

MELÉNDEZ-MARTÍNEZ, A. J.; VICARIO, I. M.; HEREDIA, F. J. Review: Analysis of carotenoids in orange juice. **Journal of Food Composition and Analysis**, v. 20, n. 7, p. 638-649, 2007.

NANOCOMPOSIX. **Guidelines for zeta potential analysis of nano particles**, 2012. Disponível em: http://cdn.shopify.com/s/files/1/0257/8237/files/nanoComposix_Guidelines_for_Zeta_Potential_Analysis_of_Nanoparticles.pdf?13692. Acesso em 09 junho 2016.

NURHADI, B.; ROOS, Y. H.; MAIDANNYK, V. Physical properties of maltodextrin DE 10: Water sorption, water plasticization and enthalpy relaxation. **Journal of Food Engineering**, v. 174, p. 68-74, 2016.

PAL, R. Rheology of Emulsions Containing Polymeric Liquids. In BECHER, P., Ed. **Encyclopedia of Emulsion Technology**. New York: Marcel Dekker, 1996.

PERRECHIL, F. A.; CUNHA, R. L. Stabilization of multilayered emulsions by sodium caseinate and κ-carrageenan. **Food Hydrocolloids**, v. 30, p. 606-613, 2013.

PERRECHIL, F. A.; PICONE, C. S. F.; CUNHA, R. L. Operação de redução de tamanho. In: TADINI, C. C.; TELIS, V. R. N.; MEIRELLES, A. J. A.; PESSOA FILHO, P. A. **Operações Unitárias na Indústria de Alimentos** 1ªed, Rio de Janeiro, LTC, p.293-322, 2016.

PLUCKNETT, K. P.; POMFRET, S. J.; NORMAND, V.; FERDINANDO, D.; VEERMAN, C.; FRITH, W. J.; NORTON, I. T. Dynamic experimentation on the confocal laser scanning microscope: application to soft-solid, composite food materials. **Journal of Microscopy**, v. 201, p. 279–290, 2001.

PUPPO, M. C.; SPERONI, F.; CHAPLEAU, N.; DE LAMBALLERIE, M.; ANON, M. C.; ANTON, M. Effect of high-pressure treatment on emulsifying properties of soybean proteins. **Food Hydrocolloids**, v. 19, p. 289-296, 2005.

RAHMAN, M. S. Glass transition data and models of foods. In: RAHMAN, M.S. (Ed.), **Food Properties Handbook**, second ed. Boca Raton: CRC Press, 2009.

RAO, M. A. **Rheology of fluid and semisolid foods**, Gaithersburg: Aspen Publication, 433 p., 1999.

RÉ, M. I. Microencapsulation by spray drying. **Drying Technology**, v. 16, p. 1195–1236, 1998.

RÉ, M. I. Formulating drug delivery systems by spray drying. **Drying Technology**, v. 24, p. 433–446, 2006.

RENKEMA, J. M. S.; GRUPPEN, H.; VAN VLIET, T. Influence of pH and ionic strength on heat-induced formation and rheological properties of soy protein gels in relation to denaturation and their protein compositions. **Journal of Agricultural and Food Chemistry**, v. 50, p. 6064-6071, 2002.

RIBEIRO, H. S.; AX, K.; SCHUBERT, H. Stability of lycopene emulsions in food systems. **Journal of Food Science**, v. 68, n. 9, p. 2730-2734, 2003.

ROCHA, G. A.; FÁVARO-TRINDADE, C. S.; GROSSO, C. R. F. Microencapsulation of lycopene by spray drying: Characterization, stability and application of microcapsules. **Food and Bioproducts Processing**, v. 90, p. 37-42, 2012.

RODRIGUEZ-AMAYA, D. B. Assessment of the provitamina A contents of foods - The brazilian experience. **Journal of Food Composition and Analysis**, v. 9, p. 196-230, 1996.

RODRÍGUEZ PATINO, J. M.; PILOSOF, A. M. R. Protein-polysaccharide interactions at fluid interfaces. **Food Hydrocolloids,** v. 25, n. 8, p. 1925-1937, 2011.

ROOS, Y. H. **Phase Transition in Foods**. California: Academic Press, 1995.

ROOS, Y. H. Glass transition temperature and its relevance in food processing. **Annual Review of Food Science and Technology**, v. 1, p. 469-496, 2010.

ROOS, Y. H.; KAREL, M. Plasticizing effect of water on thermal behavior and crystallization of amorphous food models. **Journal of Food Science**, v. 56, p. 38-56, 1991.

DE ROSSO, V. V.; MERCADANTE, A. Z. Identification and quantification of carotenoids, by HPLC-PDA-MS/MS, from amazonian fruits. **Journal of Agricultural and Food Chemistry**, v. 55, p. 5062-5072, 2007.

ROUDAUT, G.; SIMATOS, D.; CHAMPION, D.; CONTRERAS-LOPEZ, E.; LE MESTE, M. Molecular mobility around the glass transition temperature: a mini review. **Innovative Food Science and Emerging Technologies**, v. 5, n. 2, p. 127-134, 2004.

ROUDSARI, M.; NAKAMURA, A.; SMITH, A.; CORREDIG, M. Stabilizing behavior of soy soluble polysaccharide or high methoxyl pectin in soy protein isolate emulsions at low pH. **Journal of Agricultural and Food Chemistry**, v. 54, p. 1434-1441, 2006.

RUSS, J.C. **Image Analysis of Food Microstructure.** Boca Raton, FL:CRC Press, 2004.

SANTOS, M. S.; PETKOWICZ, C. L. O.; HAMINIUK, C. W. I.; CÂNDIDO, L. M. B. Polissacarídeos extraídos da gabiroba (*Campomanesia xanthocarpa* Berg): propriedades químicas e perfil reológico. **Polímeros**, v. 20, n. 5, p. 352-358, 2010.

SANTOS, M. F. G.; MARMESAT, S.; BRITO, E. S.; ALVES, R. E.; DOBARGANES, M. C. Major components in oils obtained from Amazonian palm fruits. **Grasas y Aceites**, v. 64, n. 3, p. 328-334, 2013.

SERFERT, Y.; SCHRODER, J.; MESCHER, A.; LAACKMANN, J.; RATZKE, K.; SHAIKH, M. Q.; GAUKEL, V.; MORITZ, H. U.; SCHUCHMANN, H. P.; WALZEL, P.; DRUSCH, S.; SCHWARZ, K. Spray drying behavior and functionality of emulsions with β-lactoglobulin/pectin interfacial complexes. **Food Hydrocolloids**, v. 31, p. 438-445, 2013.

SILVA, C.; RIBEIRO, A.; FERREIRA, D.; VEIGA, F. Administração oral de peptídeos e proteínas: II. Aplicação de métodos de microencapsulação. **Revista Brasileira de Ciências Farmacêuticas**, v. 39, n. 1, p. 1-19, 2003.

SILVA, S. M.; SAMPAIO, K. A.; TAHAM, T.; ROCCO, S. A.; CERIANI, R.; MEIRELLES, A. J. A. Characterization of oil extracted from buriti fruit (*Mauritia flexuosa*) grown in the Brazilian amazon region. **Journal of the American Oil Chemists Society**, v. 86, p. 611-616, 2009.

SINGH, M.; MOHAMED, A. Influence of gluten-soy protein blends on the quality of reduced carbohydrates cookies. **LWT - Food Science and Technology**, v. 40, n. 2, p. 353-360, 2007.

THAKUR, B. R.; SINGH, R. K.; HANDA, A. K.; RAO, M. A. Chemistry and uses of pectin - a review. **Critical Reviews in Food Science and Nutrition**, v. 37, n. 1, p. 47-73, 1997.

TÖMÖSKÖZI, S.; LÁSZTITY, R.; HARASZI, R. BATICZ, O. Isolation and study of the functional properties of pea proteins. **Nahrung**, v.45, n.6, p.399-401, 2001.

TROMP, R. H.; de KRUIF, C. G.; van EIJK, M.; ROLIN, C. On the mechanism of stabilization of acidified milk drinks by pectin. **Food Hydrocolloids**, v.18, p.565–572, 2004.

VAN DEN BERG, L.; VAN VLIET, T.; VAN DER LINDEN, E.; VAN BOEKEL, M. A. J. S.; VAN DE VELDE, F. Physical properties giving the sensory perception of whey proteins/polysaccharide gels. **Food Biophysics**, v. 3, n. 2, p. 198-206, 2008.

XIANQUAN, S.; SHI, J.; KAKUDA, Y.; YUEMING, J. Stability of lycopene during food processing and storage. **Journal of Medicinal Food**, v. 8, n. 4, p. 413-422, 2005.

WALSTRA, P. **Physical Chemistry of Food**, New York, NY.: Marcel Decker, 2003.

CAPÍTULO 2

Caracterização dos biopolímeros e do complexo isolado proteico de soja-pectina de alta metoxilação

O conteúdo desse capítulo está publicado como artigo científico-tecnológico no periódico Polímeros: Ciência e Tecnologia, v. 21, n. 1, p. 62-67, 2017.

Characterization of biopolymers and soy protein isolate-high-methoxyl pectin complex

Mírian Luisa Faria Freitas[1]*, Kivia Mislaine Albano[1] and Vânia Regina Nicoletti Telis[1]

1 Laboratory of Physical Measures, Department of Food Engineering and Technology, Universidade Estadual Paulista "Júlio de Mesquita Filho" campus São José do Rio Preto, 15054-000, São Paulo, Brazil.

*mirianlfreitas@yahoo.com.br

Abstract

This study aimed at characterizing the soy protein isolate and high-methoxyl pectin biopolymers individually, and the complexes formed by both at different proportions and pHs in order to find the most suitable pH and biopolymer ratios to food application as stabilizers. The biopolymers were evaluated through solubilization, charges, turbidimetry, and optical microscopy analyses; the systems with the pair of biopolymers were analyzed through turbidimetry and optical microscopy. High-methoxyl pectin showed high solubilization at all pHs investigated. The soy protein isolate showed low solubilization at pH 4.5, which is close to its isoelectric point, and complete solubilization at pH 11.0. The formation of complexes suggested an attractive interaction between the biopolymers, with high absorbance reading values and images of complexes from optical microscopy. These complexes were present in systems with pHs below the soy protein isolate's isoelectric point, with positive charges; the high-methoxyl pectin, however, had negative ones.

Keywords: attractive interaction, morphology, solubilization, turbidimetry, zeta potential.

1. Introduction

Soy has been the most used material for industrial production of protein concentrates and isolates due to its high amount of proteins and its products' good technological performance. It also represents a vegetable alternative to lactic proteins[1]. The soy protein isolate (SPI) contains at least 90% protein; it is thus virtually free from lipids and carbohydrates[2].

Pectin, probably the most complex natural macromolecule, is the most common stabilizer used in protein-based acidic beverages, positively contributing to the final product's taste, stability, and texture, even if it is added in small amounts[3-5]. Although pectins are part of the majority of plant tissues, the number of commercial sources used is very limited[4]. The mainly polysaccharide used is derived from citric fruit and classified regarding the degree of esterification in: high-methoxyl pectins, when a half or more carboxyl groups are esterified, and low-methoxyl pectins, when less than a half the carboxyl groups are esterified[6].

The formation of complexes between proteins and polysaccharides with opposite charges is a colloidal phenomenon involved in the structuring of several biological systems. There has been increasing interest in complexes formed by these biopolymers recently due to their potential applications in the food industry, being used as stabilizers in milk-based beverages, emulsifiers, foam stabilizers, fat replacers, besides being used in encapsulation, enzyme immobilization and recuperation, and protein separation processes, as explained by Dong et al.[7] in revision of the literature.

Lam et al.[6] carried out a study on pectin stability in protein acidic solutions, in which they used soy protein isolate. It was found that high-methoxyl pectin showed higher stability than low-methoxyl pectin. Jaramillo et al.[8] observed that, at a pH near the isoelectric point of the SPI (around pH 4.0), as pectin was added the protein solubilization increased, which prevented its aggregation through an electrostatic interaction. They also

verified that the resulting protein-polysaccharide complexes could bear thermal treatment, although a few changes in their properties occurred.

When the pair was used in emulsions, the polysaccharides increased the emulsion's physical stability through electrostatic and/or steric effects, because they modify the rheological properties of the interface and increase the viscosity of the emulsion[9].

Values of pH at which there are solubilization or biopolymer complexes formation do not depend or depend very little on the total concentration of the biopolymers. On the other hand, they are strongly related to the isoelectric point of the protein, the ratio between the biopolymers, their ionic strength and molar mass[10-12].

Given this context, the aim of this study was to characterize the soy protein isolate and high-methoxyl pectin biopolymers through solubilization, charges, turbidimetry, and optical microscopy analyses, besides characterizing the complex formed by the pair at different proportions and pHs, evaluating turbidimetry and optical microscopy.

2. Materials and methods

2.1 Materials

The biopolymers used were soy protein isolate (SPI) (Tovani Benzaquen Ingredientes™) and high-methoxyl pectin (HM) (CP Kelco™). For preparation of solutions, sodium azide was also used (Dinâmica™) and for pH adjustment, either 1N hydrochloric acid (Dinâmica™) or sodium hydroxide (Dinâmica™) solutions were used.

2.2 Methods

Biopolymers were characterized, individually, through solubilization, zeta potential, turbidimetry, and optical microscopy analyses at different pHs. The complex high-methoxyl pectin-soy protein isolate was

characterized through turbidimetry analyses and optical microscopy at different proportions and pHs.

2.2.1 Solubilization

Biopolymers' solubilization was determined, in triplicate, at pHs between 3.0 and 11.0 (± 0.05), according to methodology proposed by Cano-Chauca et al.[13] with some modifications. It was weighed 0.4 g of the biopolymer and completed up to 40 mL of solution with deionized water. The solutions were then moved to the shaker (Marconi, MA 830/A) for agitation for 3 hours and were left to hydrate during one night at room temperature. The next day, the desired pH was adjusted, the solutions were centrifuged at 3000×g for 5 minutes (Hermle, Z 326 K) and 20 g supernatant were transferred to previously dried Petri dishes. These were placed in a vacuum drying oven (Marconi, MA 030) at 60 °C for 48 h. Solubilization was calculated by difference in weight.

2.2.2 Preparation of Stock Solutions

Stock solutions of the soy protein isolate were prepared by solubilizing the biopolymer in deionized water and adjusting its pH to 11.0 (± 0.05), for a complete solubilization, according to the solubilization result at that pH and as suggested by Jaramillo et al.[8]. Then they were stirred for 3 h in a magnetic stirrer and allowed to hydrate during one night for a complete hydration. The solutions had their desired pHs adjusted as the analyses were carried out.

Stock solutions of high-methoxyl pectin were prepared by solubilizing them in deionized water for 3 h in magnetic stirrer and hydration during one night at room temperature. The solutions had their desired pHs adjusted as the analyses were carried out.

It was added 0.04% sodium azide in stock solutions to avoid microorganisms growth.

2.2.3 Zeta Potential

The charge analysis of soy protein isolate and high-methoxyl pectin biopolymers in 0.02% w/w solution was carried out at pHs between 3.0 and 7.0 (± 0.05). It was used a zeta potential analyzer (ZetaPALS), according to methodology proposed by Perrechil and Cunha[14]. Measurements were obtained in triplicate.

2.2.4 Turbidimetry

Solutions containing 0.05% w/w soy protein isolate or high-methoxyl pectin were analyzed individually. Besides, different quantities from each biopolymer solutions were mixed in order to obtain systems with SPI:HM proportions of 1:1, 2:1, 3:1, and 4:1 (w:w), with a final concentration of 0.05%. Individual solutions and systems were analyzed at pHs between 3.0 and 7.0 (± 0.05).

Turbidimetry analysis for each system was carried out according to methodology proposed by Antonov and Zubova[15], and Marfil[12]. After obtaining the desired pH, it were measured the absorbance reading values of the aliquots in a spectrophotometer (Biospectro SP-220) at wavelength 590 nm. According to the authors, the time between the adjustment of desired pH and absorbance reading in the spectrophotometer cannot be longer than 10 s, because there may be precipitation of the formed complexes and interference in the readings after this time.

2.2.5 Morphology

The morphology of individual solutions and elaborated systems with SPI:HM proportions of 1:1, 2:1, 3:1, 4:1, with a biopolymer concentration of 0.05%, was verified for pHs between 3.0 and 7.0 (± 0.05) using an optical microscope (Olympus CX31) with 40x magnifying lenses coupled to a digital camera (Olympus SC30).

3. Results and Discussion

3.1 Solubilization

As observed in Figure 1, high-methoxyl pectin is completely soluble, disregarding the pH of the solution. On the other hand, the soy protein isolate shows low solubilization, around 10%, at its isoelectric point (between pH 4.0 and 5.0) and the solubilization increases as it distances from this point, particularly in more alkaline conditions, reaching 100% at pH 11.0.

Figure 1. Solubilization (%) of soy protein isolate and high-methoxyl pectin vs pH.

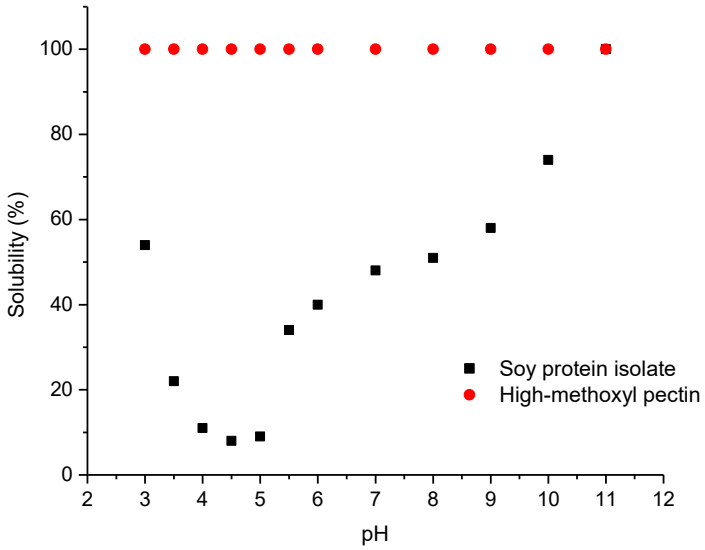

Similar results were found by both Jaramillo et al.[8], and Renkema et al.[16] when studying the soy protein behavior at pHs from 3.0 to 7.0, and 2.0 to 8.0, respectively, confirming the pH between 4.0 and 5.0 as the isoelectric point of soy protein isolate, which is characterized by the lowest solubilization due to charge neutralization.

According to Malhotra and Coupland[17] and Jaramillo et al.[8], the poor solubilization of soy protein isolate around its isoelectric point can limit its application in acid foods. The soy protein isolate presents better

functionality in conditions of higher solubilization, since it can help emulsifying hydrophobic compounds as well as binding water in food systems.

Jaramillo et al.[8] observed that the addition of pectin increased the proportion of the intermediate size fraction at the expense of the fine fraction, prevented the formation of very large aggregates and increased the solubilization of soy protein isolate close to its isoelectric point. Moreover, thermal treatment (30 min, 90 °C) enhanced the solubilization of the soy protein isolate-pectin complexes close to the isoelectric point of protein.

Rocha et al.[18] studied biodegradable composite films based on cassava starch and soy protein and verified that the increase in pH of the filmogenic solution favored solubilization, possibly due to the distance of the soy protein isoelectric point, where the maximum solubilization of the film was observed at pHs between 10 and 12.

Therefore, soy protein isolate solutions used in the other analyses were prepared at pH 11.0 and allowed to hydrate. Only after these steps they had their pH adjusted according to the necessity of the analysis.

3.2 Zeta Potential

As reported by other authors, such as Harnsilawat et al.[19], in the present study it was also observed that for polysaccharydes solutions such as high-methoxyl pectin when the pH increases, negative charges also increase, until this value reaches a plateau. To what proteins are concerned, below their isoelectric point, they acquire positive charges, whereas above this point, they acquire negative charges.

As observed in Figure 2, for the soy protein isolate, the charges close to zero were observed between pHs 4.0 and 5.0, and the curve reaches zero at pH close to 4.6, which confirms its isoelectric point.

Figure 2. Influence of pH on zeta potential (mV) of solutions of soy protein isolate and high-methoxyl pectin.

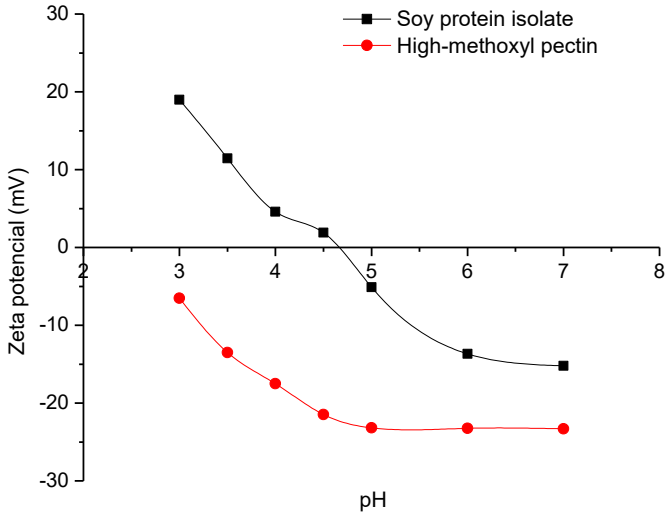

Lam et al. [6] and Jaramillo et al.[8] reported similar results in their studies on charges of soy protein isolate; it was observed that the charges were zero at pH 4.5 and 4.4, respectively.

It is possible to assume that at pHs below the protein's isoelectric point, the interaction between the protein and the pectin is attractive, once the pectin is negatively charged and the protein is positively charged[6].

For the studied biopolymers, at pH 3.5 it is possible that there is an attractive interaction and formation of complexes due to the fact that they have opposite charges and at quite high values.

3.3 Turbidimetry

The absorbance readings at different pHs for the biopolymer solutions and for the systems with different proportions of soy protein isolate:high-methoxyl pectin (SPI:HM) are shown in Figure 3.

Figure 3. Influence of pH on absorbance reading, at wavelength 590 nm, for individual biopolymer solutions and the pair at different proportions.

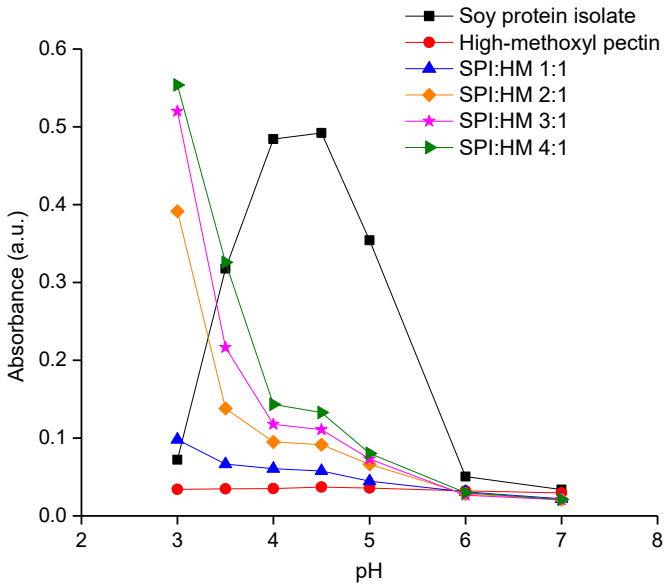

As expected, the solution containing only high-methoxyl pectin presented a low and constant absorbance reading value for all studied pHs. Once its solubilization does not depend on the pH, there was no phase separation nor precipitation.

This behavior was not observed for the soy protein isolate, which presented high absorbance values at pHs between 4.0 and 5.0. These higher absorbance values resulted along the lowest solubilization values, which suggests that the solution's turbidity is connected with the suspended particulate matter. On the other hand, for pHs lower than 4.0 and higher than 5.0, the absorbance reading values for this biopolymer were lower, resulting along higher solubilization values and, consequently, lower quantity of precitpitated matter.

For the systems in which the biopolymers were present at different concentrations, as solutions became more alkaline, the absorbance reading values became lower, which suggests a lower attractive interaction between them and lower complex formation. This result confirms the one obtained from the biopolymers charges analysis, in which at pH higher than 5.0 the

absorbance reading values were lower than 0.1 a.u. for all analyzed proportions.

For the same pH, the increase in proportion of soy protein isolate was followed by an increase in the absorbance reading value, which leads to the conclusion that a higher complex formation occurred, mainly in more acid solutions.

It is noteworthy that the systems at pH 3.0 generated absorbance reading values higher than the systems at pH 3.5. Even though they suggested a higher complex formation at pH 3.0, the systems were less stable than at pH 3.5, with a precipitation and phase separation in few minutes, which is undesirable in food systems such as emulsions.

Based on these remarks, solutions at pH 3.5 were considered ideal for an attractive interaction and complex formation between the studied biopolymers to happen, being suitable to elaborate stable food systems, such as acidic beverages based on protein or emulsions.

Jasentuliyana et al.[20] studied the interaction between the soy protein isolate and citric pectin with the objective of enhancing the use of the soy protein isolate as a turbidity agent in acidic beverages (pH 3.7). The authors then separated the soy protein isolate in two fractions, a hydrophobic and a hydrophilic one and evaluated the interaction between these and pectin through turbidity studies. They did not observe significant differences between the two fractions and reported that the higher the protein proportion, the higher the solution’s absorbance reading value, confirming the use of the soy protein isolate as an opacity agent. Besides, the systems elaborated at protein:pectin proportion of 2:1 and 1:4 showed the highest stability values throughout 28 days.

Another study on the pair formed by the soy protein isolate and high-methoxyl pectin was conducted by Albano and Telis[21], at pH 3.5. The authors confirmed the effect of stability by pectin in protein solutions close to the protein's isoelectric point. Besides, they observed the formation of small complexes that, when submitted to rheological tests, showed a slightly

pseudoplastic behavior, with a tendency to a Newtonian behavior. When the biopolymer solutions were submitted to ultrasound, it was observed that the complexes had their sizes reduced and suffered a consequent reduction of the phases separation after 24 h.

In a study on the interaction between soy protein and gum Arabic conducted by Dong et al. [7] it was found that, at pH 3.0, the addition of gum arabic in a soy protein solution increased the system's absorbance value. Moreover, the systems with a protein:polysaccharide proportion of 1.5:1 and 3:1 were instable.

3.4 Morphology

Through images obtained from optical microscopy, it was possible to observe the morphology of both the biopolymer solutions individually and the systems at different proportions for the studied pHs, confirming the results obtained through solubilization, charges, and turbidimetry tests.

For the soy protein isolate solution, the formation of aggregates was observed at pHs between 4.0 and 5.0, at which lower solubilization and higher absorbance values were noted. For the remaining pHs, there was no presence of complexes.

The pectin solution was solubilized at all different pHs, and aggregates were not noted.

For systems containing different biopolymers proportions, there was a higher formation of complexes at pHs 3.0 and 3.5, and those increased as the soy protein isolate concentration increased in the solution. These results are observed for pH 3.0 in Figure 4 and for pH 3.5 in Figure 5.

Figure 4. Images of systems at pH 3.0 with SPI:HM proportions of 1:1 (a), 2:1 (b), 3:1 (c), and 4:1 (d), obtained through optical microscopy with 40x magnifying lenses.

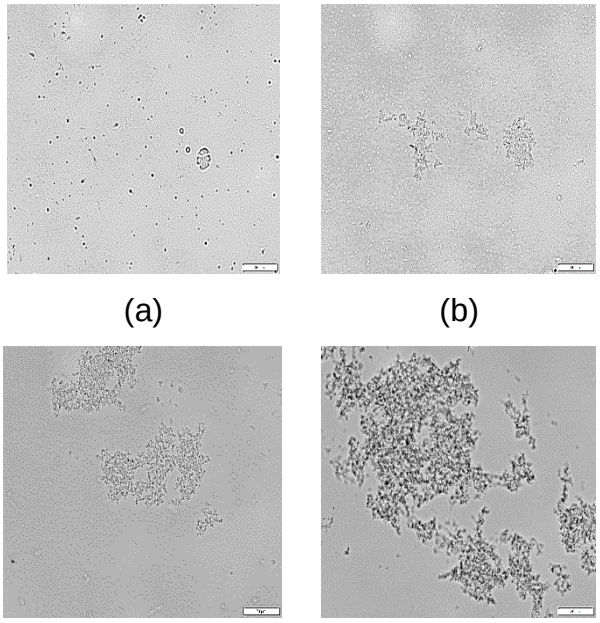

(a) (b)

(c) (d)

Figure 5. Images of systems at pH 3.5 with SPI:HM proportions of 1:1 (a), 2:1 (b), 3:1 (c), and 4:1 (d), obtained through optical microscopy with 40x magnifying lenses.

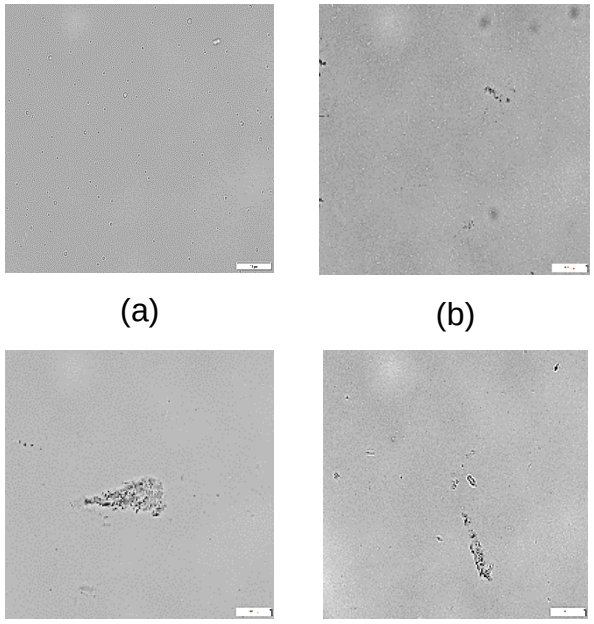

(a) (b)

(c) (d)

Although the complexes were smaller in pH 3.5, as expected by the results of turbidimetry, they were more soluble and more stable being suitable to elaborate food systems.

The systems in higher pH solutions did not present formation of complex, thus confirming a lower attractive interaction between the biopolymers.

4. Conclusions

Through tests for characterization of the biopolymers, it was observed that high-methoxyl pectin showed high solubilization, disregarding pH, and that negative charges increased as pH increased until they reached a plateau. The soy protein isolate showed low solubilization at its isoelectric point which increased in alkaline solutions, until it reached 100% at pH 11.0. Besides, positive charges below the isoelectric point and negative ones above this point were found.

In solutions with a pH lower than the isoelectric point, an attractive interaction between the soy protein isolate and high-methoxyl pectin was verified by analyzing the formation of complexes. These complexes were bigger for the systems with a higher protein proportion.

The complexes formed in pH 3.5, in the different ratios, have potential application in the food industry, for example, as emulsifiers, foam stabilizers, fat replacers or being used in encapsulation.

5. Acknowledgments

The authors acknowledge Sao Paulo Research Foundation, FAPESP (Grant n° 2014/08520-6, 2013/10842-9 and 2014/02910-7) and Coordination for the Improvement of Higher Level Personnel, CAPES.

6. References

1. Tömösközi, S., Lásztity, R., Haraszi, R., & Baticz, O. (2001). Isolation and study of the functional properties of pea proteins. *Nahrung*, 45(6), 399-

401. doi:10.1002/1521-3803(20011001)45:6<399::AID-FOOD399>3.0.CO;2-0.

2. Lam, M., Paulsen, P., & Corredig, M. (2008). Interactions of soy protein fractions with high-methoxyl pectin. *Journal of Agricultural and Food Chemistry*, 56(1), 4726–4735. doi:10.1021/jf073375d.

3. Canteri, M. H. H., Moreno, L., Wosiacki, G., & Scherr, A. P. (2012). Pectina: da matéria-prima ao produto final. *Polímeros*, 22(2), 149-157. http://dx.doi.org/10.1590/S0104-14282012005000024.

4. Santos, M. S., Petkowicz, C. L. O., Haminiuk, C. W. I., & Cândido, L. M. B. (2010). Polissacarídeos extraídos da gabiroba (*Campomanesia xanthocarpa* Berg): propriedades químicas e perfil reológico. *Polímeros*, 20, 352-358. http://dx.doi.org/10.1590/S0104-14282010005000056.

5. Tromp, R. H., de Kruif, C. G., van Eijk, M., & Rolin, C. (2004). On the mechanism of stabilization of acidified milk drinks by pectin. *Food Hydrocolloids*, 18(1), 565–572. doi:10.1016/j.foodhyd.2003.09.005.

6. Lam, M., Shen, R., Paulsen, P., & Corredig, M. (2007). Pectin stabilization of soy protein isolates at low pH. *Food Research International*, 40(1), 101-110. doi:10.1016/j.foodres.2006.08.004.

7. Dong, D., Li, X., Hua, Y., Chen, Y., Kong, X., Zhang, C., & Wang, Q. (2015). Mutual titration of soy proteins and gum arabic and the complexing behavior studied by isothermal titration calorimetry, turbidity and ternary phase boundaries. *Food Hydrocolloids*, 46(1), 28-36. doi:10.1016/j.foodhyd.2014.11.019.

8. Jaramillo, D. P., Roberts, R. F., & Coupland, J. N. (2011). Effect of pH on the properties of soy protein-pectin complexes. *Food Research International*, 44(1), 911-916. doi:10.1016/j.foodres.2011.01.057.

9. Serfert, Y., Schroder, J., Mescher, A., Laackmann, J., Ratzke, K., Shaikh, M. Q., Gaukel, V., Moritz, H. U., Schuchmann, H. P., Walzel, P., Drusch, S., & Schwarz, K. (2013). Spray drying behavior and functionality of emulsions with β-lactoglobulin/pectin interfacial complexes. *Food Hydrocolloids*, 31(1), 438-445. doi:10.1016/j.foodhyd.2012.11.037.

10. Mattison, K. W., Brittain, I. J., & Dubin, P. L. (1995). Protein-polyelectrolyte phase boundaries. *Biotechnology Progress*, 11(1), 632-637. doi:10.1021/bp00036a005.

11. Mattison, K. W., Wang, Y., Grymonpré, K., & Dubin, P. L. (1999). Micro and macro-phase behaviour in protein-polyelectrolytes systems. *Macromolecular Symposia*, 140(1), 53-76. doi:10.1002/masy.19991400107.

12. Marfil, P. H. M. (2014). *Microencapsulação de óleo de palma por coacervação complexa em matrizes de gelatina/goma arábica e gelatina/alginato* (Doctoral thesis). Universidade Estadual Paulista “Julio de Mesquita Filho”, São José do Rio Preto, São Paulo, Brazil.

13. Cano-Chauca, M., Stringheta, P. C., Ramos, A. M., & Cal-Vidal, J. (2005) Effect of the carriers on the microstructure of mango powder obtained by spray drying and its functional characterization. *Innovative Food Science & Emerging Technologies*, 6(1), 420-428. doi:10.1016/j.ifset.2005.05.003.

14. Perrechil, F. A., & Cunha, R. L. (2013). Stabilization of multilayered emulsions by sodium caseinate and κ-carrageenan. *Food Hydrocolloids*, 30(1), 606-613. doi:10.1016/j.foodhyd.2012.08.006.

15. Antonov, Y. A., & Zubova, O. M. (2001). Phase state of aqueous gelatin–polysaccharide (1)–polysaccharide (2) systems. *International Journal of Biological Macromolecules*, 29(1), 67-71. doi:10.1016/S0141-8130(01)00140-4.

16. Renkema, J. M. S., Gruppen, H., & Van Vliet, T. (2002). Influence of pH and ionic strength on heat-induced formation and rheological properties of soy protein gels in relation to denaturation and their protein compositions. *Journal of Agricultural and Food Chemistry*, 50(1), 6064-6071. doi:10.1021/jf020061b.

17. Malhotra, A., & Coupland, J. N. (2004). The effect of surfactants on the solubility, zeta potential, and viscosity of soy protein isolates. *Food Hydrocolloids*, 18(1), 101−108. doi:10.1016/S0268-005X(03)00047-X.

18. Rocha, G. O., Farias, M. G., Carvalho, C. W. P., Ascheri, J. L. R., & Galdeano, M. C. (2014). Filmes compostos biodegradáveis a base de amido de mandioca e proteína de soja. *Polímeros*, 24(5), 587-595. http://dx.doi.org/10.1590/0104-1428.1355.

19. Harnsilawat, T., Pongsawatmanit, R., & McClements, D. J. (2006). Characterization of β-lactoglobulin–sodium alginate interactions in aqueous solutions: A calorimetry, light scattering, electrophoretic mobility and solubility study. *Food Hydrocolloids*, 20(1), 577-585. doi:10.1016/j.foodhyd.2005.05.005.

20. Jasentuliyana, N., Toma, R. B., Klavons, J. A., & Medora, N. (1998). Beverage cloud stability with isolated soy protein. *Journal of the Science of Food and Agriculture*, 78(1), 389-394. doi:10.1002/(SICI)1097-0010(199811)78:3<389::AID-JSFA130>3.0.CO;2-Z.

21. Albano, K. M., & Telis, V. R. N. (2015). Rheological investigation of ultrasound effect on interactions between soy protein isolate and pectin. In: *VII Brazilian Conference on Rheology* (pp. 22-25). Curitiba: Universidade Tecnológica Federal do Paraná.

CAPÍTULO 3

Características de qualidade e comportamento térmico do óleo de buriti (*Mauritia flexuosa*)

O estudo do óleo de buriti está publicado como artigo original no periódico Grasas y Aceites, v. 68, n. 4, p. 220-228, 2017.

Quality characteristics and thermal behavior of buriti (*Mauritia flexuosa*) oil

M.L.F. Freitas[a]✉, R.C. Chisté[b], T.C. Polachini[a], L.A.C.Z. Sardella[a], C.P.M. Aranha[c], A.P.B. Ribeiro[d] , V.R. Nicoletti[a]

[a]*São Paulo State University (UNESP), Institute of Biosciences, Humanities and Exact Sciences (IBILCE), Campus São José do Rio Preto, 2265 Cristóvão Colombo Street, Jardim Nazareth, São José do Rio Preto, São Paulo, 15.054-000, Brazil.*

[b]*Faculty of Food Engineering (FEA), Institute of Technology (ITEC), Federal University of Pará (UFPA), 66075-110, Belém, Pará, Brazil.*

[c]*School of Engineering (FAEN), Federal University of Grande Dourados (UFGD), Dourados-Itahum Road Km 12, Cidade Universitária, Dourados, Mato Grosso do Sul, 79.804-970, Brazil.*

[d]*Department of Food Technology (DTA), School of Food Engineering (FEA), University of Campinas (UNICAMP), Bertrand Russel Street, Cidade Universitária, Campinas, São Paulo, 13.083-970, Brazil.*

✉Corresponding author: mirianlfreitas@yahoo.com.br

SUMMARY: This work reports a complete characterization of buriti oil. Physicochemical properties were carried out according to AOCS methodologies and thermophysical properties were measured using a controlled stress rheometer and a digital electronic density meter. β-carotene and tocopherol contents were obtained using HPLC systems. Fatty acids and acylglycerol classes were determined using GC and HPSEC systems, respectively, while triacylglycerol composition was estimated using the software PrOleos. Thermal behavior (crystallization and melting) was analyzed using a DSC. The results attested high levels of total carotenoids with β-carotene as the major one, total tocopherols with α and β-tocopherols accounting for 91% of total, and monounsaturated fatty acids mainly represented by oleic acid. It resulted in close agreement between

density and viscosity of buriti and olive oils. The crystallization and melting peaks occurred at -43.06 °C and -2.73 °C, respectively. These properties enable Buriti oil to be recommended as an excellent alternative for enriching foods with bioactive compounds.

KEYWORDS*: Carotenoids; β-carotene; Monounsaturated fatty acid; Oleic acid; Tocopherols; Triunsaturated triacylglycerols*

ORCID: Freitas MLF http://orcid.org/0000-0003-3172-6122, Chisté RC http://orcid.org/0000-0002-4549-3297, Polachini TC http://orcid.org/0000-0002-5012-6416, Sardella LACZ http://orcid.org/0000-0002-4419-2425, Aranha CPM http://orcid.org/0000-0002-6129-6218, Ribeiro APB http://orcid.org/0000-0002-6532-1265, Nicoletti VR http://orcid.org/0000-0002-2553-4629

1. INTRODUCTION

The Arecaceae family native palm trees are one of the most important plant resources in the Amazon region. Their fruits are a source of high-quality vegetable oils being not only alternative foods to the local population, but constituting important sources of oils and fats with potential applications in food, pharmaceutical, cosmetic and other industries (Santos *et al.*, 2013). Due to their chemical composition, the oils obtained from these palm trees are considered as new sources of high-added-value phytochemicals (Santos *et al.*, 2015).

Buriti (*Mauritia flexuosa*) is one of the Amazon native palms, belonging to the Arecaceae family, and it is a long-lived, single-stemmed, dioecious palm that can reach 30–40 m in height. It usually grows in permanent or periodically flooded areas along rivers, forests and savannas in northern-central Brazil, where it plays a major role in ecology, economics, and culture throughout most areas of its occurrence. Its fruit has a hard, scaly red bark that covers a soft and oily pulp; its color varies from dark yellow to reddish after complete ripeness. Extraction by cold pressing yields about 45 kg of buriti oil from 1000 kg of ripe fruits, which is considered as an Amazonian resource for cosmetic, food and pharmaceutical purposes (Albuquerque *et al.*, 2005; Silva *et al.*, 2009; Speranza *et al.*, 2016; Virapongse *et al.*, 2017).

Oils are complex mixtures containing a wide range of compounds. Apart from the major class of triacylglycerols, the unsaponifiable fraction is constituted by different groups of components, such as hydrocarbons, waxes, sterols, tocopherols and carotenoids. A complete characterization of the unsaponifiable fraction is of great interest, since the nutritional value of edible oils depends on the content and composition of biologically active compounds present in this oil fraction (Santos *et al.*, 2013). Additionaly, the characterization of oils is of big interest to predict thermophysical properties, such as density and rheological parameters (Santos *et al.*, 2005). The

specific composition of different oils makes the physical properties determination essential to provide a well-designed processing (Steffe, 1996).

Buriti oil is an important source of energy and vitamins has some similarities to palm oil, such as the reddish-yellow color and flavor (Pardauil *et al.*, 2017; Pesce *et al.*, 2009). However, buriti oil presents a high concentration of monounsaturated fatty acids, with values higher than those found in olive oil or in Brazil nuts, which are foods known to their oil with high nutritional quality due to the monounsaturated fatty acid properties of reducing blood total and LDL-cholesterol (França *et al.*, 1999; Silva *et al.*, 2009). In addition, the low concentration of polyunsaturated fatty acids gives buriti oil a high oxidative stability (Silva *et al.*, 2009). Buriti oil contains β-carotene in higher concentrations than foods widely consumed by Brazilians, such as guava, pitanga, papaya, passion fruit, carrots and other fruits from the Amazon region, including palm nuts, peach palm and tucumã (Rodriguez-Amaya, 1996; De Rosso and Mercadante, 2007). Additionally, buriti oil also presents high levels of tocopherols indicating it as a reliable source of antioxidant compounds (Bataglion *et al.*, 2015).

Carotenoids are a diversified group of lipophilic components, and β-carotene is a provitamin A compound with 100% of theoretical activity (Rodriguez-Amaya, 1996; McClements *et al.*, 2007). The prevention of cancer, heart disease and macular degeneration are among the beneficial health effects that are attributed to carotenoids due to their association with an antioxidant activity (Alquezar *et al.*, 2008; Meléndez-Martínez *et al.*, 2007). Tocopherols are important antioxidants and present vitamin E activity, especially α-tocopherol (De Greyt and Kellens, 2005).

Considering the buriti oil has high nutritional value and the growing interest of consumers for healthier products, its use in food industry could be interesting (Bovi *et al.*, 2017). In this context, this work aimed to carry out a complete characterization of buriti oil, including its physicochemical and thermophysical properties, β-carotene and tocopherols contents, fatty acids

and acylglycerol classes, as well as its thermal behavior (crystallization and melting).

2. MATERIALS AND METHODS

2.1. Chemicals

Hexane, acetonitrile, trimethylamine, methanol, ethyl acetate, isopropanol and tetrahydrofuran HPLC grade were obtained from Dinâmica (Diadema, Brazil), J. T. Baker (Phillipsburg, USA) or Vetec (Rio de Janeiro, Brazil). The samples and solvents were filtered through Millipore (Billerica, USA) membranes (0.22 and 0.45 µm) prior to HPLC analysis. Sodium hydroxide, potassium hydroxide, methanol, petroleum ether, ethyl ether analytical grade were obtained from Labsynth (Diadema, Brazil) or Dinâmica (Diadema, Brazil). Standards of β-carotene and tocopherols were obtained from Sigma-Aldrich (St. Louis, USA).

2.2. Buriti Oil

Six litres of crude buriti oil (Amazon Oil^{TM}) were obtained in Ananindeua city, Pará state, in the Brazilian Amazonian region and stored at -30 °C until analysis.

The buriti oil characterization was carried out by physicochemical analyses, thermophysical properties, β-carotene and tocopherols contents, fatty acids and acylglycerol classes and thermal analyses (crystallization and melting).

2.3. Physicochemical Analyses

The physicochemical characteristics of buriti oil were assessed by the determination of free acidity (expressed in equivalent of oleic acid) and peroxide, iodine, saponification and refractive indexes, according to AOCS (2009). All the analyses were carried out in triplicate.

2.4. Thermophysical Properties Determination

Rheology and density of crude buriti oil were investigated in triplicate at 25 ºC.

Rheology

A controlled stress rheometer, model ARG2 (TA Instruments, New Castle, USA), was used to carry out steady state flows with cone-plate geometry (52 µm gap). The shear rate varied from 0.1 s-1 to 500 s-1, and the mean shear stress was acquired through the data acquisition system. Then, the resulting rheograms were fitted to Newton model to provide the viscosity value.

Density

The density was determined using a digital electronic density meter (model DMA 4500-M, Anton Paar, Austria), in which approximately 10 mL of crude buriti oil was used for each run. After establishing the temperature, the density values were provided by the equipment.

2.5. Determination of Carotenoids and Tocopherols in Buriti Oil

Carotenoids

The content of β-carotene in buriti oil was determined by high performance liquid chromatography coupled to diode array detector (HPLC-DAD). Before the injection into the HPLC system, the crude buriti oil was submitted to saponification in 10% KOH in methanol for 14-16 hours, followed by a liquid-liquid partition using petroleum ether:ethyl ether (1:1, v/v) and the alkali was removed by washing with destiled water (De Rosso and Mercadante, 2007). The carotenoid extract was injected into a Shimadzu HPLC (Kyoto, Japan) equipped with quaternary pumps (LC-20AT) with a 10 µL loop, on-line degasser, auto sampler (SIL-20A) and a DAD detector (SPD-M20A). The compounds were separated on a C18 Shim-pack VP-ODS column (250 mm x 4.6 µm) using, as a mobile phase,

a linear gradiente of acetonitrile (0.05% triethylamine):methanol:ethyl acetate from 60:20:20 to 60:0:40 in 43 minutes and maintaining this proportion for 17 min. The flow rate was 1 mL/min, the column temperature was set at 29 °C and the chromatograms were processed at 450 nm (Silva *et al.*, 2014). The β-carotene was identified according to the following combined information: elution order on C18 column, co-chromatography with authentic standard, and UV–Vis spectrum [λ_{max}, spectral fine structure (%III/II), peak *cis* intensity (%AB/AII)] compared with the data available in the literature (De Rosso and Mercadante, 2007). The β-carotene was quantified (in triplicate) by HPLC-DAD, using external seven-point analytical curves (in duplicate) with all-*trans*-β-carotene standard (0.547–35.0 µg/mL). Total carotenoids were considered as the sum of the carotenoid peak areas in the chromatogram obtained.

Tocopherols

The tocopherol profile and total tocopherol in buriti oil was carried out according to AOCS Ce 8-89 methodology (AOCS, 2009), using the high performance liquid chromatography coupled to fluorescence detector. Before the injection into the HPLC system, the crude buriti oil was solubilized in hexane (1% w/v). The samples were injected into a Perkin Elmer SERIES 2000 HPLC, under the following chromatographic conditions: isocratic pump Perkin Elmer 250; fluorescence detector Shimadzu RF-10 AXL with excitation-290 nm and emission-330 nm; Merck analytical column 250 x 4 mm Li Chrosorb Si 60*5µm coupled to compatible guard column; mobile phase: 99:1 hexane/isopropanol (filtered and degased for 10 minutes in an ultrasonic bath), flow 1.0 mL/min; injected volume of 20.0 µL. The individual tocopherols were identified by elution order on analytical column compared with external authentic standards and quantified (in triplicate) using external analytical curves with authentic standards. Total tocopherols were considered as the sum of the individual tocopherol concentration.

2.6. Fatty Acids Composition and Acylglycerol Classes

The fatty acid composition was performed on a gas chromatograph with capillary column - CGC Agilent 6850 Series GC System, after esterification using the Hartman and Lago (1973) method. The fatty acid methyl esters were separated according to the AOCS Ce 1-62 method (AOCS, 2009) on capillary column DB-23 Agilent (50% cyanopropyl-methylpolysiloxane) with dimensions: 60 m, φ int: 0.25 mm, 0.25 μm film. Oven temperature 110 °C-5 min, 110-215 °C (5 °C/min), 215 °C-24 min; detector temperature 280 °C; injector temperature 250 °C; helium drag gas; split ratio 1:50; injected volume of 1.0 μL. The qualitative composition was determined by comparing peak retention times with those of respective fatty acid standards. Mustard oil was used as standard. The quantitative composition was determined by the peak percentage area.

The buriti oil acylglycerol classes were determined by high performance size exclusion chromatography (HPSEC) using liquid chromatograph Pelkin Elmer Series 200; refractive index detector Waters 2414; two columns, being 1 - JORDI GEL DVB 300 x 7.8 mm, 500 Å and 2 - JORDI GEL DVB 300 x 7.8 mm, 100 Å; mobile phase tetrahydrofuran; flow rate 1 mL/min; injected volume 20.0 μL. The sample was solubilized in tetrahydrofuran at 1.0% concentration. The acylglycerols separation mechanism by the HPSEC technique occurs through the molecular size difference among compounds present in reaction enviroment. In this case, the elution order is triacylglycerols, diacylglycerols, monoacylglycerols and free fatty acids.

2.7. Triacylglycerol Composition and Triacylglycerol Classes

The buriti oil triacylglycerol composition was estimated using the software PrOleos, based on the hypothesis of 1,3-random-2-random distribution, which predicts triacylglycerols molar percentage present in vegetable oils, from the fatty acid composition (Antoniosi Filho *et al.*, 1995). This software is available in the plataform

“https://lames.quimica.ufg.br/p/4035-material-didatico”. The triacylglycerol classes were estimated by triacylglycerol composition.

2.8. Crystallization and Melting

Thermal analysis for buriti oil crystallization and melting behavior was performed by differential scanning calorimetry using DSC 8000 (Pyris Series, Perkin Elmer) at 80 °C for 10 min, 80 at -80 °C (5 °C/min), -80 °C for 10 min, -80 to 80 °C (5 °C/min).

3. RESULTS AND DISCUSSION

3.1. Physicochemical and Thermophysical Analyses

The buriti oil used was crude, and due to this fact a higher percentage of free fatty acids was observed (Table 1) compared to refined oils. For example, Ribeiro *et al.* (2009) reported 0.03% FFA for refined soybean oil. The peroxide index is related to the oil oxidative state and not to its characterization itself. Santos *et al.* (2013) found 7.4 meq O_2/kg for buriti oil and reported this value within expected ranges for crude oils of good quality. The saponification and iodine values are related only to specific characteristics of each vegetable oil, such as chain length and unsaturation number (Pardauil *et al.*, 2017). Both the iodine and saponification indexes found for buriti oil were similar to that found in the literature, being 73 g/100 g and 193 mg KOH/g, respectively (Lognay *et al.*, 1987). The refractive index found for buriti oil (Table 1) was the same previously reported by the literature (Albuquerque *et al.*, 2005; Silva *et al.*, 2009).

Table 1. Physicochemical and thermophysical characteristics of buriti oil

Oil characteristics	Results
Free acidity	3.99±0.01% FFA
Peroxide index	6.86±0.38 meq O_2/kg
Iodine index	76 g/100 g
Saponification index	193 mgKOH/g
Refractive index (25 °C)	1.46±0.01
Viscosity	66.01 mPa·s
Density	909.33±0.01 kg/m³

With respect to rheology, buriti oil showed Newtonian behavior as expected in the literature for oils (Steffe, 1996). It was characterized by the linear dependence between shear rate and shear stress with R^2>0.9999 and null intercept. Newtonian viscosity presented close values to the ones published by Santos *et al.* (2005) for different vegetable oils. In the same way, viscosity of buriti oil was comparable to the values found by Ribeiro *et al.* (2017) for different commercial olive oils. These olive oils had a very similar fatty acid composition to buriti oil, which also resulted in close agreement between buriti and olive oil densities. Besides being an indicative of degradation, such properties are useful for the correct design of oil pumping, settling and filtration (Bonnet *et al.*, 2011).

3.2. β-carotene and Tocopherol Contents

Buriti oil presented high contents of carotenoids (686.89 mg/kg), with β-carotene as the major compound, accounting for 74% of total carotenoids (506.84 mg/kg), which imparts the oil orange-red color. Godoy and Rodriguez-Amaya (1994) emphasize that buriti is a very important provitamin A source, since its content in β-carotene is much higher than that found in most of Brazilian fruits. Crude palm oil shows total carotenoids of 608.39 mg/kg (Ferreira *et al.*, 2006), which is similar to the crude buriti oil in our study. In addition, natural sources of this carotene are of great interest

because only 2% of commercial β-carotene is naturally produced (Dufossé *et al.*, 2005; Ribeiro *et al.*, 2011; Speranza *et al.*, 2016).

Buriti crude oil was reported with a high amount of total carotenoids by Lognay *et al.* (1987) (1730 mg/kg), Albuquerque *et al.* (2005) (1707 mg/kg) and Silva *et al.* (2009) (1003 mg/kg) being the β-carotene the principal component.

De Rosso and Mercadante (2007) reported the identification and quantification of carotenoids in buriti pulp by HPLC-DAD using C_{30} column and coupled to mass spectrometer (APCI ionization source), and presented β-carotene as the major carotenoid (72%), followed by 13-*cis*-β-carotene (12%), 9-*cis*-β-carotene (3.6%), γ-carotene (2.9%) and *cis*-γ-carotene (1.9%) and a total carotenoid content of 513.87 mg/kg. Santos *et al.* (2015) investigated the carotenoid composition in buriti oil by HPLC-DAD. The authors reported total carotenoid content of 540.81 mg/kg with β-carotene being the principal carotenoid (55%), followed by *cis*-β-carotene (31%), lutein (6%) and *cis*-lutein (3%).

Although in our study other carotenoid peaks were observed in the chromatogram of crude buriti oil sample, it was not possible to perform the identification by the HPLC-DAD analysis, since *cis* and *trans* isomer separation were not efficient and the *cis* peaks were present at very low intensity. In the chromatogram (Figure 1) it is possible to notice the carotene peaks and β-carotene peak with the biggest area.

Figure 1. Chromatogram (processed at 450 nm), obtained by HPLC-DAD, of carotenoids from buriti oil.

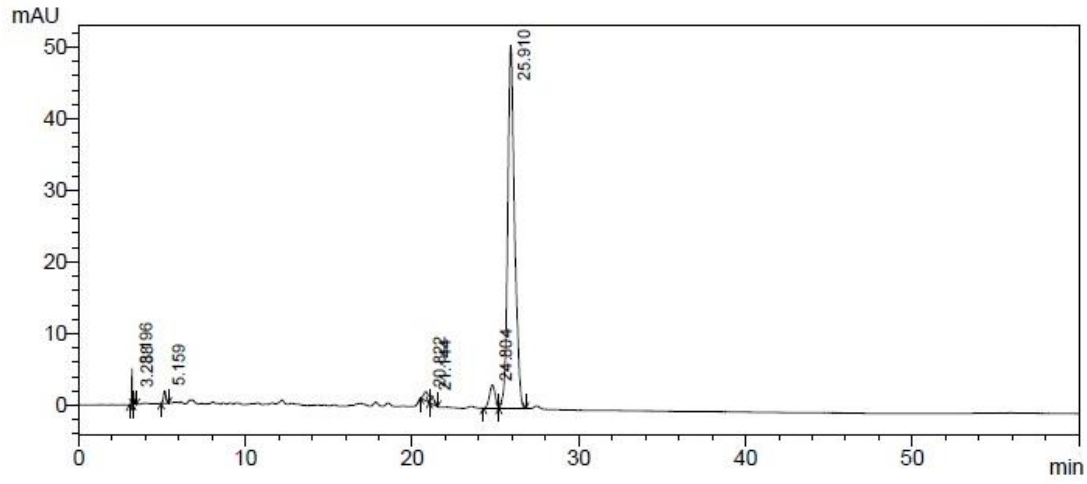

Concerning the tocopherol profile, which can be seen in Table 2, buriti oil presented a content of total tocopherol of 104.14 mg/100 g. The principal tocopherol was β-tocopherol (48%) followed by α-tocopherol (43%), in this way, they were presented in similar amount and represented 91% of total tocopherols.

Table 2. Tocopherol profile of buriti oil

Tocopherol	Content (mg/100 g)	% total tocopherol
α-tocopherol	44.89±7.84	43.11
β-tocopherol	50.13±7.42	48.13
γ-tocopherol	3.63±0.59	3.49
δ-tocopherol	5.49±0.74	5.27
Total	104.14±0.01	

Lognay *et al.* (1987) and Albuquerque *et al.* (2005) reported similar values for total tocopherols, but Lognay *et al.* (1987) presented the α-tocopherol as the major component (48.1%) while (β + γ)-tocopherol represented 48.3%. Silva *et al.* (2009) and Santos *et al.* (2013) reported

high values for total tocopherols, being 152 mg/100g and 156.7 mg/100 g, respectively. While Silva *et al.* (2009) presented β-tocopherol as the major component (45%) followed by α-tocopherol (40%), Santos *et al.* (2013) presented α-tocopherol as the major component (70%) followed by β-tocopherol (30%). These results reforced that buriti oil has a promising potential as a dietary source due to its high vitamin E content (Santos *et al.*, 2013). Such difference in reported values of unsaponified matter might be due to fact that the composition and, consequently, the nutritional value of crude buriti oil vary with the variability and/or ripening stage, the region of provenance and extraction process (Santos *et al.*, 2015; Silva *et al.*, 2009).

3.3. Fatty Acid Composition and Acylglycerol Classes

Buriti oil presented higher levels of unsaturated fatty acids than saturated fatty acids, being oleic acid the main fatty acid in buriti oil (69.58%) followed by palmitic acid (17.35%) (Table 3). Similar compositions were also related by other authors (Escriche *et al.* 1999; Albuquerque *et al.*, 2005; Silva *et al.*, 2009; Bataglion *et al.*, 2015).

Table 3. Composition of fatty acids of buriti oil

Fatty acids		Mean (%)
C12:0	Lauric acid	0.06±0.02
C14:0	Myristic acid	0.11±0.02
C15:0	Pentadecanoic acid	0.06±0.03
C16:0	Palmitic acid	17.35±0.07
C16:1	Palmitoleic acid	0.24±0.01
C17:0	Margaric acid	0.09±0.01
C17:1	Heptadecenoic acid	0.07±0.01
C18:0	Stearic acid	3.32±0.02
C18:1	Oleic acid	69.58±0.15
C18:2	Linoleic acid	7.31±0.02
C18:3	Linolenic acid	0.98±0.01
C20:0	Arachidic acid	0.20±0.01
C20:1	Gadoleic acid	0.45±0.01
C22:0	Behenic acid	0.07±0.01
C24:0	Lignoceric acid	0.11±0.04
	Saturated	21.37±0.17
	Unsaturated	78.63±0.17

The profile of fatty acids found in buriti oil revealed a good source of monounsaturated fatty acids. According to Speranza *et al.* (2016), a great interest has been placed in oils that contain these fatty acids. High oleic and low linoleic fatty acid contents help to make them more resistant to oxidation than most oils.

From the point of view of nutritional and food industry, in general, oleic acid is the most abundant omega-9 fatty acid in food and one of the most commonly fatty acids found in nature. It is monounsaturated, considered fundamental for beneficial properties in reduction of LDL-cholesterol oxidation, besides being a precursor for the production of most

of other polyunsaturated fatty acids and hormones (Syed, 2012; Watkins and German, 2008; Angelis, 2001).

Regarding the acylglycerol classes, the most abundant compounds are triacylglycerols (88%) (Table 4). Such result was similar to that reported in the literature, which follows: 92.6% of triaclylglycerols and the content of diacylglycerols, monoacylglycerols and free fatty acids being about 5% for buriti crude oil (Lognay *et al.*, 1987).

Table 4. Acylglycerol classes in buriti oil composition

Acylglycerol classes	Mean (% total lipids)
Triacylglycerols	88.33±1.16
Diacylglycerols	8.02±0.74
Monoacylglycerols + Free fatty acids	3.65±0.42

3.4. Triacylglycerol Composition and Triacylglycerol Classes

The predominant triacylglycerols were OOO, POO, OLO and POP representing 80.12% of total (Table 5). It was observed that the composition of triacylglycerol in buriti oil was extremely homogeneous, considering the low fatty acid variability of this matrix, given the high contents in oleic and palmitic acids followed by linoleic acid. This fact also justifies the large percentage of triunsaturated (U_3) and diunsaturated (SU_2) triacylglycerols in the buriti oil composition by triacylglycerol classes (Table 6).

Table 5. Triacylglycerol composition of buriti oil

Triacylglycerol		% (normalized)
C48:0	PPP	0.55±0.01
C50:1	POP	6.54±0.06
C50:2	PLP	1.03±0.04
C52:1	POS	2.53±0.02
C52:2	POO	26.41±0.06
C52:3	PLO	5.89±0.01
C52:4	PLnO	1.10±0.01
C54:2	SOO	5.37±0.02
C54:3	OOO	35.99±0.15
C54:4	OLO	11.20±0.05
C54:5	OLnO	2.64±0.01
C56:3	OGaO	0.75±0.01

P = palmitic acid, O = oleic acid, L = linoleic acid, S = stearic acid, Ln = linolenic acid, Ga = gadoleic acid.

Table 6. Triacylglycerol classes in the buriti oil composition

Triacylglycerol classes	%
S_3 (SSS)	0.55±0.01
S_2U (SUS)	10.10±0.12
SU_2 (SUU)	38.77±0.08
U_3 (UUU)	50.58±0.20

S = saturated acylglycerol, U = unsaturated acylglycerol.

Santos *et al.* (2013) carried out the buriti oil triacylglycerol profile by HPCL reporting results for OOO (39.8%), POO+PLS (35.9%) and POP (10.2%) and by GC reporting results for OOO (35.6%), POO (38.8%) and POP (9.4%). These similar results could confirm the good accuracy of the

PrOleos software, in which, Speranza *et al.* (2016) obtained a similar triacylglycerol profile for buriti oil.

Antoniosi Filho (1995) and Lognay *et al.* (1987) also found that OOO, POO and POP were the predominant triacylglycerols in the buriti oil analized, but they have not observed OLO as one of the predominant ones, reporting that it has corresponded to 1.1 and 1.8% of total triacylglycerols, respectively.

3.5. Crystallization and Melting

The crystallization temperature range was observed between -58.54 and 1.16 °C, the peak being -43.06 °C. In turn, the melting temperature range was observed between -24.51 and 18.52 °C, the peak being -2.73 °C. The crystallization and melting curves might be seen in Figure 2.

Figure 2. Thermogram of buriti oil with melting curve (above) and crystallization curve (below).

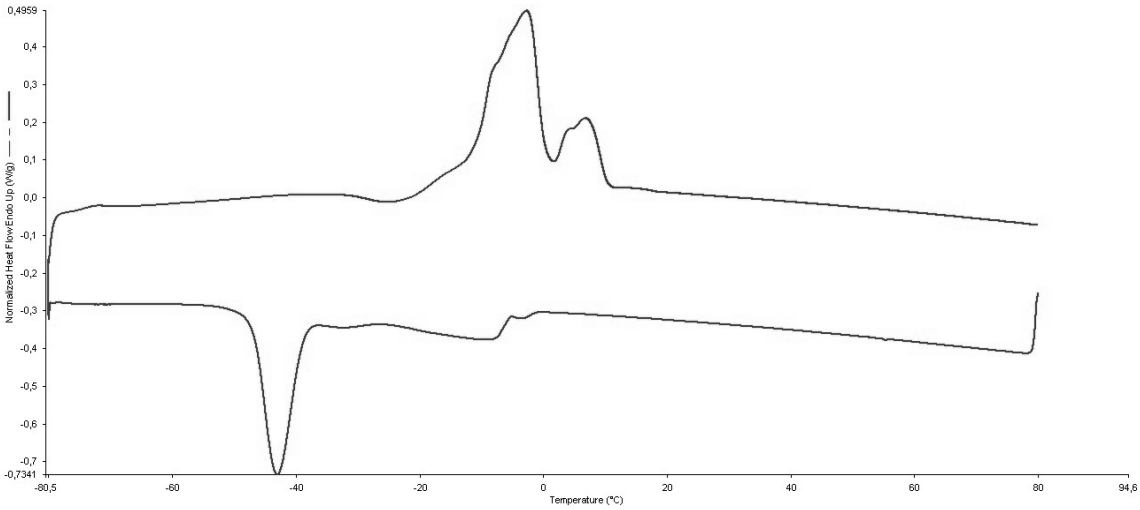

Because buriti oil is a mixture of triacylglycerols, crystallization and melting are observed in a temperature range, but not at a specific temperature. This is due to the fact that triunsaturated triacylglycerols present crystallization and melting point different from diunsaturated,

monounsaturated and trisaturated triacylglycerols, as a consequence of the different degrees of unsaturation.

It is interesting to notice that the crystallization range did not coincide with the melting range, which is a common behavior in oils as a result of the different triacylglycerol arrangements when oil is liquid or solidified.

Buriti oil has approximately 90% of triunsaturated and diunsaturated triacylglycerols, and these have lower crystallization points than monounsaturated and trisaturated ones. When oil is liquid and the temperature is gradually reduced, monounsaturated and trisaturated triacylglycerols are cristalized before the diunsaturated and triunsaturated and these last ones crystallize at a lower temperature. This behavior justifies a low crystallization temperature range.

On the other hand, when buriti oil is solidified, triacylglycerols are arranged in a more organized way, which makes the melting range higher than the crystallization and melting transitions of highly polyunsaturated fatty acids followed by melting of monounsaturated fatty acids and a small fraction of saturated fatty acids (Pardauil *et al.*, 2017). Pardauil *et al.* (2017) reported a similar crystallization curve and according to these authors and Tan and Che Man (2000), crystallization curves are reproducible and simpler than melting curves due to the oil crystallization being influenced only by chemical composition and not by initial crystalline state which is a consequence of the polymorphism phenomena of natural oils, and this cannot be established unequivocally by DSC measurements.

Crystallization and melting curves also depend on fatty acid composition. Usually, oil samples with a high degree of saturation showed higher temperatures of crystallization and melting profiles than the oils with a high degree of unsaturation (Pardauil *et al.*, 2017).

The triunsaturated triacylglycerols, prevalent in buriti oil, present melting points from −14 to 1 °C and they are important for the softness and lubricity of products at room temperature. In addition, the diunsaturated triacylglycerols, with melting points from 1 to 23 °C, are important for the

sensory textural properties and mechanical-performance of products at room temperature (O'Brien, 2009; Rodrigues and Gioielli, 2003; Bessler and Orthoefer, 1983; Speranza *et al.*, 2016).

4. CONCLUSIONS

Concerning the presented results, the buriti oil characterization attested its high quality due to high levels of carotenoids and tocopherol, with β-carotene and β-tocopherol being the principal ones in their classes, and monounsaturated fatty acids with oleic acid as the major. In this way, crude buriti oil demonstrated a high potential to be used as a bioactive ingredient for foodstuff. Furthermore, its physicochemical and thermophysical characterization is usable for developing promising products and designing new processes.

ABBREVIATIONS AND NOMENCLATURE

FFA: free fatty acids
P: palmitic acid
O: oleic acid
L: linoleic acid
S: stearic acid
Ln: linolenic acid
Ga: gadoleic acid
S: saturated acylglycerol
U: unsaturated acylglycerol

ACKNOWLEDGMENTS

The authors acknowledge Sao Paulo Research Foundation, FAPESP, Brazil, (grant numbers 2014/08520-6 and 2014/02910-7) and Coordination for the Improvement of Higher Level Personnel, CAPES, Brazil.

REFERENCES

Albuquerque MLS, Guedes I, Alcantara JP, Moreira SGC, Barbosa Neto NM, Correa DS, Zilio SC. 2005. Characterization of buriti (*Mauritia flexuosa* L.) oil by absorption and emission spectroscopies. *J. Braz. Chem. Soc.* **16**(6A), 1113-1117. http://dx.doi.org/10.1590/S0103-50532005000700004

Alquezar B, Rodrigo MJ, Zacarías L. 2008. Regulation of carotenoid biosynthesis during fruit maturation in the red-fleshed orange mutant Cara Cara. *Phytochemistry* **69**(10), 1997-2007. https://doi.org/10.1016/j.phytochem.2008.04.020

Angelis RC. 2001. Novos conceitos em nutrição. Reflexões a respeito do elo dieta e saúde. *Arq. Gastroenterol.* **38**(4), 269-271. http://dx.doi.org/10.1590/S0004-28032001000400010

Antoniosi Filho NR. 1995. *Análise de óleos e gorduras vegetais utilizando métodos cromatográficos de alta resolução e métodos computacionais.* Tese de doutorado. Universidade de São Paulo, 340p.

Antoniosi Filho NR, Mendes OL, Lanças FM. 1995. Computer prediction of triacylglycerol composition of vegetable oils by HRGC. *Chromatographia* **40**(9), 557–562. http://dx.doi.org/10.1007/BF02290268

AOCS. American Oil Chemists' Society. 2009. *Official Methods and Recommended Practices of the American Oil Chemists' Society*. 6ed, AOCS Press, Champaign.

Bataglion GA, Silva FMA, Santos JM, Barcia MT, Godoy HT, Eberlin MN, Koolen HHF. 2015. Integrative approach using GC-MS and Easy Ambient Sonic-Spray Ionization Mass Spectrometry (EASI-MS) for comprehensive

lipid characterization of buriti (*Mauritia flexuosa*) oil. *J. Braz. Chem. Soc.* **26**(1), 171-177. http://dx.doi.org/10.5935/0103-5053.20140234

Bessler TR, Orthoefer FT. 1983. Providing lubricity in food fat systems. *J. Am. Oil Chem. Soc.* **60**, 1765–1768. http://dx.doi.org/10.1007/BF02680351

Bovi GG, Petrus RR, Pinho SC. 2017. Feasibility of incorporating buriti (*Mauritia flexuosa* L.) oil nanoemulsions in isotonic sports drink. *Int. J. Food Sci. Tech.* in press. http://dx.doi:10.1111/ijfs.13499

Bonnet JP, Devesvre L, Artaud J, Moulin P. 2011. Dynamic viscosity of olive oil as a function of composition and temperature: A first approach. *Eur. J. Lipid Sci. Technol.* **113**, 1019–1025. http://dx.doi.org/10.1002/ejlt.201000363

De Rosso VV, Mercadante AZ. 2007. Identification and quantification of carotenoids, by HPLC-PDA-MS/MS, from amazonian fruits. *J. Agric. Food Chem.* **55**, 5062-5072. http://dx.doi.org/10.1021/jf0705421

De Greyt WD, Kellens M. 2005. Deodorization, in Shahidi F (Ed.) *Bailey's Industrial Oil & Fat Products* 6ªed, v.5. John Wiley & Son, New York, 341-383. http://dx.doi.org/10.1002/047167849X

Dufossé L, Galaup P, Yaron A, Arad SM, Blanc P, Murthy KNC, Ravishankar GA. 2005. Microorganisms and microalgae as source of pigments for food use: A scientific oddity or an industrial reality? *Trends Food Sci. Technol.* **16**, 389–406. https://doi.org/10.1016/j.tifs.2005.02.006

Escriche I, Restrepo J, Serra JA, Herrera LF. 1999. Composition and nutritive value of Amazonian palm fruits. *Food Nutr. Bull.* **20**(3), 361-364. https://doi.org/10.1177/156482659902000314

Ferreira CD, Conceição EJL, Machado BAS, Hermes VS, Rios AO, Druzian JI, Nunes IL. 2016. Physicochemical characterization and oxidative stability of microencapsulated crude palm oil by spray drying. *Food Bioprocess Tech.* **9**, 124-136. https://doi.org/10.1007/s11947-015-1603-z

França LF, Reber G, Meireles MAA, Machado NT, Brunner G. 1999. Supercritical extraction of carotenoids and lipids from buriti (*Mauritia flexuosa*), a fruit from the Amazon region. *J. Supercrit. Fluids.* **14**, 247-256. https://doi.org/10.1016/S0896-8446(98)00122-3

Godoy HT, Rodriguez-Amaya DB. 1994. Occurrence of cis-isomers of provitamin A in Brazilian fruits. *J. Agric. Food Chem.* **42**, 1306-1313. https://doi.org/10.1021/jf00042a011

Hartman L, Lago RCA. 1973. Rapid preparation of fatty acid methyl esters from lipids. *Lab. Pract.* **22**(6), 475-476.

Lognay G, Trevejo E, Jordan E, Marlier M, Severin M, Ortiz de Zarate I. 1987. Investigaciones sobre el aceite de Mauritia Flexuosa L. *Grasas Aceites* **38**(5), 303-307. http://hdl.handle.net/2268/84543

McClements DJ, Decker EA, Weiss J. 2007. Emulsion-based delivery systems for lipophilic bioactive components. *J. Food Sci.* **75**(8), 109-124. https://doi.org/10.1111/j.1750-3841.2007.00507.x

Meléndez-Martínez AJ, Vicario IM, Heredia FJ. 2007. Review: Analysis of carotenoids in orange juice. *J. Food Comp. Anal.* **20**(7), 638-649. https://doi.org/10.1016/j.jfca.2007.04.006

O`Brien RD. 2009. *Fats and Oils: Formulating and Processing for Applications.* 3ed. CRC Press, New York.

Pardauil JJR, Molfetta FA, Braga M, Souza LKC, Filho GNR, Zamian JR, Costa CEF. 2017. Characterization, thermal properties and phase transitions of amazonian vegetable oils. *J. Therm. Anal. Calorim.* **127**, 1221-1229. https://doi.org/10.1007/s10973-016-5605-5

Pesce C, Rocha ES, Filho NR, Zoghbi MGB. 2009. *Oleaginosas da Amazônia.* 2ed. Museu Paraense Emílio Goeldi, Brasilia.

Ribeiro APB, Masuchi MH, Grimaldi R, Gonçalves LAG. 2009. Interesterificação química de óleo de soja e óleo de soja totalmente hidrogendo: Influência do tempo de reação. *Quim. Nova* **32**(4), 939-945. http://dx.doi.org/10.1590/S0100-40422009000400021

Ribeiro BD, Barreto DW, Coelho MAZ. 2011. Technological aspects of β-carotene production. *Food Bioprocess Technol.* **4**, 693–701. http://dx.doi.org/10.1007/s11947-011-0545-3

Ribeiro EF, Polachini TC, Carvalho GR, Telis-Romero J, Cabral RAF. 2017. Thermophysical properties of different olive oils: Evaluating density and rheology through a fluid dynamic approach. *Eur. J. Lipid Sci. Technol.* **119**, 1-10. http://dx.doi.org/10.1002/ejlt.201600316

Rodrigues JN, Gioielli LA. 2003. Chemical interesterification of milkfat and milkfat-corn oil blends. *Food Res. Int.* **36**, 149–159. https://doi.org/10.1016/S0963-9969(02)00130-8

Rodriguez-Amaya DB. 1996. Assessment of the provitamina A contents of foods - The brazilian experience. *J. Food Composit. Anal.* **9**, 196-230. https://doi.org/10.1006/jfca.1996.0028

Santos MFG, Alves RE, Ruíz-Méndez MV. 2013. Minor components in oils obtained from Amazonian palm fruits. *Grasas Aceites* **64**(5), 531-536. http://dx.doi.org/10.3989/gya.048913

Santos MFG, Marmesat S, Brito ES, Alves RE, Dobarganes MC. 2013. Major components in oils obtained from Amazonian palm fruits. *Grasas Aceites* **64**(3), 328-334. http://dx.doi.org/10.3989/gya.023513

Santos MFG, Alves RE, Roca M. 2015. Carotenoid composition in oils obtained from palm fruits from the Brazilian Amazon. *Grasas Aceites* **66**(3), 1-8. http://dx.doi.org/10.3989/gya.1062142

Santos JCO, Santos IMG, Souza AG. 2005. Effect of heating and cooling on rheological parameters of edible vegetable oils. *J. Food Eng.* **67**(4), 401–405. https://doi.org/10.1016/j.jfoodeng.2004.05.007

Silva SM, Sampaio KA, Taham T, Rocco SA, Ceriani R, Meirelles AJA. 2009. Characterization of oil extracted from buriti fruit (*Mauritia flexuosa*) grown in the Brazilian amazon region. *J. Am. Oil Chem. Soc.* **86**(7), 611-616. https://doi.org/10.1007/s11746-009-1400-9

Silva CP, Sousa MSB, Siguemoto ES, Soares RAM, Areas JAG. 2014. Chemical composition and antioxidant activity of jatobá-do-cerrado (*Hymenaea stigonocarpa* Mart.) flour. *Food Sci. Technol.* **34**(3), 597-603. http://dx.doi.org/10.1590/1678-457x.6405

Speranza P, Oliveira Falcão A, Alves Macedo J, Silva LHM, Rodrigues AMC, Alves Macedo G. 2016. Amazonian buriti oil: Chemical characterization and antioxidant potential. *Grasas Aceites* **67**(2), 1-9. http://dx.doi.org/10.3989/gya.0622152

Steffe FL. 1996. *Rheological Methods in Food Process Engineering*, Freeman Press, East Lansing.

Syed A. 2012. Future of omega-9 oils, in Thiyam-Holländer U, Michael Eskin NA, Matthäus B (Ed.) *Canola and Rapessed Production, Processing, Food Quality, and Nutrition*. CRC Press, Boca Raton, 79-100. http://dx.doi.org/10.1201/b13023-6

Tan CP, Che Man YB. 2000. Differential scanning calorimetric analysis of edible oils: Comparison of thermal properties and chemical composition. *J. Am. Oil Chem. Soc.* **77**(2), 143-155. http://dx.doi.org/10.1007/s11746-000-0024-6

Virapongse A, Endress BA, Gilmore MP, Horn C, Romulo C. 2017. Ecology, livelihoods, and management of the *Mauritia flexuosa* palm in South America. *Glob. Ecol. Conserv.* **10**, 70-92. http://dx.doi.org/10.1016/j.gecco.2016.12.005

Watkins SM, German JB. 2008. Unsaturated fatty acids, in Akoh CC, Min DB (Ed.) *Food Lipids – Chemistry, Nutrition, and Biotechnology*. 3ed, CRC Press, Boca Raton, 514-530. http://dx.doi.org/10.1201/9781420046649.ch20

CAPÍTULO 4

Estabilidade, microestrutura e reologia de emulsões de óleo de buriti (*Mauritia flexuosa*) afetadas pela proporção de isolado proteico de soja/pectina de alta metoxilação, teor de óleo e pressão de homogeneização

Esse capítulo será submetido como artigo científico para possível publicação.

Stability, microstructure, and rheology of buriti (*Mauritia flexuosa*) oil emulsions as affected by soy protein isolate/high-methoxyl pectin ratio, oil content, and homogenization pressure

Mírian Luisa Faria Freitas[a*], Ana Paula Badan Ribeiro[b], Vânia Regina Nicoletti[a]

[a]*São Paulo State University (UNESP), Institute of Biosciences, Humanities and Exact Sciences (IBILCE), Campus São José do Rio Preto, 2265 Cristóvão Colombo Street, Jardim Nazareth, São José do Rio Preto, São Paulo, 15.054-000, Brazil. E-mail: mirianlfreitas@yahoo.com.br; vanianic@ibilce.unesp.br*

[b]*Department of Food Technology (DTA), School of Food Engineering (FEA), University of Campinas (UNICAMP), Bertrand Russel Street, Cidade Universitária, Campinas, São Paulo, 13.083-970, Brazil. E-mail: anabadan@fea.unicamp.br*

[*]Corresponding author:
São Paulo State University (UNESP), Institute of Biosciences, Humanities and Exact Sciences (IBILCE), Campus São José do Rio Preto, 2265 Cristóvão Colombo Street, Jardim Nazareth, São José do Rio Preto, São Paulo, 15.054-000, Brazil.
E-mail: mirianlfreitas@yahoo.com.br
Telephone number: 55 17 98116-8134

Abstract: Buriti (*Mauritia flexuosa*) oil has a high concentration of monounsaturated fatty acids, carotenoids and tocopherols, recognized as a reliable source of antioxidant compounds. Emulsion technology is a suitable way of encapsulating, protecting and releasing bioactive lipid compounds for food industries. At pH below protein isoelectric point, oil in water (O/W) emulsion stability can be improved by electrostatic interactions between protein-polysaccharide around the oil droplets. In addition, polysaccharides contribute to emulsion stability by increasing viscosity of the continuous phase. The aim of this work was the production of buriti oil emulsions using soy protein isolate (SPI) and high-methoxyl pectin (HMP) as stabilizers, investigating the effects of oil content, SPI:HMP ratio, and homogenization pressure according to a rotable central composite (RCCD) 2^3 experimental design. The emulsions were evaluated regarding stability, droplet size, electrical conductivity, electrical charge, microstructure, and rheological behavior. An optmized emulsion was produced with 28% buriti oil, 55% SPI, and homogenization pressure of 380 bar. This emulsion was stable for at least 7 days, presenting reduced droplet size (4.58 µm (OM) and 38.18 µm (LD)), lower electrical conductivity (2.23 mS/cm) and higher modulus of negative charges (-17.65 mV). The mechanical spectra showed that the emulsion behaved as a viscoelastic gel under oscillatory, non-destructive shearing, whereas shear-thinning behavior took place under steady shear conditions.

Keywords: Carotenoids; confocal laser scanning microscopy; electrical conductivity; high-methoxyl pectin; soy protein isolate; viscoelaticity.

1. INTRODUCTION

Emulsion technology is a suitable way of encapsulating, protecting, and modulating the release of bioactive lipid compounds for use in food and pharmaceutical industries. On the other hand, emulsions are thermodynamically unstable systems and require addition of emulsifiers

and/or stabilizers, as well as the use of mechanical forces (homogenization process) to attain kinectic stability (McClements et al., 2007). Proteins are surface-active molecules that act as surfactants and prevent the coalescence of dispersed droplets: they spontaneously migrate from the bulk volume to the oil-water interface, as the free energy of proteins at the interface is lower than in the continuous phase (Walstra, 2003). The emulsion stabilizing properties of proteins may be enhanced by their potential electrostatic interactions with charged polysaccharides, which results in complex amphiphilic structures. These complexes or association colloids do not require a special legislation and may improve emulsion stability and textural attributes (Benichou et al, 2002; Dickinson, 2003; Lam et al., 2007; Perrechil and Cunha, 2013).

Soy protein isolate (SPI) contains at least 90% protein, being practically free of lipids and carbohydrates. The main components of these proteins are the β-conglycinin (7S) and glycinin (11S) fractions, wich represent more than 85% of the total soybean proteins (Lam et al., 2008). These two fractions have emulsifying action, presenting ability to stabilize emulsions by forming an adsorbed layer at the oil/water interface (Singh and Mohamed, 2007). Pectin, probably the most complex natural macromolecule, is the most commonly used stabilizer in protein based acidic beverages, and contributes positively to flavor, stability and texture of final products, even when added in small amounts (Tromp et al., 2004; Canteri et al., 2012). The key characteristic of pectin molecules is a linear chain of (1→4)-linked α-D-galactopyranosyl-uronic acid units in addition to neutral sugars such as L-rhamnose. High-methoxyl pectins (HMP) possess more than half of their carboxyl groups in the methyl ester form and at low pH the highly hydrated and charged carboxylate groups turn to uncharged and slightly hidrated carboxylic acid gropus, leading to association of the pectin molecules and formation of a polymer network that entraps water (BeMiller and Whistler, 1996).

At pH below 4.6, which corresponds to the isoelectric point of SPI, the negatively charged HMP interacts with protein positive charges to form a biopolymer double layer, preventing droplet coalescence and stabilizing the emulsion (Gancz et al., 2005; Freitas et al., 2017a). Protein-polysaccharide complexes enhance emulsion stability through electrostatic and/or steric phenomena, by modifying interfacial rheological properties and increasing emulsion viscosity (Serfert et al., 2013). In order to provide steric stabilization, it is desirable that, in addition to the hydrophobic groups that will keep permanently attached to the oil droplets' surface, the macromolecular structure at the oil-water interface presents a large fraction of hydrophilic chain segments that will protrude from the surface and increase the stabilizing layer thickness. At the same time, if this macromolecular structure contains charged groups that contribute to increasing the net repulsive electrostatic interactions, it would help to prevent aggregation of adjacent droplets caused by the attractive van der Waals forces (Dickinson, 2003).

The homogeneization step is of crucial importance to modulate physico-chemical and organoleptic properties, such as texture, taste, appearance, and stability of emulsified systems (McClements, 1999). High-pressure homogenization equipment is effective in reducing droplet sizes of pre-existing coarse emulsions: the fluid is pumped through a small adjustable orifice, located between the valve and its support, generating a combination of intense shear and cavitation in turbulent regime, thus promoting droplet size reduction (Schultz et al., 2004). Good results have been reported for emulsions stabilized with protein-polysaccharide complexes subjected to high-pressure homogenization (Perrechil and Cunha, 2013).

Knowledge of the rheological properties of emulsions is important for a number of reasons, which include the design of processing equipment (McKenna and Lyng, 2003), estimation of sensory attributes related to texture, and flow properties. In addition, rheological assays can provide

fundamental information on structural organization and interactions between emulsion components (McClements, 1999). The rheological behavior of concentrated emulsions ranges between the limit of dilute emulsions – with a linear dependence of viscosity on concentration and negligible interactions between droplets - and emulsions containing closely packed spherical droplets – in which it is impossible to increase the number of droplets without deforming the existing ones. The increase of droplet concentration in emulsions results in increased Newtonian viscosity at low shear rates, followed by appearance of strong non-Newtonian effects. As the droplet concentration increases, the Newtonian viscous flow is replaced by a viscoplastic behaviour with a step-like decrease of the apparent viscosity that is typical for multi-component systems with a coagulate structure formed by the dispersed phase, and reflects the breackage of the structure at a certain shear rate that is associated to a yield stress. The increase in concentration also enhances the influence of the droplet size on the emulsions rheology, as it influences the volume-to-surface area ratio. In addition, other rheological effects may appear at high concentrations, such as shearing time effects. These time effects are due to structural arrangements between the interfacial layers in the closely packed droplets, which are destroyed by deformation and restores at rest. The interaction between droplets and evolution of their shape in flow can also result in viscoelastic effects (Rao, 1999; McClements, 1999; Walstra, 2003; Derkach, 2009).

Native palm trees belonging to the *Aracaceae* family are among the most useful vegetable resources in the Amazon region. Buriti (*Mauritia flexuosa*) oil has a high concentration of monounsaturated fatty acids, with values higher than those found in olive oil or Brazil nuts, foods known to have high nutritional quality oils due to the properties of reducing blood cholesterol. In addition, the low concentration of polyunsaturated fatty acids gives the buriti oil a higher oxidative stability (Silva et al., 2009). Buriti oil contains β-carotene in higher concentrations than foods widely consumed

by Brazilians, such as guava, pitanga, papaya, passion fruit, carrots and other fruits from the Amazon region, including palm nuts, peach palm and tucumã (Rodriguez-Amaya, 1996; De Rosso and Mercadante, 2007). Additionally, buriti oil also presents high levels of tocopherols, indicating it as a reliable source of antioxidant compounds (Bataglion et al., 2015; Freitas et al., 2017b). When used as food additives, carotenoids and tocopherols are relatively unstable because they are sensible to light, oxygen, temperature and self-oxidation (non-enzymatic cleavage), which causes their rapid degradation (Xianquan et al., 2005; Guinazi et al., 2009). Emulsification and microencapsulation may be effective for protecting carotenoids and tocopherols from adverse effects of environment during storage (McClements et al., 2007).

Considering this context, the aim of this work was to investigate the production of buriti oil emulsions by high pressure homogeneization using soy protein isolate and high-methoxyl pectin as stabilizers, as well as characterizing the resulting systems by evaluating their stability, droplet size, electrical conductivity, electrical charge, optical microscopy, scanning electron microscopy, confocal laser scanning microscopy, and rheological behavior.

2. MATERIALS AND METHODS

2.1. Materials

The raw materials used were buriti oil (Amazon Oil Industry^{TM}), soy protein isolate (SPI) (Tovani Benzaquen Ingredientes^{TM}) and high-methoxyl pectin (HMP) (CP Kelco^{TM}). Preparation of samples used deinozed water, sodium azide (Dinâmica^{TM}), hydrochloric acid (Dinâmica^{TM}) or sodium hydroxide (Dinâmica^{TM}) solutions (1 N), and McIlvaine buffer (pH 3.5) prepared using disodium phosphate and citric acid (Dinâmica^{TM}).

2.2. Preparation of buriti oil emulsions

Oil-in-water emulsions were prepared with different oil contents, different contents of SPI in the continuous phase, and different applied homogenization pressures. The HMP content was not included as an independent variable in the experimental design, since it was added in the amount necessary to attain a fixed total concentration of biopolymers (SPI + HMP) in the continuous phase of the emulsion. The assays were carried out according to a rotable central composite design (RCCD) 2^3 to analyze the effects of 3 independent variables (Rodrigues and Iemma, 2009). Five assays were added at the central point of the experimental design, totalizing 19 assays according to Table 1. The following polynomial model was fitted to the data:

$$y = \beta_0 + \beta_1 x_1 + \beta_2 x_2 + \beta_3 x_3 + \beta_{11} x_1^2 + \beta_{22} x_2^2 + \beta_{33} x_3^2 + \beta_{12} x_1 x_2 + \beta_{13} x_1 x_3 + \beta_{23} x_2 x_3 \quad (1)$$

in which y is the response variable, x_1 is the oil content (% relative to total weight of emulsion), x_2 is the SPI content (% relative to total weight of SPI + HMP in the emulsion), x_3 is the homogeneization pressure (bar), and β_i and β_{ij} are the fitted coeficients.

The results were subjected to analysis of variance (ANOVA) and the fitted model was tested regarding the lack of fit and coefficient of regression using a statistical software. The lack of fit were not statistical significant ($p \leq 0.05$) and the coefficient of regression were statistical significant ($p > 0.05$) for all fitted models.

Table 1. Buriti oil emulsion assays with coded variables and real values, according to RCCD 2^3 experimental design and final emulsion composition, in wt%.

Assay	Rotable Central Composite Design (RCCD)			Emulsion composition[a]			
	Oil (%) (x_1)	SPI (%)[a](x_2)	Pressure (bar) (x_3)	Oil (%)	SPI (%)	HMP (%)	Water (%)
O14S56P240	-1 (14%)	-1 (56%)	-1 (240 bar)	14.00	1.20	0.93	83.87
O14S56P360	-1 (14%)	-1 (56%)	+1 (360 bar)	14.00	1.20	0.93	83.87
O14S74P240	-1 (14%)	+1 (74%)	-1 (240 bar)	14.00	1.70	0.60	83.70
O14S74P360	-1 (14%)	+1 (74%)	+1 (360 bar)	14.00	1.70	0.60	83.70
O26S56P240	+1 (26%)	-1 (56%)	-1 (240 bar)	26.00	1.02	0.80	72.18
O26S56P360	+1 (26%)	-1 (56%)	+1 (360 bar)	26.00	1.02	0.80	72.18
O26S74P240	+1 (26%)	+1 (74%)	-1 (240 bar)	26.00	1.45	0.50	72.05
O26S74P360	+1 (26%)	+1 (74%)	+1 (360 bar)	26.00	1.45	0.50	72.05
O10S65P300	-1.68 (10%)	0 (65%)	0 (300 bar)	10.00	1.49	0.81	87.70
O30S65P300	+1.68 (30%)	0 (65%)	0 (300 bar)	30.00	1.16	0.63	68.21
O20S50P300	0 (20%)	-1.68 (50%)	0 (300 bar)	20.00	0.96	0.96	78.08
O20S80P300	0 (20%)	+1.68 (80%)	0 (300 bar)	20.00	1.74	0.44	77.82
O20S65P200	0 (20%)	0 (65%)	-1.68 (200 bar)	20.00	1.30	0.70	78.00
O20S65P400	0 (20%)	0 (65%)	+1.68 (400 bar)	20.00	1.30	0.70	78.00
O20S65P300	0 (20%)	0 (65%)	0 (300 bar)	20.00	1.30	0.70	78.00
O20S65P300	0 (20%)	0 (65%)	0 (300 bar)	20.00	1.30	0.70	78.00
O20S65P300	0 (20%)	0 (65%)	0 (300 bar)	20.00	1.30	0.70	78.00
O20S65P300	0 (20%)	0 (65%)	0 (300 bar)	20.00	1.30	0.70	78.00
O20S65P300	0 (20%)	0 (65%)	0 (300 bar)	20.00	1.30	0.70	78.00

[a]SPI (%): percent value relative to the total weight of SPI + HMP in the emulsion; [b]Percent contents relative to total weight of the emulsion.

All the emulsions were prepared using McIlvaine buffer at pH 3.5, which is below the isoelectric point of SPI and allows the biopolymers in solution to acquire opposite charges in a sufficient amount to form electrostatic complexes that remain dispersed in the aqueous phase (Freitas et al., 2017a). Stock solutions of SPI (3 g/100 g) were prepared by dispersing the protein in half of the required water and adjusting pH 11.0 (± 0.05) with NaOH for complete solubilization, subjected to magnetic stirring for 3 h, left at rest overnight (25 °C) for complete hydration, and finally completing the water content with buffer pH 3.5. Stock solutions of HMP (2 g/100 g) were prepared by dispersion in buffer solution at pH 3.5, 3 h under magnetic stirring, and overnight hydration at 25 °C. Sodium azide 0.04%

was added to stock solutions to prevent microorganism growth (Freitas et al., 2017a).

Buriti oil was dispersed in the SPI stock solution using Ultra Turrax stirrer (T-25, IKA, Germany) at 15000 rpm for 4 minutes, followed by addition of HMP stock solution, and dispersion at 15000 rpm for 4 minutes using the same stirrer, according to methodology described by Kaltsa et al., (2013), with some modifications. After this procedure, the coarse emulsion was homogenized at high pressure in a double stage homogenizer (SPX Flow Technology, Lab Serie APV-2000), without sample recirculation.

2.3. Caracterization of buriti oil emulsions

The emulsions were stored at 25 °C for a 7-day period after production. After this time, they were analyzed, in triplicate, regarding stability, droplet size, electrical conductivity and electrical charge, morphology by optical microscopy and scanning electron microscopy (SEM), and rheology. Confocal laser scanning microscopy (CLSM) was performed on the same day of emulsion preparation with fluorescent dyes, in order to avoid fluorescence losses. In the emulsions that destabilized throughout this period, the analyses were performed using samples from the creamed phase. The analytical procedures are described as follows.

2.3.1. *Stability*

Transparent tubes containing the emulsions were closed and stored at 25 °C. When phase separation took place, there was formation of a lower density upper phase (cream). The creaming index (CI), indicative of emulsion stability, was determined as the ratio between the lower phase height (H) and the emulsion initial height (H_0) in the tube, according to Equation 2 (Perrechil and Cunha, 2013).

$$CI(\%) = 100\frac{H}{H_0} \quad (2)$$

2.3.2. *Droplet size by optical microscopy (OM) and laser diffraction (LD)*

The average droplet size was evaluated using an optical microscope (Olympus, CX31) with a 40× magnification objective coupled with a digital camera (Olympus, SC30), and software Image-Pro Plus 6.0 (Media Cybernetics, Inc.). A minimum number of 300 droplets to be measured in order to give significant results was defined after comparing the average sizes calculated from 100 to 800 droplets applying a Tukey's test. There were no significant differences ($p > 0.05$) among the calculated average size, with satisfactory results for size distribution and standard deviation, when measuring 300 droplets or more.

In addition to optical microscopy, droplet size distribution was evaluated by laser diffraction (Mastersizer 2000 with Hydro 2000S dispersion unit, Malvern). The samples were dispersed in deionized water at 10 % obscuration and kept under stirring during analysis. The refractive indexes used for droplets and dispersant phase were 1.46 (buriti oil) and 1.33 (deionized water), respectively. Taking into account that some samples showed bimodal particle size distribution, the mode of the cumullative frequency distribution was adopted as the most representative particle size (Walstra, 2003).

2.3.3. *Electric conductivity*

The emulsion electrical conductivity was measured using a conductivity meter (Seven Compact, Mettler Toledo) at room temperature (Levic et al., 2015).

2.3.4. *Charge analysis*

Electrical charges were analyzed by zeta potential measurements (Zetasizer NanoZ, Malvern). The emulsion or cream phase samples were dispersed to a concentration of 0.05% in ultrapure water followed by pH 3.5 adjustment using HCl solution to maintain the dispersing medium as close

as possible to the emulsions continuous phase, according to methodology proposed by Abdolmaleki et al., (2016).

2.3.5. *Rheological behavior*

Rheological analyses were performed on an AR-2000EX (TA Instruments, Delaware, USA) rheometer with geometry of serrated parallel plates of 40 mm diameter and gap of 300 μm at 25 °C. To avoid droplet crushing, the distance between parallel plates (gap) was defined as being at least 10 times larger than the maximum droplet size (Steffe, 1996). Viscosity curves were obtained from steady shear assays and the viscoelastic properties were determined from oscillatory shear tests.

Steady shear

Steady shear tests were performed following downward (100 to 0.1 s^{-1}) and upward (0.1 to 100 s^{-1}) shear rate ramps to obtain apparent viscosity versus shear rate curves. The Sisko viscosity model (Equation 3) was fitted to experimental data.

$$\eta_{ap} = \eta_{\infty}\dot{\gamma} + K\dot{\gamma}^{(n-1)} \quad (3)$$

In which η_{ap} is the apparent viscosity (Pa.s), η_{∞} is the infinite-shear viscosity (Pa.s), $\dot{\gamma}$ is the shear rate (s^{-1}), K is the consistency index ($Pa.s^n$), n is the flow behavior index (dimensionless) (Marfil et al. 2012).

Oscillatory shear

The viscoelastic properties were evaluated along frequency sweeps between 0.03 and 30 rad/s at maximum deformation of 0.001, which was in the linear viscoelastic region. A Power Law model was applied in order to describe the frequency (ω) dependence on the storage (G') and loss (G'') moduli, according to Equations 4 and 5.

$$G' = k'\omega^{n'} \quad (4)$$

$$G" = k"\omega^{n"} \quad (5)$$

In which *k'*, *k"*, *n'* and *n"* are the corresponding fitting parameters.

The fitting quality of Sisko (Eq. 3) and Power Law models (Eqs. 4 and 5) were evaluated by the coefficient of determination, R^2, and the root mean squared errors, *RMSE*.

2.3.6. *Analyses of the emulsion morphology*

CLSM

Analyses by CLSM were carried out according to Lamprecht et al. (2000) and Mukai-Correa et al., (2005), using fluorescein isothiocyanate (FITC) to interact with SPI and Rhodamine B to interact with HMP. The dyes were dissolved in dimethyl sulfoxide (DMSO, 1 mg/mL) and added at a ratio of 50 µL/2.5 g of polymer in stock solutions. The emulsions were then prepared as described in item 2.2. Images were collected in a ZEISS LSM 710 microscope with 40×-magnification with the laser adjusted to green/red fluorescence mode, at wavelengths of 488 nm and 543 nm to visualize FITC and Rhodamine B, respectively. Green and red fluorescent images were obtained from the two separate channels and, then, overlaid and analyzed by Zen 2010 software.

SEM

SEM images were obtained in a TM 3000 (Hitachi) microscope with a 600×-magnification. The samples were inserted into the chamber and immobilized by vacuum application during image capture.

2.4. Experimental validation of the RCCD models

Experimental validation of the models resulting from the RCCD (Equation 1) was carried out based on the results of stability, droplet size,

electrical conductivity and electrical charge. Selected values for buriti oil content, SPI content, and homogeneization pressure were applied to produce an emulsion and the corresponding experimental results were compared with those predicted by the fitted models. In addition, this emulsion was characterized by rheological and morphological analyses (items 3.2.5 and 3.2.6).

3. RESULTS AND DISCUSSION

The emulsions prepared with different buriti oil and SPI contents and subjected to varied homogeneization pressures, according to the RCCD presented in Table 1, were characterized regarding stability (*CI*), droplet size (by OM and LD), electrical conductivity, and electrical charge after 7 days of preparation. The obtained results (Table 2) were used to fit empirical models (Eq. 1) and the regression coefficients for the coded second-order polynomial fitted equations, as well as the determination coefficients (R^2), for each one of the dependent variables are given in Table 3. Some non-significant effects were eliminated, and the resulting equations were tested for adequacy and fitness by the analysis of variance (ANOVA). The fitted models were suitable, showing significant regression, low residual values, no lack of fit and satisfactory determination coefficients.

Table 2. Stability (creaming index, *CI*), droplet size (obtained by optical microscopy, OM, and by laser diffraction, LD), electrical conductivity, and electrical charge (zeta potential) of emulsions. The values into brackets are standard deviations.

Assays	*CI* (%)	Droplet size OM (μm)	Droplet size LD (μm)	Electrical conductivity (mS/cm)	Zeta potential (mV)
O14S56P240	28.00 (±0.63)	3.41 (span 1.24)	25.97 (±0.28)	2.87 (±0.01)	-20.28 (±1.25)
O14S56P360	11.70 (±0.58)	2.94 (span 1.12)	38.88 (±0.59)	3.08 (±0.01)	-20.00 (±0.83)
O14S74P240	20.27 (±1.24)	3.36 (span 1.18)	51.48 (±1.16)	2.47 (±0.01)	-16.27 (±1.18)
O14S74P360	22.34 (±1.62)	2.39 (span 1.29)	51.72 (±1.95)	2.81 (±0.01)	-18.30 (±2.07)
O26S56P240	3.67 (±6.36)	4.38 (span 1.29)	39.48 (±2.72)	2.29 (±0.01)	-20.50 (±0.97)
O26S56P360	0.00 (±0.00)	4.50 (span 1.86)	42.44 (±0.55)	2.18 (±0.01)	-22.23 (±0.58)
O26S74P240	11.56 (±0.57)	5.67 (span 1.93)	40.18 (±0.21)	2.00 (±0.01)	-15.17 (±1.30)
O26S74P360	14.71 (±1.55)	4.70 (span 1.31)	35.04 (±0.51)	2.38 (±0.01)	-15.55 (±0.55)
O10S65P300	35.62 (±1.93)	2.93 (span 1.09)	46.49 (±0.34)	2.82 (±0.01)	-20.40 (±0.75)
O30S65P300	0.00 (±0.00)	6.76 (span 2.37)	40.55 (±0.77)	2.16 (±0.01)	-21.92 (±0.82)
O20S50P300	13.96 (±5.88)	3.87 (span 1.44)	43.15 (±0.84)	2.53 (±0.01)	-22.33 (±0.70)
O20S80P300	16.36 (±1.41)	4.25 (span 1.70)	66.27 (±0.80)	2.02 (±0.01)	-15.30 (±0.61)
O20S65P200	17.33 (±0.50)	3.59 (span 1.36)	37.41 (±0.26)	2.27 (±0.01)	-19.55 (±1.24)
O20S65P400	10.11 (±1.54)	2.97 (span 0.93)	53.07 (±1.21)	2.47 (±0.01)	-14.60 (±1.74)
O20S65P300	16.56 (±0.57)	3.81 (span 1.14)	51.54 (±0.77)	2.31 (±0.01)	-20.72 (±1.75)
O20S65P300	14.48 (±1.48)	3.95 (span 1.40)	50.27 (±1.51)	2.70 (±0.01)	-18.68 (±1.43)
O20S65P300	18.18 (±4.83)	3.88 (span 1.34)	49.01 (±0.73)	2.21 (±0.01)	-17.77 (±1.39)
O20S65P300	14.03 (±0.93)	3.40 (span 1.27)	48.02 (±0.36)	2.38 (±0.01)	-17.65 (±0.67)
O20S65P300	13.40 (±2.03)	3.27 (span 1.05)	43.22 (±0.49)	2.44 (±0.01)	-20.58 (±0.36)

Table 3. Coded second-order regression coefficients for creaming index (*CI*), droplet size (by OM and LD), electrical conductivity, and zeta potential. *n.s.: non-significant (p > 0.10).

Regression analysis coefficients	*CI* (%)	Droplet size OM (μm)	Droplet size LD (μm)	Electrical conductivity (mS/cm)	Zeta potential (mV)
β_0	16.27	3.77	49.34	2.44	-19.45
β_1	-13.10	0.99	n.s.*	-0.26	n.s.
β_2	7.66	n.s.	5.16	-0.12	2.16
β_3	-0.60	-0.25	2.73	0.09	n.s.
β_{11}	n.s.	0.37	-3.35	n.s.	n.s.
β_{22}	n.s.	n.s.	n.s.	n.s.	n.s.
β_{33}	n.s.	-0.19	-2.75	n.s.	0.87
β_{12}	9.28	0.26	-5.63	n.s.	n.s.
β_{13}	n.s.	n.s.	n.s.	n.s.	n.s.
β_{23}	10.66	-0.20	n.s.	n.s.	n.s.
R^2	0.88	0.94	0.71	0.74	0.66

3.1. Stability

The creaming index was significantly affected ($p \leq 0.10$) by the oil content (β_1), SPI content (β_2), and homogenization pressure (β_3). In addition, there were significant interactions between oil and SPI contents (β_{12}), as well as between SPI content and homogenization pressure (β_{23}) (Table 3). The oil content and homogenization pressure had negative effects, whereas SPI content had a positive effect on creaming index, being important to remember that the higher the *CI*, the higher the emulsion instability.

The increase of emulsion stability with increasing concentration of the dispersed phase is probably related to the higher viscosity associated to the increased concentration of emulsion droplets (Derkach 2009). In addition, the buriti oil used is a crude oil and has about 12% of diacylglycerols and monoacylglycerols, compounds which are recognized by their emulsifying properties (Freitas et al., 2017b). In such a way, it is possible to suggest that the increase in oil content lead to an increasing content of these compounds, which could contribute to lower *CI* values, or

higher emulsion stability. On the other hand, lower SPI contents in the continuous phase also imply in higher HMP contents (Table 1), which suggests that a minimum content of HMP is important to increasing the continuous phase viscosity and preventing oil droplets diffusion, wich could contribute to increase the stability and lower *CI* values (Albano and Nicoletti, 2018). In turn, higher homogenization pressures may contribute to production of smaller oil droplets, resulting in a more homogeneous and, consequently, more stable system, with lower creaming index (Kaltsa et al., 2013).

3.2. Droplet size

With respect to droplet size measured by OM, the variables with significant effects ($p \leq 0.10$) were the oil content (linear, β_1, and quadratic, β_{11}), homogenization pressure (β_3 and β_{33}), the interactions between oil and SPI contents (β_{12}) and between SPI content and homogenization pressure (β_{23}). Whereas the oil content and the interaction between oil and SPI contents had positive effects on droplet size, the homogenization pressure and the interaction between SPI content and homogenization pressure had negative effects. This suggests that high HMP levels helped to stabilize the emulsions, although the smaller amount of SPI was not sufficient to produce emulsions with small droplets, since a larger amount of protein would be needed to cover the larger interfacial area.

The droplet sizes determined by laser diffraction (LD) were represented by the distribution mode and were significantly affected ($p \leq 0.10$) by the oil content (β_{11}), SPI content (β_2), homogenization pressure (β_3 and β_{33}) and by the interaction between oil and SPI contents (β_{12}). The SPI content and homogenization pressure presented positive effects, whereas the oil content, homogenization pressure, and the interaction between oil and SPI contents presented negative effects. It is interesting to note the large difference between the results for droplet size determined by OM and LD. Differences could also be observed concerning the variables that

exerted significant effects on these results. The laser diffraction technique applied requires sample dilution, which does not happen in the optical microscopy technique. This fact led to the hypothesis that the dilution was not enough to completely disperse the oil droplets, which remained arranged in clusters. This hypothesis was confirmed by observing the emulsions at the same dilution in the optical microscope. Despite the observed differences, the results from LD are relevant, since this is the standard technique used for droplet size analysis in emulsions (Diao et al., 2016; Murray and Phisarnchananan, 2016; Abdolmaleki et al., 2016).

3.3. Electrical conductivity

The electrical conductivity was significantly affected ($p \leq 0.10$) by the oil content (β_1), SPI content (β_2) and homogenization pressure (β_3). The oil and SPI contents presented negative effects and the homogenization pressure presented positive effect on the electrical conductivity of emulsions or of cream phases. These results can be explained considering that the systems with higher SPI contents had lower HMP contents and, taking into account that pectin helps to mantain oil droplets apart from each other, in these systems there was a great possibility that oil droplets were floculated, or even merged (coalescence) in the creamed phase, leading to lower electrical conductivity values. On the other hand, in emulsions subjected to higher homogenization pressures, smaller oil droplets and greater homogeneity are expected, thus, resulting in higher electrical conductivity values.

According to Bruttel (2004), in oil-in-water emulsions, water has a higher dielectric constant and presents positive charges, whereas the oil has a lower dielectric constant and presents negative charges. When the water phase is bound to stabilizers, that is, the emulsion has maximum viscosity, its stability will also be maximum and due this fact the electrical conductivity is minimal.

3.4. Analysis of the droplet charge

The zeta potential, or electrokinetic potential, is related to the electrophoretic mobility and gives a measure of the net charge on the surface of a macromolecule, being used to describe the surface charge of polyeletrolites or of dispersed droplets; as well as the electrical conductivity, zeta potential is related to emulsion stability. The more charged the droplets, greater is the repulsion among them, which contributes to a more stable suspension. In order to prevent irreversible oil droplet flocculation, an emulsion should present a zeta potential greater than 25 mV (in modulus), characterizing a metastable system (Hunter, 2001). All the emulsions prepared according to the RCCD presented negative zeta potential, varying in the range of -22.33 (±0.70) to -14.60 (±1.74) mV (Table 2). At pH 3.5, SPI is positively charged and HMP has a slightly larger negative charge than SPI (Freitas et al., 2017a), thus suggesting that pectin presence was determinant for the net charge of emulsions, reinforcing the hypothesis that protein acts at oil/water interface and pectin, in addition to interacting with protein, covers droplets as a second layer, also acting as a stabilizer in the continuous phase (Dickinson, 2003).

Stable emulsions (O26S56P240, O26S56P360, and O30S65P300) showed high charge modulus (Table 2). However, these values were lower than 25 mV and this may be an indication that these emulsions would not remain stable for a long time. The emulsion with lower SPI content (50%) and, consequently, higher HMP content (O20S50P300) presented higher charge modulus, while those with lower HMP contents (20 or 26%) (O14S74P240, O14S74P360, O26S74P240, O26S74P360, and O20S80P300) presented lower charge modulus. The emulsion O20S65P400, despite not having the lowest HMP contents (35%), resulted in the lowest charge modulus (-14.60 ± 1.74 mV). The homogenization pressure (400 bar) might have contributed to this lower negative charge, since the smaller droplets produced result in larger surface area covered by SPI and available to interact with HMP. This greater interaction might

contribute to further neutralization of available negative charges. Another interesting observation is that emulsions with high charge modulus presented smaller droplet sizes measured by LD (O14S56P240, O14S56P360, O26S56P240, O36S65P300, and O20S50P300). This suggests that, in these systems, there were stronger repulsive forces between droplets and thus the size of clusters measured by LD were smaller. In agreement with the above discussion, the variables with significant effects ($p \leq 0.10$) on zeta potential were SPI content (β_2) and homogenization pressure (β_{33}), both having positive effects on zeta potential, i.e., increasing SPI and homogenization pressure caused lower charge modulus.

3.5. Rheological behavior of emulsions

Steady shear

Figure 1 shows apparent viscosity curves corresponding to emulsions O14S74P360, O26S56P360, O26S74P240, and O26S74P360, which were chosen for presentation due to differences in their formulations (Table 1) and for possibility of comparing one variable at a time, while maintaining the other constant.

Figure 1. Apparent viscosity curves obtained for downward (closed symbols) and upward (open symbols) shear rate ramps of emulsions O14S74P360 (squares), O26S56P360 (circles), O26S74P240 (triangles) and O26S74P360 (stars).

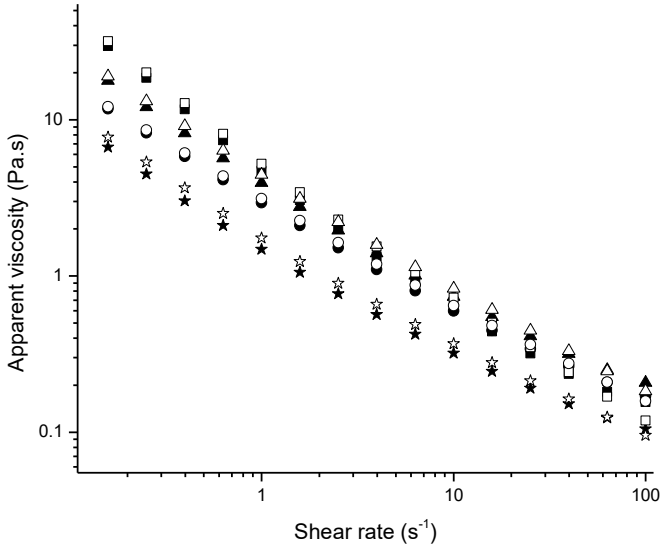

The emulsions showed similar shear-thinning behavior, with their apparent viscosity decreasing with increasing shear rate. Comparing the emulsions O26S56P360 (circles) and O26S74P360 (stars) produced with the same oil content and homogenization pressure, slightly higher viscosity values were observed in the emulsion with the lower SPI content and, consequently, higher HMP content. On the other hand, comparing the emulsions O26S74P240 (triangles) and O26S74P360 (stars) that were produced with the same composition, it was noted that the higher homogenization pressure slightly reduced the apparent viscosity, probably because of the smaller oil droplets produced, which is in accordance with the discussion regarding the creaming index (item 3.1), as well as the results observed in previous works (Derkach, 2009; Kaltsa et al., 2013; Albano and Nicoletti, 2018).

The Sisko model (Equation 3) presented satisfatory fit to the apparent viscosity curves (Table 4), resulting in determination coefficients above 0.9 low values of RMSE for both downward and upward shear rate ramps. The pseudoplastic behavior is explained by structure modification of the long

chain molecules, such as those of SPI and HMP present in the continuous phase, as well as by modification of oil-droplet aggregates due to the increase of velocity gradient, or shear rate (Walstra, 2003). This behavior has been commonly observed in concentrated emulsions (Derkach, 2009; Kaltsa et al., 2013; Perrechil and Cunha, 2013; Albano and Nicoletti, 2018). Infinite-shear viscosity provides information on how the system behaves when submited to high shear conditions, such as spraying or extrusion (Marfil et al., 2012). Under these conditions, the buriti oil emulsions or creamed phases would have reduced apparent viscosity but still higher than water viscosity.

The apparent viscosity curves corresponding to the downward and upward shear rate ramps practically overlap, suggesting that the rheological behavior of the emulsions was independent of the shearing time, which could be an interesting characteristic for industrial processing such as pumping and tube flowing.

Table 4. Consistency index (*K*), flow behavior index (*n*), infinite-shear viscosity (η_∞) and determination coefficient (R^2) for the Sisko model fittet to apparent viscosity curves and consistency index (*K'* e *K"*), flow behavior index (*n'* e *n"*), determination coefficient (R^2), and root mean squared error (*RMSE*) for the Power Law fitted to viscoelasticity data of emulsions O14S74P360, O26S56P360, O26S74P240 and O26S74P360.

Sisko viscosity model										
Assays	**Downward shear rate ramp**					**Upward shear rate ramp**				
	K **(Pa.s^n)**	***n***	η_∞ **(Pa.s)**	R^2	***RMSE***	***K*** **(Pa.s^n)**	***n***	η_∞ **(Pa.s)**	R^2	***RMSE***
O14S74P360	4.54	0.01	0.17	0.99	0.04	5.25	0.03	0.10	0.99	0.14
O26S56P360	2.82	0.23	0.11	0.99	0.02	3.04	0.25	0.09	0.99	0.01
O26S74P240	3.69	0.15	0.20	0.99	0.05	4.36	0.21	0.11	0.99	0.03
O26S74P360	1.28	0.11	0.14	0.99	0.05	1.72	0.19	0.07	0.99	0.03

Power Law model fitted to frequency sweeps									
Assays	***K'*** **(Pa.s$^{n'}$)**	***n'***	R^2	***RMSE***	***K"*** **(Pa.s$^{n"}$)**	***n"***	R^2	***RMSE***	$n_{r,av}$
O14S74P360	12.10	0.09	0.99	0.20	1.83	0.18	0.93	0.20	0.13
O26S56P360	16.76	0.09	0.99	0.13	2.61	0.19	0.87	0.41	0.14
O26S74P240	16.75	0.11	0.99	0.30	2.84	0.19	0.89	0.42	0.15
O26S74P360	7.41	0.11	0.98	0.27	1.49	0.23	0.89	0.27	0.17

Oscillatory shear

The storage (*G'*) and loss (*G"*) moduli as functions of frequency for the emulsions O14S74P360, O26S56P360, O26S74P240, and O26S74P360 can be visualized in Figure 2(a).

Figure 2. Storage (*G'*- closed symbols) and loss (*G"*- open symbols) moduli as functions of frequency (a) and loss tangent, Tan (*δ*) (b) for the emulsions O14S74P360 (squares), O26S56P360 (circles), O26S74P240 (triangles), and O26S74P360 (stars).

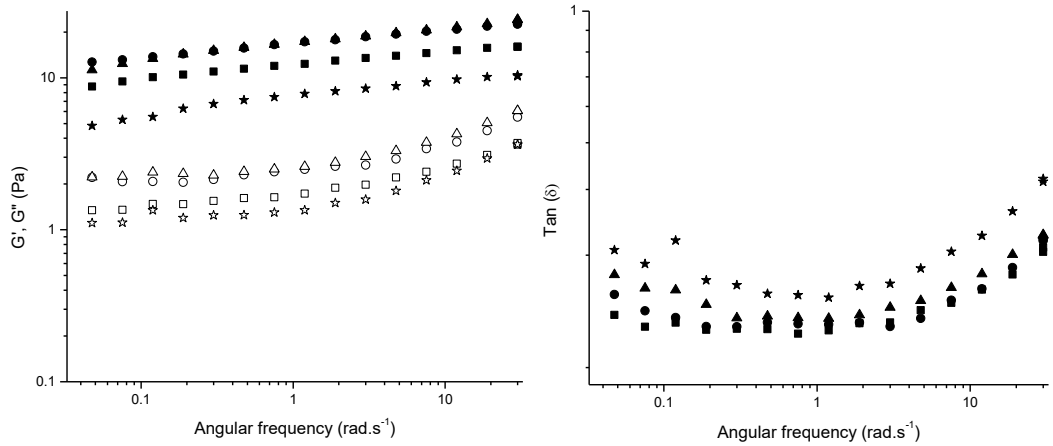

(a) (b)

In all the emulsions analysed, *G'* presented values greater than *G"* for the entire studied frequency range, showing that the emulsions and creamed phases presented elastic characteristics weak-gel behavior. Weak or physical gels are frequency dependent, with *G' > G"* but with no crossing-over, whereas true or elastic gels present constant *G'* along frequency sweeps (Steffe, 1996; Chamberlain and Rao, 2000). In opposition to a true gel, which will breakdown when subjected to high shear (steady shear assays), a weak gel will flow under similar conditions (Ikeda and Nishinari, 2001; Albano et al., 2014).

The samples differed on storage and loss modulus magnitude, and the O26S74P360 emulsion (stars) presented the lowest modulus. The O14S74P360 (squares) assay was the most unstable system, and despite

this, its cream showed similar viscoelastic results to O26S56P360 (circles) assay, which was stable emulsion.

An appropriate approach to analyzing the mechanical spectra of biopolymer systems is based on fitting a Power Law model (Equations 4 and 5) to *G'* and *G"* versus frequency data. The fitting parameters obtained for the studied emulsions can be found in Table 4. It is possible to observe that the Power Law could be fitted to experimental data with high coefficients of determination ($R^2 > 0.87$) and *RMSE* < 0.43. For biopolymer systems that behave as true gels, the loss and storage modulus are congruent for several decades of frequency and this behavior results in a constant value of the loss tangent, Tan (*δ*), in which δ is the phase angle between stress (*σ*) and strain (*γ*). These relations can be expressed as Equations 6 and 7 (Lopes da Silva and Golçalves, 1994; Richter, 2007, Albano et al., 2014).

$$G'(\omega) \propto G"(\omega) \propto \omega^{n_r}, \text{with } 0 < n_r < 1 \quad (6)$$

$$\frac{G"}{G'} = tan(\delta) = tan\left(\frac{n_r \pi}{2}\right) \quad (7)$$

The parameter n_r is the relaxation exponent and Equation 7 predicts that *G"* > *G'* for $n_r > 0.5$, *G'* > *G"* for $n_r < 0.5$, and *G"* = *G'* for $n_r = 0.5$. A gel with n_r approaching 1 is a purely viscous gel, whereas n_r approaching 0 suggests a purely elastic gel (Chambon and Winter, 1987; Rodd et al., 2001). Values of *n'* and *n"* can provide useful information regarding the viscoelastic nature of materials (Richter, 2007; Albano et al., 2014). The buriti oil emulsions or creamed phases showed *n'* < *n"* < 0.24 (Table 4) and the relative magnitudes obtained for *n'* and *n"* are typical of weak physical gels, especially at low frequency. Values of Tan (*δ*) were included in Figure 2(b).

3.6. Microscopic analyses

Optical microscopy

Optical microscopy was used to observe the emulsions or creamed phase morphology and it was also possible to analyze and compare oil droplets arrangement among different assays. Figure 3 shows the images collected with a 40×-magnification for the assays O14S74P360, O26S56P360, O26S74P240, and O26S74P360.

Figure 3. Images of the assays O14S74P360 (a), O26S56P360 (b), O26S74P240 (c), and O26S74P360 (d) obtained by optical microscopy with a 40×-magnification objective (bars correspond to 20 µm).

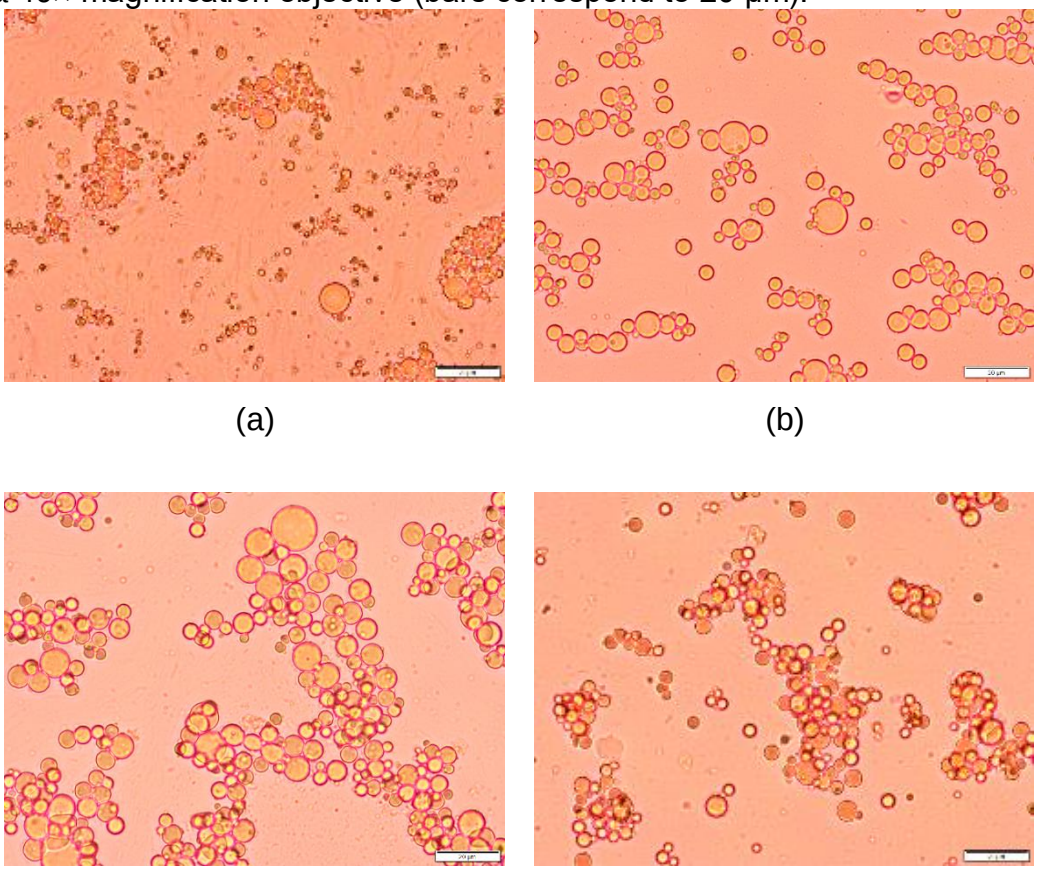

(a) (b)

(c) (d)

Through the images it is possible to note dispersed oil droplets in the continuous phase. In addition, these droplets were mostly arranged in clusters, suggesting that although the systems were negatively charged,

these charges were not sufficient to mantain and the oil droplets completely dispersed throughout the continuous phase, indicating that the emulsions were probably destabilized by the flocculation phenomena.

The assays O14S74P360 (Figure 3a) and O26S74P360 (Figure 3d) differ in oil content and larger oil droplets could be observed in assay O26S74P360 (Figure 3d). This might confirm the model fitted in Table 3, in which the oil content had positive effect on the droplet size measured by optical microscopy. The assay O26S56P360 (Figure 3b) was prepared with a lower SPI content in the wall material and therefore, a higher pectin content comparing to the O26S74P360 (Figure 3d) assay. It was possible to observe that the assay O26S56P360 had a higher pectin excess, which caused a higher negative charge and consequently lower flocculation. This agrees with the model presented in Table 3, in which the SPI content positively influenced the droplet size measured by LD. The emulsions O26S74P240 (Figure 3c) and O26S74P360 (Figure 3d) were produced using different homogenization pressures, and the sample O26S74P360 had a smaller droplet size due to the higher homogenization pressure.

Confocal laser scanning microscopy

The images corresponding to the emulsions O14S74P360, O26S56P360, O26S74P240, and O26S74P360 (Figure 4) were obtained in a confocal microscope with a 40×-magnification. SPI can be visualized in green and HMP in red due to interaction with fluorescent dyes FITC and Rhodamine B, respectively.

Figure 4. Images of the assays O14S74P360 (a), O26S56P360 (b), O26S74P240 (c), and O26S74P360 (d) obtained by confocal laser scanning microscopy with a 40×-magnification.

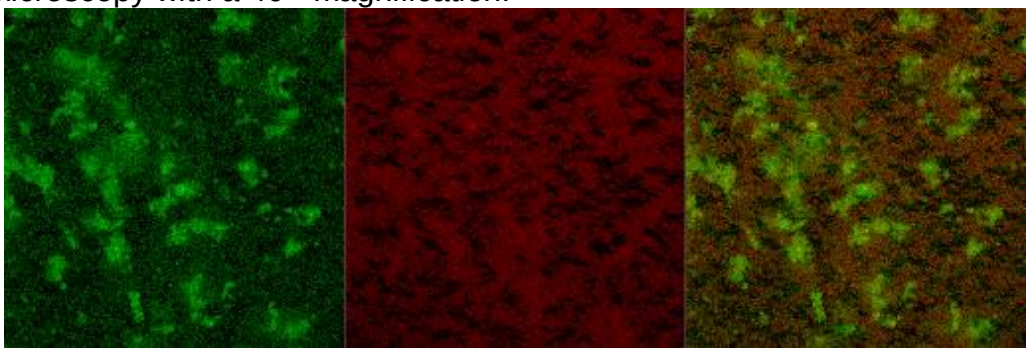

(a1) (a2) (a3)

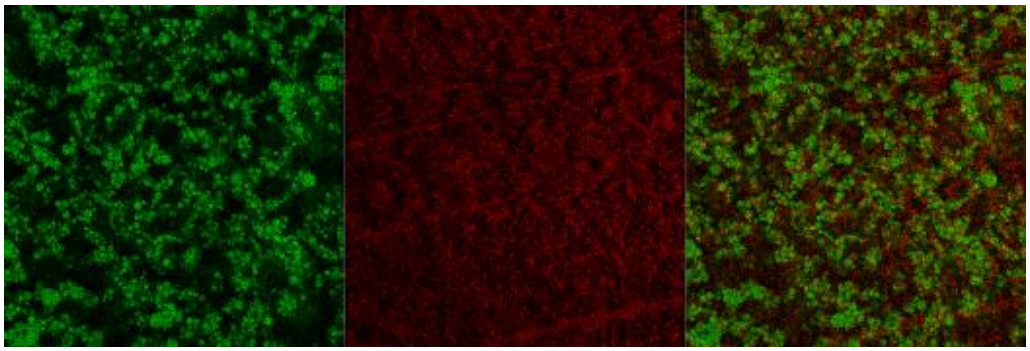

(b1) (b2) (b3)

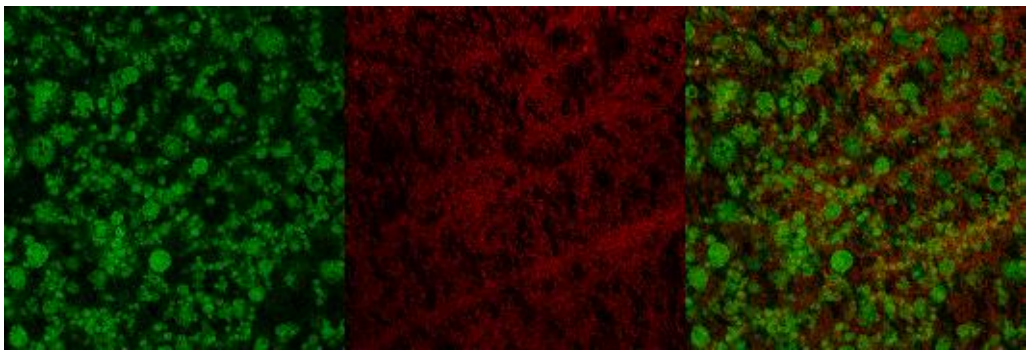

(c1) (c2) (c3)

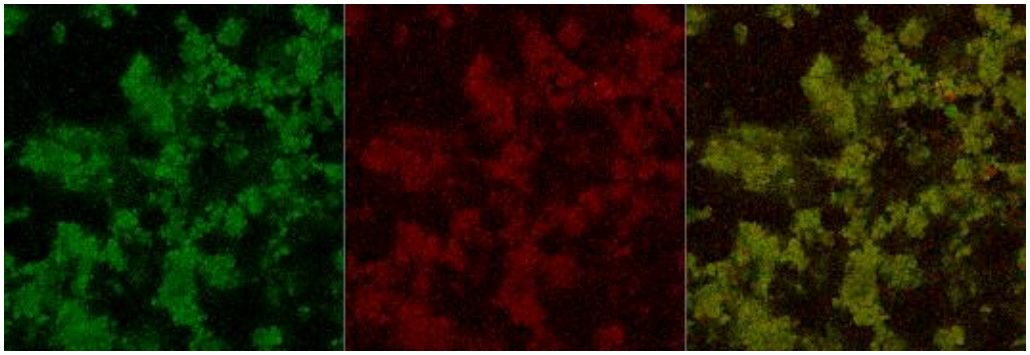

(d1) (d2) (d3)

Through the collected images it was possible to observe that the SPI covered the oil droplets, which were presented as green spheres when observed individually (Figure 4a1, b1, c1, d1). High-methoxyl pectin, in turn, interacted with protein and this interaction could be observed as the orange regions in the overlaps (Figure 4a3, b3, c3, d3). In addition, HMP is also dispersed in the continuous phase presenting as a net when observed individually (Figure 4a2, b2, c2, d2) and in red regions in overlapped images. The pectin excess in the samples seems to contribute to emulsion stability, preventing droplet movement, in addition to increasing the repulsion among them due to excess of negative charges.

The emulsion O26S56P360 (Figure 4b) was stable for more than 7 days and it was possible to notice a different microstructure from the others, presenting smaller droplets that were homogeneously distributed in the continuous phase, with lower degree of flocculation. On the other hand, droplet clusters could be clearly visualized in the images of assays O14S74P360 (Figure 4a) and O26S74P360 (Figure 4d).

Scanning electron microscopy

The microstructure of emulsions or creamed phases was also analyzed by scanning electron microscopy. Figure 5 shows images collected at 600×-magnification for the assays O14S74P360, O26S56P360, O26S74P240, and O26S74P360.

Figure 5. Images of assays O14S74P360 (a), O26S56P360 (b), O26S74P240 (c), and O26S74P360 (d) by scanning electron microscopy at 600×-magnification.

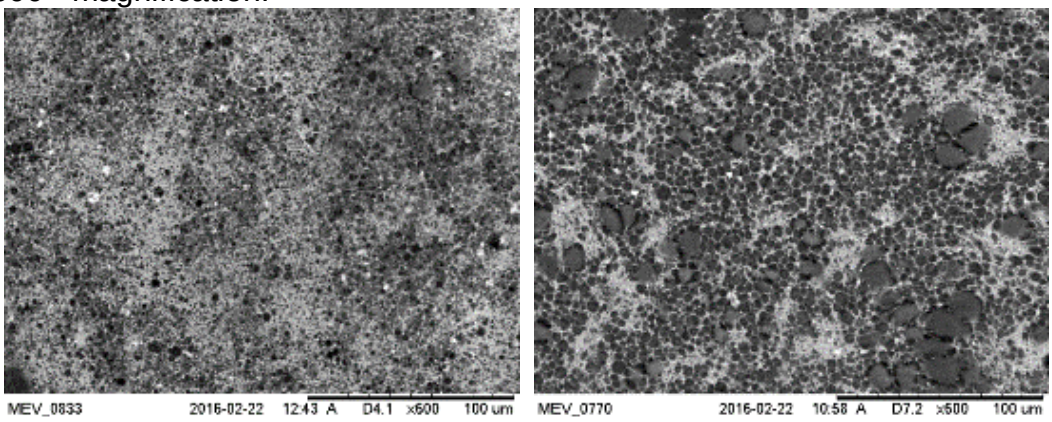

(a) (b)

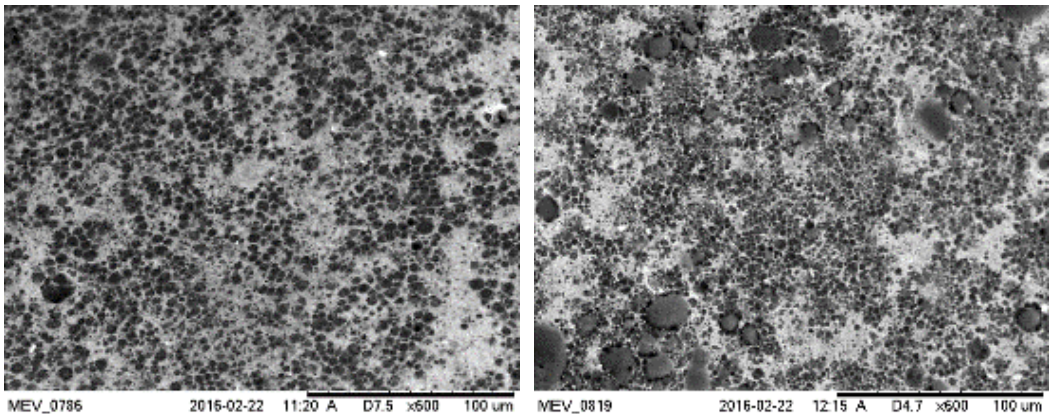

(c) (d)

It was possible to note a dense continuous phase, probably due to presence of high-methoxyl pectin excess and buriti oil droplets embedded into this biopolymer matrix. Comparing the images, once more it was possible to notice a difference in morphology comparing different formulations. The droplets of O14S74P360 assay (Figure 5a), for example, are small and more flocculated, presenting regions containing only continuous phase (lighter regions). Droplets of different sizes could be noted comparing images of O26S56P360 (Figure 5b) and O26S74P360 (Figure 5d) assays.

3.7. Experimental validation of the models obtained for emulsion production

In order to produce a stable emulsion with high carotenoids and tocopherols content, which corresponds to a higher buriti oil content, with reduced size droplets, low electrical conductivity, and high electrical charge, the optimal values for the independent variables were fixed as 28% buriti oil, 55% SPI, and homogenization pressure of 380 bar.

The observed results, as well as those predicted by the regression models (Table 3) for the validation assay are presented in Table 5, as well as the fitting and relative errors. The obtained results were consistent with those expected and, due to proximity of the experimental and predicted results, the relative errors were low, suggesting that the experimental design was adequate to obtain predictive models for production of buriti oil emulsions.

Table 5. Experimental results and values predicted by the regression models and errors for the RCCD validation assay.

Analyses	Experimental results	Predict results	Fitting error	Relative error (%)
Creaming index (%)	0.00 (±0.00)	- *	-	-
Droplet size OM (µm)	4.58 (±1.14)	5.01	0.43	8.58
Droplet size LD (µm)	38.18 (±0.34)	44.47	6.29	14.14
Electrical conductivity (mS/cm)	2.23 (±0.03)	2.34	0.11	4.70
Zeta potential (mV)	-17.65 (±0.73)	-20.11	-2.46	12.23

*The model predicts that there would be no creaming index.

The images obtained by optical microscopy, SEM and CLSM (Figure 6) allowed to observe the optimized buriti oil emulsion morphology.

Figure 6. Images of the RCCD validation assay obtained by optical microscopy with a 40×-magnification objective (a) (bars correspond to 20 µm), SEM with a 600×-magnification (b), and CLSM with a 40×-magnification (c1, c2 and c3).

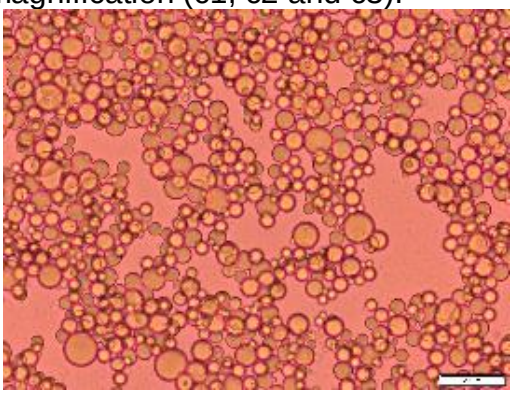

(a)

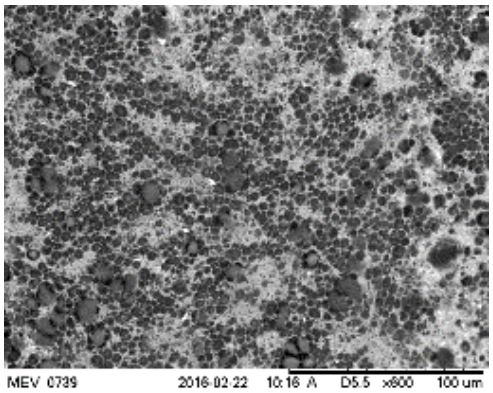

(b)

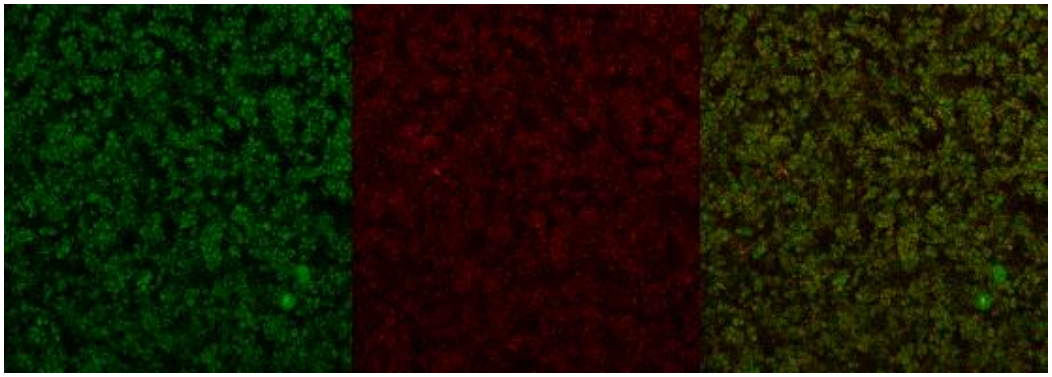

(c1) (c2) (c3)

Figure 7 shows the apparent viscosity curves (Figure 7a) obtained by steady shear tests, the mechanical spectra obtained by oscillatory shear (Figure 7b) and phase angle (Figure 7c) of optimized buriti oil emulsion. The pseudoplastic behavior of this system was confirmed by the Sisko viscosity model good fitting. The mechanical spectra revealed the sample was located in the viscoelastic plateau region and its microstructure revealed weak gel characteristics.

Figure 7. Apparent viscosity curves (a), storage (*G'* - closed symbols) and loss (*G"* - open symbols) moduli as a function of frequency (b), and loss tangent, Tan (*δ*) (c) for the RCCD validation assay.

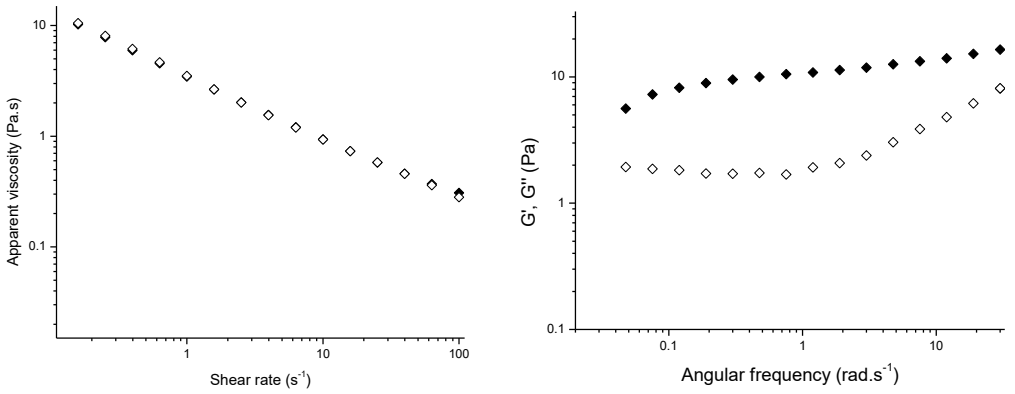

(a)

(b)

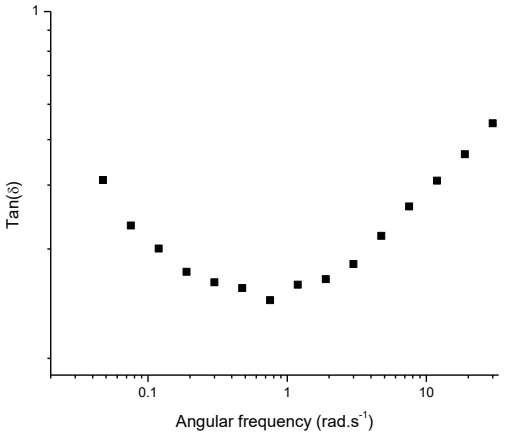

(c)

4. CONCLUSIONS

The RCCD experimental design was suitable for investigating formation of buriti oil emulsions stabilized by SPI and HMP electrostatic interactions. Through this investigation, it was possible to obtain an optimized emulsion, produced with 28% buriti oil, 55% SPI in the continuous phase, and homogenized at 380 bar, which was stable for at least 7 days, presenting reduced droplet size (4.58 µm), low electrical conductivity (2.23

mS/cm), and high modulus of negative charges (-17.65). This emulsion presented behavior typical of a weak gel. An excess of pectin in the continuous phase was observed to contribute to the emulsion stability.

5. ACKNOWLEDGEMENTS

This work was supported by the Sao Paulo Research Foundation, FAPESP, Brazil [grant numbers 2014/08520-6, 2014/02910-7] and Coordination for the Improvement of Higher Level Personnel, CAPES, Brazil.

6. REFERENCES

Abdolmaleki, K., Mohammadifar, M. A., Mohammadi, R., Fadavi, G., Meybodi, N. M., 2016. The effect of pH and salt on the stability and physicochemical properties of oil-in-water emulsions prepared with gum tragacanth. Carbohydr. Polym. 140(1), 342-348.

Albano, K. M., Franco, C. M. L., Telis, V. R. N., 2014. Rheological behavior of Peruvian carrot starch gels as affected by temperature and concentration, Food Hydrocoll. 40(1), 30-43.

Albano, K. M., Nicoletti, V. R., 2018. Ultrasound impact on whey protein concentrate-pectin complexes and in the O/W emulsions with low oil soybean content stabilization. Ultrason. Sonochem. 41(1), 562–571.

Bataglion, G. A., Silva, F. M. A., Santos, J. M., Barcia, M. T., Godoy, H. T., Eberlin, M. N., Koolen, H. H. F., 2015. Integrative approach using GC-MS and Easy Ambient Sonic-Spray Ionization Mass Spectrometry (EASI-MS) for comprehensive lipid characterization of buriti (*Mauritia flexuosa*) oil. J. Braz. Chem. Soc. 26(1), 171-177.

BeMiller, J. N., Whistler, R. L., 1996. Carbohydrates. In: Fennema, O. R. (Ed.). Food Chemistry. New York, USA: Marcel Decker.

Benichou, A., Aserina, A., Garti, N., 2002. Protein-polysaccharide interactions for stabilization of food emulsions. J. Disper. Sci. Technol. 23(1-3), 93-123.

Bruttel, P. A., 2004. Conductometry – Conductivity measurement. Herisau, Switzerland: Metrohm Ltd.

Canteri, M. H. H., Moreno, L., Wosiacki, G., Scherr, A. P., 2012. Pectina: da matéria-prima ao produto final. Polímeros 22(2), 149-157.

Chamberlain, E. K., Rao, M. A., 2000. Effect of concentration on rheological properties of acid-hydrolyzed amylopectin solutions. Food Hydrocoll. 14(2), 163-171.

Chambon, F., Winter, H. H., 1987. Linear viscoelasticity at the gel point of a crosslinking PDMS with imbalanced stoichiometry. J. Rheol. 31(8), 683-697.

De Rosso, V. V., Mercadante, A. Z., 2007. Identification and quantification of carotenoids, by HPLC-PDA-MS/MS, from amazonian fruits. J. Agric. Food Chem. 55(1), 5062-5072.

Derkach, S. R., 2009. Rheology of emulsions. Adv. Colloid Interface Sci. 151 (1), 1–23.

Diao, X., Guana, H., Zhao, X., Chena, Q., Kong, B., 2016. Properties and oxidative stability of emulsions prepared with myofibrillar protein and lard diacylglycerols. Meat Sci. 115(1), 16–23.

Dickinson, E., 2003. Hydrocolloids at interfaces and the influence on the properties of dispersed systems. Food Hydrocoll. 17(1), 25-39.

Freitas, M. L. F., Albano, K. M., Telis, V. R. N., 2017a. Characterization of biopolymers and soy protein isolate-high-methoxyl pectin complex. Polímeros 27(1), 62-67.

Freitas, M. L. F., Chisté, R. C., Polachini, T. C., Sardella, L. A. C. Z., Aranha, C. P. M., Ribeiro, A. P. B., Nicoletti, V. R., 2017b. Quality characteristics and thermal behavior of buriti (*Mauritia flexuosa* L.) oil. Grasas Aceites, 68(4), 220-228.

Gancz, K., Alexander, M., Corredig, M., 2005. Interactions of high methoxyl pectin with whey proteins at oil/water interfaces. J. Agric. Food Chem. 53(1), 2236-2241.

Guinazi, M., Milagres, R. C. R. M., Pinheiro-Sant'Ana, H. M., Chaves, J. B. P., 2009. Tocoferois e tocotrienois em óleos vegetais e ovos. Quím. Nova 32(8), 2098-2103.

Hunter, R. J., 2001. Foundations of Colloid Science. New York, USA: Oxford University Press.

Ikeda, S., Nishinari, K., 2001. "Weak-gel" type rheological properties of aqueous dispersions of nonaggregated k-carrageenan helices. J. Agric. Food Chem. 49(9), 4436-4441.

Kaltsa, O., Michon, C., Yanniotis, S., Mandala, I., 2013. Ultrasonic energy input influence on the production of sub-micron o/w emulsions containing whey protein and common stabilizers. Ultrason. Sonochem. 20(1), 881-891.

Lam, M., Paulsen, P., Corredig, M., 2008. Interactions of soy protein fractions with high-methoxyl pectin. J. Agric. Food Chem. 56(1), 4726–4735.

Lam, M., Shen, R., Paulsen, P., Corredig, M., 2007. Pectin stabilization of soy protein isolates at low pH. Food Res. Int. 40(1), 101-110.

Lamprecht, A., Schafer, U. F., Lehr, C. M., 2000. Characterization of microcapsules by confocal laser scanning microscopy: Structure, capsule wall composition and encapsulation rate. Eur. J. Pharm. Biopharm. 49(1), 1-9.

Levic, S., Lijakovic, I. P., Dordevic, V., Rac, V., Rakic, V., Knudsen, T. S., Pavlovic, V., Bugarski, B., Nedovic, V., 2015. Characterization of sodium alginate/D-limonene emulsions and respective calcium alginate/D-limonene beads produced by electrostatic extrusion. Food Hydrocoll. 45(1), 111-123.

Lopes da Silva, J. A., Gonçalves, M. P., 1994. Rheological study into the ageing process of high methoxyl pectin/sucrose aqueous gels. Carbohydr. Polym. 24(1), 235-245.

Marfil, P. H. M., Telis-Romero, J. Telis, V. R. N., 2012. Rheological behavior of biopolymer suspensions. In V. R. N. TELIS (Ed.), Biopolymer engineering in food processing (pp. 69-110). Boca Raton, USA: CRC Press.

McClements, D. J., 1999. Food emulsions. Principles, practice, and techniques. Boca Raton, USA: CRC Press.

McClements, D. J., Decker, E. A., Weiss, J., 2007. Emulsion-based delivery systems for lipophilic bioactive components. J. Food Sci. 75(8), 109-124.

McKenna, B. M., Lyng, J. G., 2003. Introduction to food rheology and its measurements. In B. M. McKenna (Ed.), Texture in food, volume 1: Semi-solid foods (pp. 130-160). Boca Raton, USA: CRC Press.

Mukai-Correa, R., Prata, A. S., Alvim, I. D., Grosso, C., 2005. Caracterização de microcápsulas contendo caseína e gordura vegetal higrogenada obtidas por gelificação iônica. BJFT, 8(1), 73-80.

Murray, B. S., Phisarnchananan, N., 2016. Whey protein microgel particles as stabilizers of waxy corn starch + locust bean gum water-in-water emulsions. Food Hydrocoll. 56(1), 161-169.

Perrechil, F. A., Cunha, R. L., 2013. Stabilization of multilayered emulsions by sodium caseinate and κ-carrageenan. Food Hydrocoll. 30(1), 606-613.

Rao, M. A., 1999. Rheology of fluid and semisolid foods. Gaithersburg, USA: Aspen Publication.

Richter, S., 2007. Comparison of critical exponents determined by rheology and dynamic light scattering on irreversible and reversible gelling systems. Macromol. Symp. 256(1), 88-94.

Rodd, A. B., Cooper-White, J., Dunstan, D. E., Boger, D. V., 2001. Gel point studies for chemically modified biopolymer networks using small amplitude oscillatory rheometry. Polymer, 42(1), 185-198.

Rodrigues, M. I., Iemma, A. F., 2009. Planejamento de experimentos e otimização de processos, second ed. Campinas, Brazil: Casa do Espírito Amigo Fraternidade Fé e Amor.

Rodriguez-Amaya, D. B., 1996. Assessment of the provitamina A contents of foods - The Brazilian experience. J. Food Compos. Anal. 9(1), 196-230.

Schultz, S., Wagner, G., Urban, K., Ulrich, J., 2004. High-pressure homogenization as a process for emulsion formation. Chem. Eng. Technol. 27(1), 361–368.

Serfert, Y., Schroder, J., Mescher, A., Laackmann, J., Ratzke, K., Shaikh, M. Q., Gaukel, V., Moritz, H. U., Schuchmann, H. P., Walzel, P., Drusch, S., Schwarz, K., 2013. Spray drying behavior and functionality of emulsions with β-lactoglobulin/pectin interfacial complexes. Food Hydrocoll. 31(1), 438-445.

Silva, S. M., Sampaio, K. A., Taham, T., Rocco, S. A., Ceriani, R., Meirelles, A. J. A., 2009. Characterization of oil extracted from buriti fruit (Mauritia flexuosa) grown in the Brazilian amazon region. J. Am. Oil Chem. Soc. 86(1), 611-616.

Singh, M., Mohamed, A., 2007. Influence of gluten-soy protein blends on the quality of reduced carbohydrates cookies. Food Sci. Technol. 40(2), 353-360.

Steffe, F. L., 1996. Rheological methods in food process engineering. East Lansing, USA: Freeman Press.

Tromp, R. H., de Kruif, C. G., van Eijk, M., Rolin, C., 2004. On the mechanism of stabilization of acidified milk drinks by pectin. Food Hydrocoll. 18(1), 565–572.

Walstra, P., 2003. Physical chemistry of foods. New York, USA: Marcel Decker.

Xianquan, S., Shi, J., Kakuda, Y., Yueming, J., 2005. Stability of lycopene during food processing and storage. J. Med. Food 8(4), 413-422.

CAPÍTULO 5

Efeito da adição de maltodextrina em emulsões óleo em água para produção de microcápsulas de óleo de buriti (*Mauritia flexuosa*) por secagem por atomização

Esse estudo será submetido como artigo científico para possível publicação.

Effect of maltodextrin addition in oil-in-water emulsion for production of buriti (*Mauritia flexuosa*) oil microcapsules by spray drying

Mírian Luisa Faria Freitas[a*], Yrjö Henrik Ross[b], Ana Paula Badan Ribeiro[c], Vânia Regina Nicoletti[a]

[a]*São Paulo State University (UNESP), Institute of Biosciences, Humanities and Exact Sciences (IBILCE), Campus São José do Rio Preto, 2265 Cristóvão Colombo Street, Jardim Nazareth, São José do Rio Preto, São Paulo, 15.054-000, Brazil.*

[b]*University College Cork (UCC), College of Science, Engineering and Food Science, School of Food and Nutritional Sciences, College Road, Cork, Postal Code T12 YN60, Ireland.*

[c]*University of Campinas (UNICAMP), Department of Food Technology (DTA), School of Food Engineering (FEA), Bertrand Russel Street, Cidade Universitária, Campinas, São Paulo, 13.083-970, Brazil.*

[*]Corresponding author:
São Paulo State University (UNESP), Institute of Biosciences, Humanities and Exact Sciences (IBILCE), Campus São José do Rio Preto, 2265 Cristóvão Colombo Street, Jardim Nazareth, São José do Rio Preto, São Paulo, 15.054-000, Brazil.
e-mail: mirianlfreitas@yahoo.com.br
Telephone number: 55 17 98116-8134

Abstract: Buriti (*Mauritia flexuosa*) oil presents high concentration of monounsaturated fatty acids and is a recognized source of bioactive compounds such as β-carotene and tocopherols. In addition to the difficulty of dispersing lipids in food products, unsaturated fatty acids are susceptible to oxidation, whereas bioactive compounds are sensitive to temperature, light, oxygen, and moisture. Lipid encapsulation presents some advantages such as retarding oxidation, increasing stability and modulating release of lipophilic compounds. This work aimed to produce carotenoid-rich microcapsules by spray drying of buriti oil emulsions stabilized by soy protein isolate (SPI) and high-methoxyl pectin (HMP), added with maltodextrin as a drying aid. Microcapsules were produced by spray drying of emulsions containing 28 g/100 g buriti oil and 1.8 g/100 g wall material (55 g/100 g SPI and 45 g/100 g HMP) added with maltodextrin at different contents: 0.75, 1.00, and 1.25 g maltodextrin/g total solids in the emulsion. The microcapsules were analyzed for colour, moisture content, encapsulation yield, particle size distribution, encapsulation efficiency and retention of carotenoids, encapsulation efficiency and retention of oil, water sorption, water plasticization and mechanical relaxation, and morphology by optical and scanning electron microscopy. Significant differences ($p \leq 0.05$) were observed in colour, yield, encapsulation efficiency, and carotenoid retention. Microcapsules produced with higher maltodextrin content presented lower colour intensity, but the hue angle was around 77°, between orange and yellow; on the other hand, the highest maltodextrin content resulted in higher yield (58.4% w/w), encapsulation efficiency (63.7% w/w), and carotenoid retention (53.3% w/w). Moisture content was around 0.70% w/w (d.b.) and particle size distribution was unimodal, with mean diameter around 30 μm. The glass transition and relaxation temperatures of the microcapsules were dependent on relative humidity and mechanical relaxation occurred at least 30 °C above the glass transition temperature. The microcapsules were poly-nucleated, spherical, with few wrinkles, no apparent cracks, and presence of some aggregates. The

results showed that the produced buriti oil microcapsules are suitable for application in carotenoid enrichment of foods, as well as a natural dye.
Keywords: Bioactive compounds, carotenoid-rich microcapsules, emulsion spray drying, protein/pectin complex, encapsulation efficiency, carotenoid retention, scanning electron microscopy, glass transition temperature, relaxation temperature.

1. INTRODUCTION

Native palm trees belonging to the Arecaceae family are among the most useful vegetable resources in the Amazonia. The fruits of these palm trees are not only alternative foods for the local population, but also source of a high-quality oil (Santos et al., 2013). Buriti oil has a high concentration of monounsaturated fatty acids, in higher content than those found in foods recognized to present high nutritional quality oils, such as olive oil or Brazil nut oil (França et al., 1999; Silva et al., 2009). Buriti oil also contains β-carotene in higher concentrations than foods widely consumed by Brazilians, such as carrots, guava, pitanga, papaya, passion fruit and other fruits from the Amazonia, including palm nuts, peach palm and tucumã (Rodriguez-Amaya, 1996; De Rosso and Mercadante, 2007), besides presenting high levels of tocopherols (Freitas et al., 2017).

Carotenoids are a diversified group of lipophilic components, with β-carotene being a pro-vitamin A, with 100% of activity (Rodriguez-Amaya, 1996; McClements, Decker and Weiss, 2007). Tocopherols are important antioxidants and present vitamin E activity, especially α-tocopherol (De Greyt and Kellens, 2005).

In general, lipids are difficult to disperse in food products, and polyunsaturated fatty acids are especially susceptible to oxidation, resulting in unpleasant aromas and formation of toxic compounds. In addition, the bioactive compounds present in lipids are sensitive to temperature, light, oxygen and moisture (Guinazi et al., 2009). Microencapsulation by spray

drying is a feasible process to overcome these difficulties (Gouin, 2004; Gharsallaoui et al. 2007).

The interfacial structure preservation is of utmost importance to ensure high efficiency of microencapsulation and to maintain the desired functionality. Accordingly, emulsions drying requires the use of a wall material capable to forming a continuous matrix in order to cover the oil droplets in dried material (Serfert et al., 2013). The chemical functionality, solubilization, and diffusion of the encapsulated material throught the matrix determine the degree of core retention during microcapsule production by atomization, so that the stability during storage is highly dependent on the wall material composition (Gharsallaoui et al., 2007).

Proteins and polysaccharides are normally used as natural hydrocolloids in the food industry. The combination, in the same system, of the protein advantages (rapid adsorption compared to polysaccharide) and polysaccharides (steric repulsion or viscosity enhancement) to stabilize emulsions has been increasingly studied (Aberkane, Roudaut and Saruel, 2014). The emulsifying and stabilizing properties of proteins and polysaccharides contribute to emulsions with better stability and functional characteristics (Bouyer et al., 2012). Lam et al. (2007) demonstrated that high-methoxyl pectin (HMP) showed higher stability than low-methoxyl pectin in acidic solutions of soy protein isolate (SPI). Jaramillo, Roberts and Coupland (2011) observed that soy protein isolate-pectin complexes near the SPI isoelectric point were able to withstand heat treatment, despite some modifications in their properties.

Carbohydrates such as starches, maltodextrins, and corn syrup are generally used to microencapsulate food ingredients. These materials are considered as good encapsulating agents because of their low viscosities at high solid content and good solubilization, but most of them lack the interfacial properties required for high microencapsulation efficiency and are generally associated with other encapsulating materials, such as proteins or gums (Gharsallaoui et al., 2007). Maltodextrins provide good oxidative

stability to the encapsulated oil but exhibit poor emulsifying ability providing low emulsion stability and low oil retention (Kenyon, 1995). In contrast, proteins have an amphiphilic character that provide physical-chemical and functional properties necessary to encapsulate hydrophobic materials. Pectin, in turn, is a polymer capable of assisting in stable emulsions production at low concentration (Gharsallaoui et al., 2007).

The spray drying technique was successfully used by Serfert et al. (2013) to encapsulate fish oil emulsion stabilized by β-lactoglobulin and pectin with addition of glucose syrup, reaching microencapsulation efficiency above 95%. Aberkane, Roudaut, and Saruel (2014) observed maximun encapsulation efficiency and minimun lipid oxidation in microcapsules produced by adding maltodextrin to oil emulsions rich in omega-3 fatty acids stabilized by pea protein and pectin before spray drying.

Encapsulation processes generally use materials capable of forming vitreous structures to protect the interest compounds. The vitreous state of these solids forms during the drying process by fast removal of water, leading the material to go through a reversible glass transition (Roos, 2010). Water sorption and water plasticization are important physicochemical properties of microcapsules and are related to stability during processing and storage (Roos, 1995; Rahman, 2009). Correlation between water sorption and water plasticization is often used to determine critical moisture content (CMC) and critical water activity (CAW) for defined processing or storage temperatures (Roos, 1995; Nurhadi; Roos; Maidannyk, 2016). Plasticization of non-crystalline structures due to increasing temperature or moisture sorption reduces the relaxation time exponentially above the glass transition, resulting in a rapid deterioration of the product, whereas materials with water content below their respective CMC, present greater stability, especially in terms of physical stability (Roos, 1995; Roos, 2010).

Considering this scenario, this work aimed the production and characterization of microcapsules by spray drying of buriti oil-in-water

emulsions stabilized by SPI and HMP in order to improve the oil compounds stability, as well as broadening its application possibilities in food industry.

2. MATERIAL AND METHODS

2.1. Material

The raw materials used were buriti oil (Amazon Oil Industry™), soy protein isolate (SPI) (Tovani Benzaquen Ingredientes™), high-methoxyl pectin (HMP) (CP Kelco™), and maltodextrin DE 10 (Get do Brasil™). Preparation of samples used deinozed water, sodium azide (Dinâmica™), hydrochloric acid (Dinâmica™) or sodium hydroxide (Dinâmica™) solutions (1 N), and McIlvaine buffer (pH 3.5) prepared using disodium phosphate and citric acid (Dinâmica™).

2.2. Buriti oil emulsion preparation

Previous studies carried out by the research group permited the development of a stable buriti oil emulsion for more than 7 days and with a high content of carotenoids and tocopherols. This emulsion was elaborated containing 28 g/100 g buriti oil and 1.8 g/100 g wall material, which was composed of 55 g/100 g SPI and 45 g/100 g HMP.

The emulsion was prepared using McIlvaine buffer at pH 3.5, which is below the isoelectric point of SPI and allows the biopolymers in solution to acquire opposite charges in a sufficient amount to form electrostatic complexes that remain dispersed in the aqueous phase (Freitas, Albano and Telis, 2017). Stock solutions of SPI (3 g/100 g) were prepared by dispersing the protein in half of the required water and adjusting pH 11.0 (± 0.05) with NaOH for complete solubilization, subjected to magnetic stirring for 3 h, left at rest overnight (25 °C) for complete hydration, and finally completing the water content with buffer pH 3.5. Stock solutions of HMP (2 g/100 g) were prepared by dispersion in buffer solution at pH 3.5, 3 h under magnetic stirring, and overnight hydration at 25 °C. Sodium azide 0.04%

was added to stock solutions to prevent microorganism growth (Freitas, Albano and Telis, 2017).

Buriti oil was dispersed in the SPI stock solution using Ultra Turrax stirrer (T-25, IKA, Germany) at 15000 rpm for 4 minutes, followed by addition of HMP stock solution, and dispersion at 15000 rpm for 4 minutes using the same stirrer. After this procedure, the coarse emulsion was homogenized at 380 bar in a double stage homogenizer (SPX Flow Technology, Lab Serie APV-2000), without sample recirculation.

2.3. Microencapsulation by spray drying

Buriti oil microcapsules were produced using the buriti oil emulsion added with maltodextrin DE 10, in the ratios of 1:0.75; 1:1 and 1:1.25 [solids present in the emulsion]:[maltodextrin]. The maltodextrin dispersion into emulsion was performed using Ultra Turrax stirrer at 15000 rpm for 10 minutes.

According to Rosenberg, Kopelman and Talmon (1990) and Gharsallaoui et al. (2007) the emulsion viscosity has a significant effect on microencapsulation by spray drying, with high viscosities interfering in atomization process and leading to large elongated droplets formation which adversely affects the drying rate. To minimize this effect, the emulsions were maintained at 40 °C during feed into the system.

The emulsions were dried in a spray dryer (B-290, Büchi, Switzerland) using double-fluid spray nozzle. The equipment was fed through a peristaltic pump and, after some tests, the defined drying conditions were: feeed flow rate 3 mL/min, atomization air rate of 500 L/h, inlet air temperature 180 °C, and aspiration of 35 m^3/h. The outlet air temperature was measured during drying and varied between 119 and 123 °C.

2.4. Characterization of the microcapsules

2.4.1. Color parameters

Color parameters were measured using a Konica Minolta colorimeter (CR-S, Konica Minolta, Japan) calibrated for the CIELab coordinates, measuring the parameter *L** (lightness) and the chromaticity coordinates *a** (+*a** = red, -*a** = green) and *b** (+*b** = yellow, -*b** = blue), through which Chroma (*C*) (Equation 1) and Hue Angle (*h*) (Equation 2) were calculated.

$$C = \sqrt{(a^*)^2 + (b^*)^2} \quad (1)$$

$$h = \tan^{-1}\left(\frac{b^*}{a^*}\right) \quad (2)$$

2.4.2. Moisture content

The moisture content of microcapsules was determined gravimetrically by drying 1.5 g of samples in a vacuum oven (Marconi, MA 030) at 70 °C until constant weight.

2.4.3. Encapsulation yield

The encapsulation yield was determined as the ratio between the mass of solids in the dried powder and the mass of solids in the emulsion feed to the dryer. The calculation was carried out by Equation 3:

$$YV(\%) = \frac{m_{sol,pow}}{m_{sol,feed}} \times 100 = \frac{m_{pow} \times X_{sol,pow}}{m_{feed} \times X_{sol,feed}} \times 100 \quad (3)$$

in which *YV* is the yield value (% w/w), *m* is the mass (g), and X_{sol} is the solids content (g solids/g powder or feed). The subscripts *pow* and *feed* refer to the dried powder and the emulsion fed to the dryer, respectively.

2.4.4. Particle size distribution

Particle size distribution was measured by static light scattering method using the instrument Horiba LA-950E (Particle Sizing Systems,

Japan). The mean particle diameter $D_{[4,3]}$ or De Brouckere diameter and the width of particle size distribution, *span*, were calculated according to Equations 4 and 5, respectively.

$$D_{[4,3]} = \frac{\sum n_i d_i^4}{\sum n_i d_i^3} \quad (4)$$

$$Span = \frac{D_{90} - D_{10}}{D_{50}} \quad (5)$$

in which *n* is the particle number, *d* is the particle diameter and D_{10}, D_{50} and D_{90} are the diameters at 10%, 50% and 90% cumulative volumes, respectively (Jafari, He and Bhandari, 2007).

2.4.5. Encapsulation efficiency (EEC) and retention (RTC) of carotenoids

The encapsulation efficiency (EEC) and retention (RTC) of carotenoids were calculated by quantifying the initial carotenoids present in buriti oil (IC), the carotenoids present on microcapsule surface (SC), and the total carotenoids present in microcapsules (TC), as described by Aranha (2015) with some modifications. The amount of carotenoids in buriti oil (IC) was determined by wheighing an aliquot of 25 mg of buriti oil into a 10 mL volumetric flask and completing the volume with chloroform. The absorbance was measured (spectrophotometer Biospectro SP-220) at 465 nm and carotenoids, expressed in β-carotene, were determined by Equation 6:

$$C = \frac{Abs \times V \times 10^4}{2396 \times m} \quad (6)$$

in which *C* is the carotenoid concentration (μg of β-carotene/g sample), *Abs* is the absorbance reading ($\dot{A}$), *V* is the dilution volume (mL), and *m* is the sample mass (g).

The carotenoids present on microcapsule surface (SC) where quantified by mixing 50 mg of microcapsules and 5 mL of chloroform in a capped test tube and stirring manually for one minute. After stirring, the

organic phase was filtered and transferred to a 5 mL volumetric flask and the volume was completed with chloroform. The absorbance was measured at 465 nm and the carotenoids, expressed in β-carotene, were determined by Equation 6.

The total carotenoids present in the microcapsules (TC) were analyzed by dispersing 100 mg of microcapsules in 20 mL of McIlvaine buffer at pH 7.4, stirring in a vortex (Phoenix Luferco AP 56) for 30 seconds, and resting for 12-14 hours. Then, 25 mL of chloroform were added to the dispersion, stirred in vortex for 30 seconds and sonicated (Ultrasonic Cleaner 5040D) for 20 minutes, forming a two-phase system. The aqueous and organic phases were separated by centrifugation (Hermle centrifuge, Z 326 K) at 1800 rpm for 10 minutes and the organic phase was transferred to a 25 mL volumetric flask, completing the volume with chloroform. The absorbance was read at 465 nm and the carotenoids, expressed in β-carotene, were determined by Equation 6.

The encapsulation efficiency (EEC) and retention (RTC) of carotenoids were calculated, respectively, by Equations 7 and 8:

$$\%EEC = \frac{TC-SC}{TC} \times 100 \quad (7)$$

$$\%RTC = \frac{TC \times m_{pow}}{IC \times m_{oil}} \times 100 \quad (8)$$

in which m_{pow} is the total mass of microcapsules powder obtained e m_{oil} is the total mass of oil in the emulsion.

2.4.6. Encapsulation efficiency (EEO) and retention (RTO) of oil

The encapsulation efficiency (EEO) and retention (RTO) of buriti oil were calculated based on the oil content initially present in the emulsion (IO), the oil present on microcapsule surface (SO) and total oil present in the microcapsules (TO), based on methodology described in item 2.4.5 and methodology described by Tonon, Grosso and Hubinger (2011).

The oil present on microcapsule surface (SO) was quantified by mixing 50 mg of microcapsules and 5 mL of chloroform in a capped test tube and stirring manually for one minute; the organic phase was then filtered and transferred to a Petri dish. The solvent was first allowed to evaporate at room temperature in a fume hood, and then in an oven at 60 °C until constant weight. The extracted oil residue was taken as the surface oil.

The total oil present in the microcapsules (TO) was analyzed by dispersing 100 mg of microcapsules in 20 mL of McIlvaine buffer at pH 7.4, stirring in a vortex (Phoenix Luferco AP 56) for 30 seconds, and resting for 12-14 hours. The dispersion was mixed with 25 mL of chloroform under vortex stirring for 30 seconds and sonication (Ultrasonic Cleaner 5040D) for 20 minutes, forming a two-phase system. The aqueous and organic phases were separated by centrifugation (Hermle centrifuge, Z 326 K) at 1800 rpm for 10 minutes and the organic phase was transferred to a Petri dish. The solvent was first allowed to evaporate at room temperature in a fume hood, and then in an oven at 60 °C until constant weight. The total oil was taken as the extracted oil residue.

The encapsulation efficiency (EEO) and retention (RTO) of buriti oil were calculated, respectively, by Equations 9 and 10:

$$\%EEO = \frac{TO-SO}{TO} \times 100 \quad (9)$$

$$\%RTO = \frac{TO \times m_{pow}}{IO} \times 100 \quad (10)$$

in which m_{pow} is the total mass of powder obtained.

2.4.7. Water sorption isotherms

Water sorption isotherms were determined by storing the microcapsules in desiccators containing different saturated salt solutions: LiCl, CH_3COOK, $MgCl_2$, K_2CO_3, $Mg(NO_3)_2$, $NaNO_2$, and NaCl, correponding to water activity values of 0.11, 0.23, 0.33, 0.43, 0.53, 0.65, and 0.75,

respectively, at room temperature (Nurhadi, Roos and Maidannyk, 2016). During storage in vacum desiccators, the samples were weighed regularly along three weeks. The equilibrium water content for microcapsules at each water activity was calculated based on the weight gain. Analysis were carried out in triplicate. A second order polynomial (Equation 11) was fitted to relate water activity of microcapsules and their water content.

$$\frac{a_w}{X} = a \cdot {a_w}^2 + b \cdot a_w + c \quad (11)$$

in which a_w is the water activity and X is the water content (g water/g dry solids).

2.4.8. Water plasticization

About 10 mg of buriti oil microcapules where wheighed in a standard 40 µl aluminum pan and equilibrated in desiccators over various relative humidities for three weeks. The pans were then hermetically sealed and analyzed in a differential scanning calorimeter (DSC, Mettler Toledo, Schwerzebach, Switzerland). Three cycles of scanning were used (heating-cooling-heating) at heating rate of 5 °C/min and cooling rate of 10 °C/min. The temperature scanning range at a_w of 0.11 was 0 - 120 °C, and at a_w of 0.23; 0.33; 0.43; 0.53; 0.65 and 0.75 was 0 - 100 °C. The second heating scans were used to determine the glass transition temperatures using the STARe software version 8.10 (Mettler Toledo Schwerzenbach, Switzerland).

2.4.9. Mechanical relaxation

The mechanical relaxation of buriti oil microcapsules at a_w of 0.11; 0.23; 0.33; 0.43; 0.53 and 0.65 was studied using a dynamic mechanical analyzer (Tritec 2000 DMA, Triton Technology Ltd., UK) according to Fan and Roos (2016). The storage modulus, *E'*, and loss modulus, *E"*, as functions of temperature at different frequencies (0.5, 1, 2, and 5 Hz) were determined. The DMA instrument was balanced or set at zero to determine

the zero displacement position and return the force to the zero position before starting an experiment. Samples of approximately 100 mg were spread on a metal pocket-forming sheet (Triton Technology Ltd., UK). The sheet with the sample was crimped along a pre-scored line to form a thin sandwich pocket. This pocket was attached directly between the clamps (the fixed clamp and the driveshaft clamp) inside the measuring head of the DMA. The length, width, and thickness (~1.5 mm) of the sample pocket between the clamps were measured. Triplicate samples of each material were analyzed using dynamic measurements and recorded using DMA software version 1.43.00. Samples were scanned in heating from 20 to 140 °C at rate of 2 °C/min. During dynamic heating, the samples were analyzed for relaxation temperature, *T*, determined from the peak temperature of $\tan(\delta) = E''/E'$.

The structural relaxation time, τ, and the relaxation temperature, *T*, were modeled and analyzed using the Williams-Landel-Ferry, WLF, model (Equation 12). The τ was defined by oscillation frequency set in DMA measurement ($\tau = 1/2\,\pi f$). The WLF model constants C_1 and C_2 can be derived from a plot of $1/\log(\tau/\tau_g)$ against $1/(T - T_g)$ using experimental relaxation times, τ, with the assumption of $\tau_g = 100\,s$ at the onset temperature of the calorimetric glass transition, T_g (Fan and Roos, 2016).

$$\log\left(\frac{\tau}{\tau_g}\right) = \frac{C_1(T-T_g)}{C_2+(T-T_g)} \tag{12}$$

2.4.10. Particle morphology

Optical microscopy

The microcapsule morphology was analyzed using an optical microscope (Olympus, CX31) with a 40×-magnification objective coupled with a digital camera (Olympus, SC30). The samples were dispersed on a slide using mineral oil and covered with a slide cover slip.

Scanning electron microscopy

SEM images were obtained in an INSPECT EBSD microscope with 500 and 1000×-magnification. The samples were immobilized on suitable supports with adhesive tape and covered with gold.

2.4.11. Statistical analysis

The microcapsule characterization results were submitted to Analysis of Variance (ANOVA) and Tukey's Test in order to detect significant differences of averages values at the probability level of 5% ($p \leq 0.05$).

3. RESULTS AND DISCUSSION

3.1. Color parameters

The microcapsules of buriti oil were analyzed by the color parameters: *L** (lightness), the chromaticity coordinates *a** (+*a** = red, -*a** = green) and *b** (+*b** = yellow, -*b** = blue), Chroma (*C*), and Hue Angle (*h*). Table 1 presents the averages obtained for these parameters along with the Tukey's averages test results.

The samples differed significantly from each other ($p \leq 0.05$) for all color parameters. Sample 1:0.75, containing the lowest maltodextrin content, presented the lowest lightness (*L**), whereas sample 1:1.25, containing the highest maltodextrin content, presented the highest lightness (*L**), suggesting that lower maltodextrin contents produce microcapsules with more intense color. In addition, sample 1:0.75 presented higher values for the chromaticity coordinates *a** and *b** and sample 1:1.25 presented lower values for these coordinates, showing that the microcapsules produced with lower maltodextrin contents presented more intense red/yellow coloration. Regarding to Chroma (*C*), sample 1:0.75 presented the highest value and sample 1:1.25 had the lowest one, that is, the higher

the maltodextrin content, the lower color saturation of the buriti oil microcapsules. Although the sample 1:0.75 had the lowest value and the sample 1:1.25, the highest value for Hue Angle (h), it is important to note that even these values were significantly different ($p \leq 0.05$), they differ in less than one radian degree and that all samples presented values for this parameter in the first quadrant and around 90 °, that is, closer to yellow color (90 °) in detriment to red color (0 °).

Table 1. Mean values obtained for the parameters of color lightness (*L**), chromaticity coordinates (*a** and *b**), Chroma (*C*) and Hue Angle (*h*); moisture content (dry basis); encapsulation yield; mean diameter and span; encapsulation efficiency (EEC) and retention (RTC) of carotenoids; and encapsulation efficiency (EEO) and retention (RTO) of oil of buriti oil microcapsules.

	Ratio (solids in the emulsion):(maltodextrin)		
	1:0.75	**1:1**	**1:1.25**
Color parameters			
*L**	76.93^{c} (±0.16)	78.18^{b} (±0.03)	79.41^{a} (±0.07)
*a**	19.88^{a} (±0.30)	18.52^{b} (±0.13)	17.42^{c} (±0.38)
*b**	83.57^{a} (±1.01)	79.54^{b} (±0.40)	79.05^{b} (±1.03)
C	85.90^{a} (±1.05)	81.67^{b} (±0.42)	80.94^{b} (±1.09)
h (degree)	76.62^{c} (±0.04)	76.90^{b} (±0.04)	77.57^{a} (±0.11)
Moisture content			
Moisture content (d.b.) (% w/w)	$0.68^{n.s.}$ (±0.02)	$0.71^{n.s.}$ (±0.04)	$0.70^{n.s.}$ (±0.04)
Encapsulation yield			
Yield value (% w/w)	50.45^{c} (±0.01)	51.35^{b} (±0.02)	58.37^{a} (±0.03)
Particle size			
Mean diameter (μm)	$35.35^{n.s.}$ (±13.54)	$30.40^{n.s.}$ (±0.14)	$32.34^{n.s.}$ (±0.97)
Span value	$1.66^{n.s.}$ (±0.40)	$1.52^{n.s.}$ (±0.01)	$1.86^{n.s.}$ (±0.05)
Encapsulation efficiency (EEC) and retention (RTC) of carotenoids			
EEC (% w/w)	54.88^{b} (±0.29)	$59.98^{a,b}$ (±1.63)	63.75^{a} (±4.68)
RTC (% w/w)	48.76^{b} (±0.19)	47.89^{b} (±1.16)	53.31^{a} (±1.81)
Encapsulation efficiency (EEO) and retention (RTO) of oil			
EEO (% w/w)	52.43^{c} (±1.65)	60.17^{b} (±0.98)	65.70^{a} (±0.87)
RTO (% w/w)	52.79^{b} (±0.72)	51.47^{b} (±0.42)	56.38^{a} (±1.53)

Average values with equal letters in the same line do not present significant difference ($p > 0.05$) according to Tukey's test.
n.s.: Non-significant ($p > 0.05$).

3.2. Moisture content

It is noted that the variation in maltodextrin content did not significantly influence the microcapsules moisture content (d.b.) ($p > 0.05$) (Table 1). In addition, the relatively low values found are characteristic of powder products from spray drying due to atomization of fluids into small

droplets in the drying chamber at high temperatures (Gharsallaoui et al., 2007).

Low values for moisture content, below 2%, were also found by Botrel et al. (2014) studying fish oil microcapsules produced by spray drying using soy protein isolate or inulin as wall material, and by Carneiro et al. (2013) studying flaxseed oil microcapsules produced by spray drying containing maltodextrin in combination with various polymers in the wall material.

3.3. Encapsulation yield

The encapsulation yield obtained for the different samples of buriti oil microcapsules was higher than 50% and significantly different ($p \leq 0.05$) from each other (Table 1). The sample 1:1.25, produced with the highest maltodextrin content, presented the highest encapsulation yield, confirming the funcionality of the used drying aid.

3.4. Particle size distribution

Particle sizes were measured by static light scattering and the result, based on the particle volume, was obtained as mean particle diameter, $D_{[4,3]}$. In addition, it is important to observe the particle size distribution and the *span*, which is related to data dispersion, that is, the width of the size distribution (Table 1). Figure 1 shows the typical particle size distribution curves for buriti oil microcapsules samples.

Figure 1. Particle size distribution of microcapsules prepared in ratio (solids in the emulsion):(maltodextrin): (a) 1:0.75, (b) 1:1, and (c) 1:1.25.

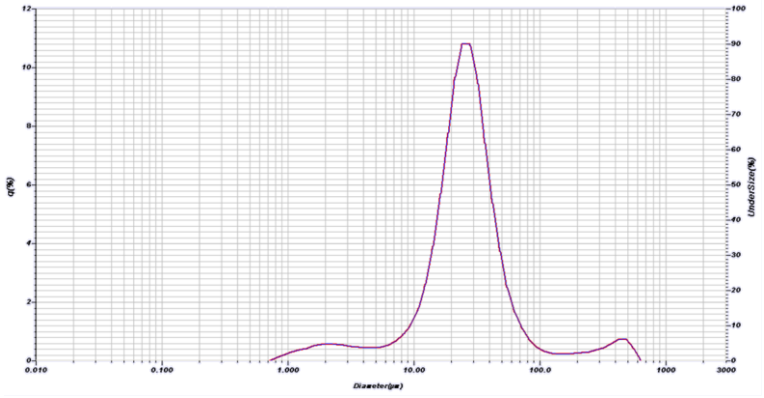

(a)

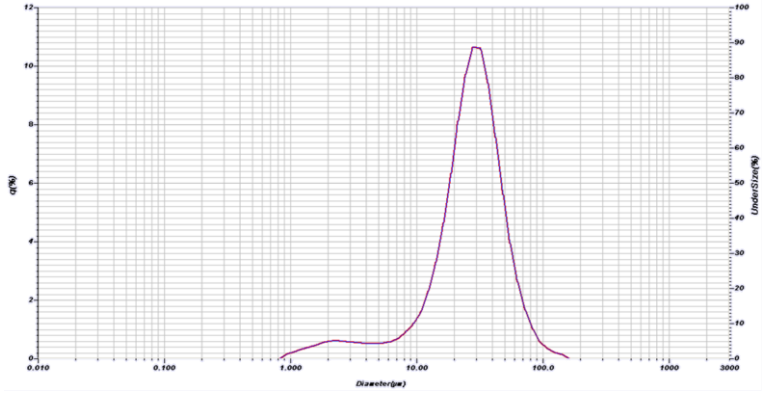

(b)

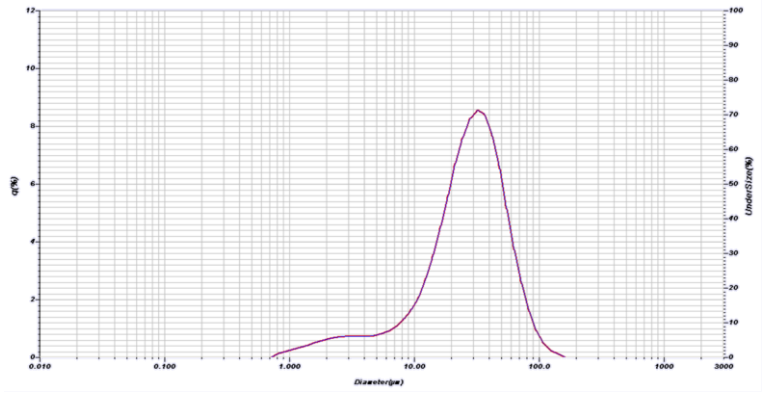

(c)

The samples did not present significant difference ($p > 0.05$) among them for mean diameter and *span*, suggesting that the difference in maltodextrin content did not interfere in these parameters. In fact,

considering these extensive range of size distribution as presented, the mean diameters were very close.

In the particle size distribution curve of sample 1:0.75, it is interesting to note the presence of a small amount of particle with larger sizes, a behavior that was not observed in samples 1:1 and 1:1.25. This fact suggests particle agglomeration and flake formation.

In a study conducted by Aberkane, Roudaut and Saurel (2014) on encapsulation of oil rich in polyunsaturated fatty acids by spray drying, using pea protein and pectin as wall material and with addition of maltodextrin, a wide range of microcapsule size distribution (from 0.3 to 400 µm) was reported besides the presence of particle agglomerates.

Carneiro et al. (2013) studied linseed oil microcapsules produced by spray drying containing maltodextrin in combination with various polymers in wall material and found particle sizes significantly different ($p \leq 0.05$) among the samples, from 15.32 µm to 23.03 µm. According to these authors, this difference can be explained by different viscosities of the emulsions to be dried, since a high viscosity emulsion produces larger droplets during atomization and, consequently, larger size particles. The authors also reported large particle size distribution with bimodal distribution, which was attributed to a particularity observed in powders.

When producing fish oil microcapsules by spray drying with soy protein isolate or inulin as wall material, Botrel et al. (2014) concluded that particles size was influenced by drying temperature, wall material composition and oil content in the emulsion.

3.5. Encapsulation efficiency (EEC) and retention (RTC) of carotenoids

The encapsulation efficiency of carotenoids (*EEC*) is related to carotenoid content inside and outside the microcapsules, while retention of carotenoids (*RTC*) refers to total carotenoids content in the microcapsules in relation to carotenoid content in the emulsion. In this way, the microcapsules of buriti oil presented encapsulation efficiency of carotenoids

over 54% and retention of carotenoids over 48%, expressed as β-carotene content (Table 1).

The samples were significantly different ($p \leq 0.05$) and the sample 1:1.25, containing the highest maltodextrin content, presented the highest values for *EEC* and *RTC*, confirming that the use of higher drying aid concentrations may contribute to production of a more effective encapsulation matrix for bioactive compounds protection.

3.6. Encapsulation efficiency (EEO) and retention (RTO) of oil

As observed for encapsulation efficiency and retention of carotenoids, the sample 1:1.25, containing the highest maltodextrin content, had the highest values for encapsulation efficiency (*EEO*) and retention (*RTO*) of buriti oil, differing significantly ($p \leq 0.05$) from the other samples. It is interesting to observe that the values obtained for *EEC* and *EEO* were close, although the encapsulation efficiency of carotenoids was slightly lower. This fact could also be observed comparing *RTC* and *RTO*. One possible reason might be the use of different methodologies, since the carotenoids were expressed in β-carotene content, neglecting the other carotenoids present in buriti oil. On the other hand, small losses of carotenoids may have occurred during the drying process due the exposition at drying air, although, according to Dubernet and Benoit (1986) and Gharsallaoui et al. (2007) the low exposure time and rapid water evaporation keep microcapsules core below 40 °C despite the high temperatures normally used in this process.

3.7. Water sorption

Understanding water sorption behaviour of food systems is of great importance, especially for food systems with high hygroscopicity, such as microcapsules produced by spray dryer. Water sorption isotherms are considered as important processing and storage tools and one of the best

ways of representing food sorption characteristics, from which food stability can be predicted (Brett et al., 2009).

The curves that relate water activity with water content, or sorption isotherms, for the buriti oil microcapsules stored at room temperature are presented in Figure 2. In addition, the curves predicted by the fitted model to experimental data also can be seen.

Figure 2. Water sorption isotherms of buriti oil microcapsules and water content calculated using the second order polynomial model.

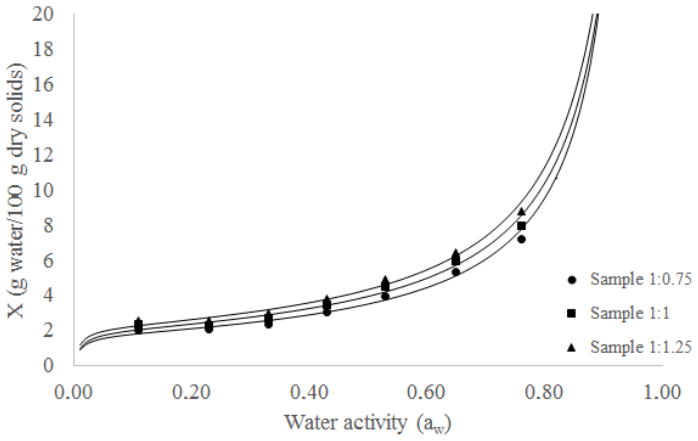

The water sorption in foods is a very complex phenomenon, consisting of several different mechanisms that depend on the material structure and composition (Staudt et al., 2013). The samples with different maltodextrin contents behaved in a similar way, but the sample with higher maltodextrin content had slightly higher water contents when stored in higher water activities. The second order polynomial parameters are presented in Table 2 and the model good fit can be confirmed by the values of determination coefficients (R^2) higher than 0.93.

Table 2. The second order polynomial parameters of buriti oil microcapsules water sorption.

	Ratio (solids in the emulsion):(maltodextrin)		
	1:0.75	**1:1**	**1:1.25**
a	-0.60	-0.51	-0.47
b	0.58	0.50	0.46
c	0.0062	0.0057	0.0042
R^2	0.9352	0.9405	0.9405

3.8. Water plasticization

The water plasticization phenomenon relates water content and glass trasition temperature of an amorphous phase. The glass transition temperature of food materials is generally reduced due to an increase in the product water content and water activity (Nurhadi, Roos and Maidannyk, 2016).

The glass transition is reversible, and it occurs over a temperature range. Well below the glass transition, molecules are frozen in their positions, and their molecular motions are limited to rotations and vibrations, which results in the solid-like characteristics of the material. When a glass is heated to above the glass transition, molecules gain translational mobility and enter the supercooled, liquid-like state with a concomitant appearance of viscous flow. In cooling to below the glass transition, the amorphous material vitrifies to a solid-like, brittle, and transparent structure typical of the glassy state (Sperling, 2006; Roos, 2010). These properties and significant differences of the solid- and liquid-like states of amorphous materials make the glass transition perhaps the most important state transition responsible for processing, stability, and quality characteristics of food materials bein recognized in dehydrated foods (Roos, 2010).

Considering the water effect on the food hygroscopic region, it is expected a decrease in the glass transition temperature with increasing water content (Slade and Levine, 1991; Telis and Martínez-Navarrete, 2009). This behavior was confirmed by Telis and Martínez-Navarrete (2009) when studying grapefruit juice powder with different drying aids, including

maltodextrin. In addition, Nurhadi, Roos and Maidannyk (2016), studying the physical properties of maltodextrin DE 10, reported glass transition temperatures between 95 °C for a_w = 0.11 and 17 °C for a_w = 0.75.

For the buriti oil microcapsules (Table 3), this behavior was observed for a_w between 0.33 and 0.75, with glass transition temperatures between 49 and 5 °C, respectively. For a_w of 0.11 and 0.23 it was not possible to observe the glass transition temperatures, possibly because of the difficulty in detecting T_g for samples with low water content. It was also possible to observe that the microcapsules containing different maltodextrin contents presented similar values for T_g, at the same a_w.

3.9. Mechanical relaxation

Structural relaxations correspond to impeded kinetic molecular rearrangements and relate to time-dependent changes of thermodynamic, mechanical or dielectric properties, after a perturbation such as temperature or pressure change (Fan and Roos, 2016). Relaxation time is the time required for disturbance recovery (Le Meste et al., 2002). Structural relaxations and relaxation time may be related to particle structure, viscosity and mechanical properties, which control the quality and stability of food materials, particularly at temperatures close to and above the glass transition (Fan and Roos, 2016).

The frequency-dependent relaxation of amorphous polymers is governed by moisture, water activity and temperature (Roos and Karel, 1991) due the fact of these parameters affect the glass transition.

The results presented in Table 3 confirm the dependence of the relaxation temperature of buriti oil microcapsules with frequency and water activity. The samples prepared with different maltodextrin contents showed similar relaxation temperatures for the same frequency and a_w. However, a slight increase in the relaxation temperature was noted with increasing frequency for the same a_w, and a decrease in the relaxation temperature with increasing a_w. It was not possible to detect the relaxation temperatures

for microcapsules in a_w = 0.75, possibly because these values would be lower the values possible to detect by the methodology used.

Table 3. Glass transition and relaxation temperatures at different frequencies of buriti oil microcapsules at various water activity.

Water activity	Frequency (Hz)	Temperature (°C)	Ratio (solids in the emulsion):(maltodextrin) 1:0.75	1:1	1:1.25
0.11	-	T_g	n.d.	n.d.	n.d.
	0.5	Relaxation temperature	97 (±4)	96 (±3)	106 (±3)
	1		98 (±4)	100 (±2)	109 (±2)
	2		100 (±4)	101 (±4)	110 (±3)
	5		104 (±4)	103 (±4)	113 (±2)
0.23	-	T_g	n.d.	n.d.	n.d.
	0.5	Relaxation temperature	97 (±1)	99 (±3)	99 (±2)
	1		100 (±1)	101 (±2)	101 (±3)
	2		103 (±1)	103 (±3)	103 (±1)
	5		105 (±1)	107 (±2)	105 (±1)
0.33	-	T_g	41 (±13)	49 (±9)	44 (±11)
	0.5	Relaxation temperature	94 (±3)	94 (±4)	92 (±3)
	1		96 (±2)	97 (±3)	93 (±2)
	2		97 (±1)	97 (±2)	96 (±4)
	5		101 (±2)	100 (±2)	98 (±3)
0.43	-	T_g	36 (±3)	40 (±7)	40 (±11)
	0.5	Relaxation temperature	84 (±3)	82 (±3)	86 (±3)
	1		85 (±1)	84 (±3)	86 (±2)
	2		88 (±1)	86 (±3)	88 (±3)
	5		90 (±1)	88 (±3)	91 (±2)
0.53	-	T_g	31 (±7)	38 (±3)	43 (±2)
	0.5	Relaxation temperature	64 (±1)	63 (±2)	63 (±1)
	1		66 (±1)	65 (±3)	65 (±1)
	2		69 (±2)	67 (±2)	66 (±1)
	5		70 (±2)	70 (±2)	69 (±1)
0.65	-	T_g	29 (±6)	31 (±3)	23 (±5)
	0.5	Relaxation temperature	50 (±1)	55 (±2)	54 (±2)
	1		52 (±1)	57 (±3)	55 (±2)
	2		54 (±1)	59 (±3)	57 (±2)
	5		57 (±1)	62 (±2)	61 (±1)
0.75	-	T_g	5 (±1)	7 (±3)	7 (±2)
	0.5	Relaxation temperature	n.d.	n.d.	n.d.
	1		n.d.	n.d.	n.d.
	2		n.d.	n.d.	n.d.
	5		n.d.	n.d.	n.d.

It was possible to observe that the mechanical relaxation occurred approximately 30 °C above the T_g for higher a_w and this difference increased with decreasing a_w. According to Telis and Martínez-Navarrete (2009), a single value of $\Delta T = T - T_g \approx$ -20 °C could be taken as the critical limit to the safe storage of the powders, regardless of their composition.

The WLF model was fitted to correlate the structural relaxation time, τ, and the relaxation temperature, T. Roos (2012) recommended that WLF equation was valid over the temperature range within the rubbery or supercooled liquid state and was also used to describe time and temperature dependent behavior of amorphous materials. The WLF model parameters of microcapsules at various water activity can been seen in Table 4, and experimental and teoretical values are presented in Figure 3.

It was possible to observe the model good fit, the similarity among samples and to confirm that the structural relaxations occur in lower $\Delta T = T - T_g$ for higher a_w.

Table 4. The Williams-Landel-Ferry model parameters of buriti oil microcapsules at various water activity.

		Ratio (solids in the emulsion):(maltodextrin)		
		1:0.75	**1:1**	**1:1.25**
a_w 0.11	**C_1**	1.28	1.40	1.16
	C_2	-98.82	-103.43	-93.93
	R^2	0.9161	0.9684	0.9997
a_w 0.23	**C_1**	3.05	2.40	1.84
	C_2	-103.67	-99.77	-84.93
	R^2	0.9953	0.9794	0.9991
a_w 0.33	**C_1**	1.73	1.62	2.01
	C_2	-88.76	-74.02	-84.98
	R^2	0.9789	0.9497	0.9656
a_w 0.43	**C_1**	1.95	2.04	1.54
	C_2	-83.90	-75.06	-72.66
	R^2	0.9723	0.9917	0.9159
a_w 0.53	**C_1**	3.44	5.50	15.24
	C_2	-79.14	-82.50	-137.59
	R^2	0.9897	0.9909	0.9979
a_w 0.65	**C_1**	13,83	9.30	4.96
	C_2	-137.92	-112.79	-89.90
	R^2	0.9910	0.9772	0.9651

Figure 3. Mechanical relaxation according to WLF model of microcapsules prepared in ratio (solids in the emulsion):(maltodextrin): (a) 1:0.75, (b) 1:1, and (c) 1:1.25.

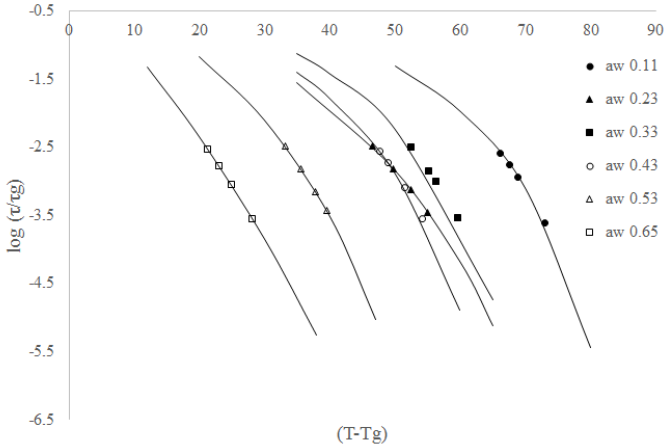

(a)

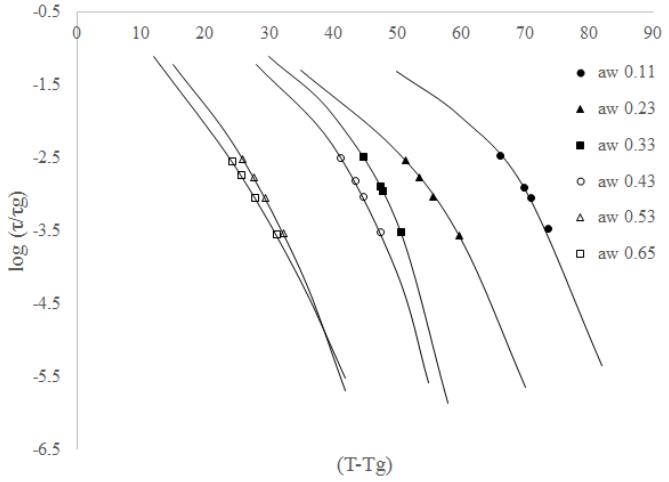

(b)

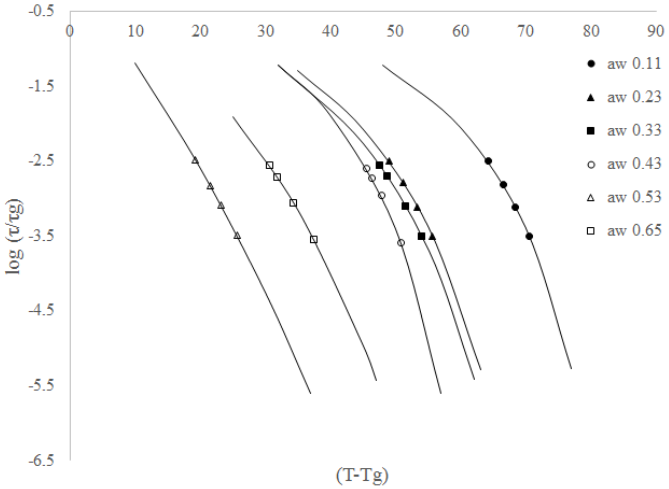

(c)

3.10. Particle morphology

Optical microscopy

Optical microscopy was used to observe the buriti oil microcapsules morphology and, thus, complement the information obtained by the physico-chemical analyzes. Figure 4 presents the images collected by an optical microscope with 40×-magnification. It was possible to observe that the samples were morphologically similar, with the encapsulated oil not in a single nucleus, but in many nucleus, characterizing poly-nucleated microcapsules (Silva et al., 2003).

Figure 4. Micrographics of buriti oil microcapsules prepared in ratio (solids in the emulsion):(maltodextrin): (a) 1:0.75, (b) 1:1, and (c) 1:1.25 obtained by optical microscopy with 40×-magnification (bar is equivalent to 20 µm).

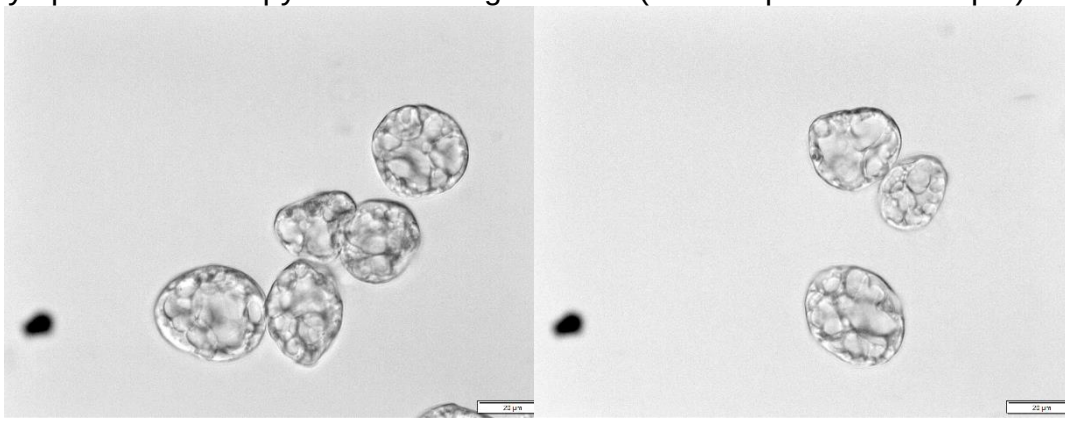

(a1) (a2)

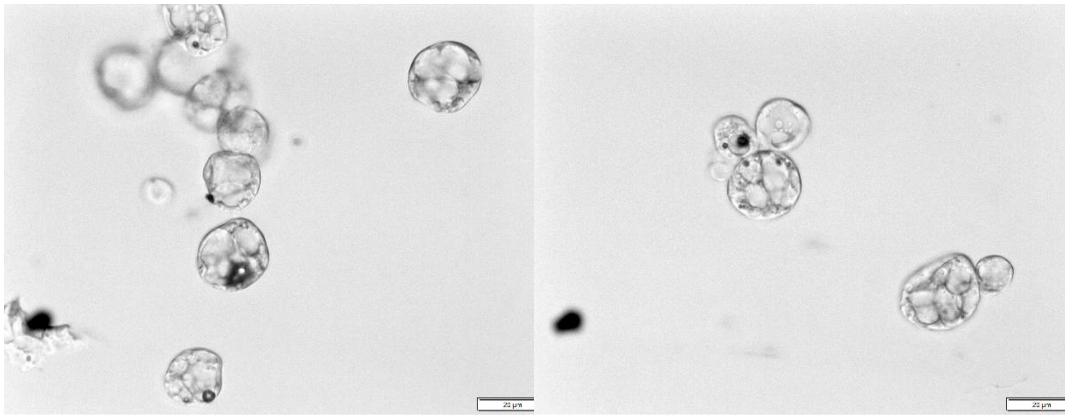

(b1) (b2)

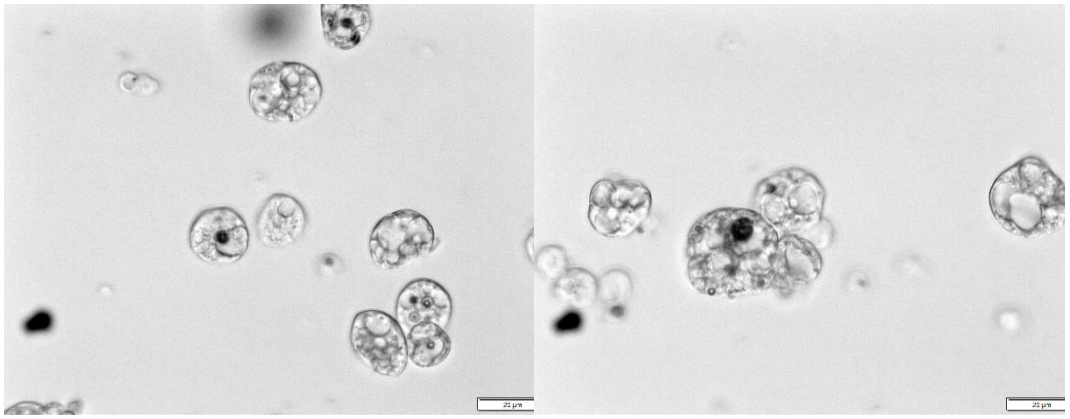

(c1) (c2)

Scanning electron microscopy

The microcapsules microstructure was also analyzed by scanning electron microscopy and the images collected with 500× and 1000×-magnification are presented in Figure 5. It was possible to observe microcapsules in different sizes and to note the presence of flakes formed by caking, as suggested in the analysis of particle size distribution curves (Figure 1).

The microcapsules were spherical and presented smooth surface with few wrinkles and no apparent cracks, characteristic morphology of microcapsules produced by spray drying of oil-in-water emulsions. According to Dziezak (1988) and Gharsallaoui et al. (2007) when the atomized emulsion enters into the hot air chamber, the water is rapidly evaporated, and the microcapsule assumes the spherical shape of the dispersed oil droplets in the emulsion.

Microcapsules of polyunsaturated fatty acids rich oil produced by spray drying using pea protein and pectin with addition of maltodextrin as wall material, studied by Aberkane, Roudaut and Saurel (2014), and linseed oil microcapsules produced by spray drying containing maltodextrin in combination with other polymers as wall material, analyzed by Carneiro et al. (2013), also presented spherical shape, different sizes and no apparent cracks. These characteristics were considered an advantage, since they imply that the capsules would have less gas permeability, increasing protection and retention of the active material.

Figure 5. Micrographics of buriti oil microcapsules prepared in ratio (solids in the emulsion):(maltodextrin): (a) 1:0.75, (b) 1:1, and (c) 1:1.25 obtained by scanning electron microscopy with 500×-magnification (a1, b1, and c1) and 1000×-magnification (a2, b2, and c2).

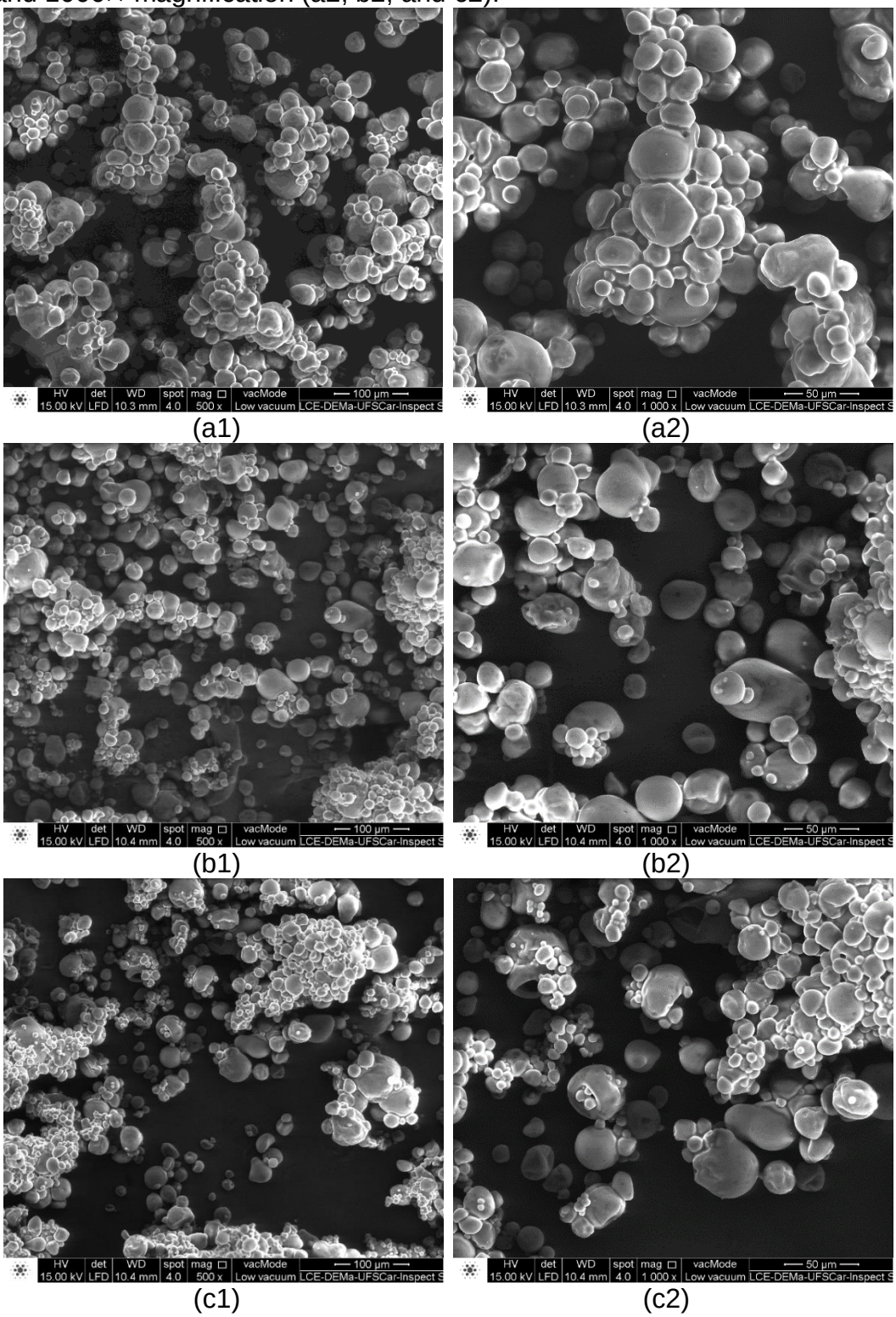

4. CONCLUSIONS

Carotenoid-rich microcapsules with satisfactory results for encapsulation yield and retention of bioactive compounds were produced by spray drying of oil-in-water emulsion with addition of maltodextrin as drying aid.

The microcapsules produced with addition of different maltodextrin contents presented significant differences ($p \leq 0.05$) with respect to color parameters, encapsulation yield, encapsulation efficiency and retention of carotenoid, and encapsulation efficiency and retention of buriti oil. The sample with the highest maltodextrin content presented less intense coloration, but in contrast, presented the highest encapsulation yield, encapsulation efficiency and retention of bioactive compounds.

The glass transition and relaxation temperatures of the microcapsules were dependent on water activity. The relaxation temperature increased with frequency and decreased with a_w. In addition, the mechanical relaxation occurred at least 30 °C above the glass transition temperature.

The observed results showed that the produced buriti oil microcapsules are suitable for application in carotenoid enrichment of foods, as well as a natural dye.

5. ACKNOWLEDGMENTS

The authors acknowledge the financial support from the Sao Paulo Research Foundation, FAPESP, Brazil [grant numbers 2014/08520-6, 2014/02910-7] and Coordination for the Improvement of Higher Level Personnel, CAPES, Brazil [grant number 88881.132893/2016-01].

6. REFERENCES

Aberkane, L.; Roudaut, G.; Saurel, R. Encapsulation and oxidative stability of PUFA-rich oil microencapsulated by spray drying using pea protein and pectin. Food and Bioprocess Technology, v. 7, p. 1505-1517, 2014.

Aranha, C. P. M. Microencapsulação por gelificação iônica e interação eletrostática do corante de buriti (*Mauritia flexuosa* L. f.), 116p. Tese (Doutorado em Engenharia e Ciência de Alimentos) – Universidade Estadual Paulista "Julio de Mesquita Filho", São José do Rio Preto, 2015.

Botrel, D. A.; Borges, S. V.; Fernandes, R. V. B.; Carmo, E. L. Optimization of fish oil spray drying using a protein:inulin system. Drying Technology, v. 32, p. 279-290, 2014.

Bouyer, E.; Mekhloufi, G.; Rosilio, V.; Grossiord, J. L.; Agnely, F. Proteins, polysaccharides, and their complexes used as stabilizers for emulsions: alternatives to synthetic surfactants in the pharmaceutical field? International Journal of Pharmaceutics, v. 436, p. 359–378, 2012.

Brett, B.; Figueroa, M.; Sandoval, A. J.; Barreiro, J. A.; Müller, A. J. Moisture sorption characteristics of starchy products: oat flour and rice flour. Food Biophysics, v. 4, p. 151–157, 2009.

Carneiro, H. C. F.; Tonon, R. V.; Grosso, C. R. F.; Hubinger, M. D. Encapsulation efficiency and oxidative stability of flaxseed oil microencapsulated by spray drying using different combinations of wall materials. Journal of Food Engineering, v. 115, p. 443-451, 2013.

De Greyt, W. D.; Kellens, M. Deodorization. In: Shahidi, F. Bailey's Industrial Oil & Fat Products 6ªed, v.5, New York, John Wiley & Son, p.341-383, 2005.

De Rosso, V. V.; Mercadante, A. Z. Identification and quantification of carotenoids, by HPLC-PDA-MS/MS, from amazonian fruits. Journal of Agricultural and Food Chemistry, v. 55, p. 5062-5072, 2007.

Dubernet, C.; Benoit, J. P. La microencapsulation: Ses techniques et ses applications en biologie. L'actualité chimique, v. 10, p. 19–28, 1986.

Dziezak, J. D. Microencapsulation and encapsulated ingredients. Food Technology, v. 42, p. 136–151, 1988.

Fan, F.; Roos, Y. H. Structural relaxations of amorphous lactose and lactose-whey protein mixtures. Journal of Food Engineering, v. 173, p. 106-115, 2016.

França, L. F.; Reber, G.; Meireles, M. A. A.; Machado, N. T.; Brunner, G. Supercritical extraction of carotenoids and lipids from buriti (*Mauritia flexuosa*), a fruit from the Amazon region. The Journal of Supercritical Fluids, v. 14, p. 247-256, 1999.

Freitas, M. L. F.; Albano, K. M.; Telis, V. R. N. Characterization of biopolymers and soy protein isolate-high-methoxyl pectin complex. Polímeros: Ciência e Tecnologia, v. 27, p. 62-67, 2017.

Freitas, M. L. F.; Chisté, R. C.; Polachini, T. C.; Sardella, L. A. C. Z.; Aranha, C. P. M.; Ribeiro, A. P. B.; Nicoletti, V. R. Quality characteristics and thermal behavior of buriti (*Mauritia flexuosa* L.) oil. Grasas y Aceites, v. 68, n. 4, p. 220-228, 2017.

Gharsallaoui, A.; Roudaut, G.; Chambin, O.; Voilley, A.; Saurel, R. Applications of spray-drying in microencapsulation of food ingredients: an overview. Food Research International, v. 40, n. 9, p. 1107–1121, 2007.

Gouin, S. Micro-encapsulation: Industrial appraisal of existing technologies and trends. Trends in Food Science and Technology, v. 15, p. 330–347, 2004.

Guinazi, M.; Milagres, R. C. R. M.; Pinheiro-Sant'Ana, H. M.; Chaves, J. B. P. Tocoferois e tocotrienois em óleos vegetais e ovos. Química Nova, v. 32, n. 8, p. 2098-2103, 2009.

Jafari, S. M.; He, Y.; Bhandari, B. Production of sub-micron emulsions by ultrasound and microfluidization techniques. Journal of Food Engineering, v. 82, p. 478-488, 2007.

Jaramillo, D. P.; Roberts, R. F.; Coupland, J. N. Effect of pH on the properties of soy protein-pectin complexes. Food Research International, v. 44, p. 911-916, 2011.

Kenyon, M. M. Modified starch, maltodextrin, and corn syrup solids as wall materials for food encapsulation. In S. J. Risch; G. A. Reineccius (Eds.), Encapsulation and Controlled Release of Food Ingredients. Washington, DC, American Chemical Society. ACS symposium series, v. 590, p. 42–50, 1995.

Lam, M.; Shen, R.; Paulsen, P.; Corredig, M. Pectin stabilization of soy protein isolates at low pH. Food Research International, v. 40, p. 101-110, 2007.

Le Meste, M.; Champion, D.; Roudaut, G.; Blond, G.; Simatos, D. Glass transition and food technology: A critical appraisal. Journal of Food Science, v. 67, p. 2444–2458, 2002.

McClements, D. J.; Decker, E. A.; Weiss, J. Emulsion-based delivery systems for lipophilic bioactive components. Journal of Food Science, v. 75, n. 8, p. 109-124, 2007.

Nurhadi, B.; Roos, Y. H.; Maidannyk, V. Physical properties of maltodextrin DE 10: Water sorption, water plasticization and enthalpy relaxation. Journal of Food Engineering, v. 174, p. 68-74, 2016.

Rahman, M. S. Glass transition data and models of foods. In: RAHMAN, M.S. (Ed.), Food Properties Handbook, second ed. Boca Raton: CRC Press, 2009.

Rodriguez-Amaya, D. B. Assessment of the provitamina A contents of foods - The brazilian experience. Journal of Food Composition and Analysis, v. 9, p. 196-230, 1996.

Roos, Y. H.; Karel, M. Plasticizing effect of water on thermal behavior and crystallization of amorphous food models. Journal of Food Science, n. 56, p. 38-56, 1991.

Roos, Y. H. Phase Transition in Foods. California: Academic Press, 1995.

Roos, Y. H. Glass transition temperature and its relevance in food processing. Annual Review of Food Science and Technology, v. 1, p. 469-496, 2010.

Roos, Y. H. In: Bhandari, B.; Roos, Y. H. (Eds.). Food Materials Science and Engineering: Phase and State Transitions and Related Phenomena in Foods, first ed. Blackwell Publishing Ltd, 2012.

Rosenberg, M.; Kopelman, I. J.; Talmon, Y. Factors affecting retention in spray-drying microencapsulation of volatile materials. Journal of Agricultural and Food Chemistry, v. 38, p. 1288–1294, 1990.

Santos, M. F. G.; Marmesat, S.; Brito, E. S.; Alves, R. E.; Dobarganes, M. C. Major components in oils obtained from Amazonian palm fruits. Grasas y Aceites, v. 64, n. 3, p. 328-334, 2013.

Serfert, Y.; Schroder, J.; Mescher, A.; Laackmann, J.; Ratzke, K.; Shaikh, M. Q.; Gaukel, V.; Moritz, H. U.; Schuchmann, H. P.; Walzel, P.; Drusch, S.; Schwarz, K. Spray drying behavior and functionality of emulsions with β-lactoglobulin/pectin interfacial complexes. Food Hydrocolloids, v. 31, p. 438-445, 2013.

Silva, C.; Ribeiro, A.; Ferreira, D.; Veiga, F. Administração oral de peptídeos e proteínas: II. Aplicação de métodos de microencapsulação. Revista Brasileira de Ciências Farmacêuticas, v. 39, n. 1, p. 1-19, 2003.

Silva, S. M.; Sampaio, K. A.; Taham, T.; Rocco, S. A.; Ceriani, R.; Meirelles, A. J. A. Characterization of oil extracted from buriti fruit (*Mauritia flexuosa*) grown in the Brazilian amazon region. Journal of the American Oil Chemists Society, v. 86, p. 611-616, 2009.

Slade, L.; Levine, H. Beyond water activity: recent advances based on an alternative approach to the assessment of food quality and safety. Critical Reviews in Food Science and Nutrition, v. 30, n. 2-3, p. 115-360, 1991.

Sperling, L. H. Introduction to Physical Polymer Science. 3rd ed., New York: Wiley, 845 pp., 2006.

Staudt, P. B.; Tessaro, L. C.; Marczak, L. D. F.; Soares, R. P.; Cardozo, N. S. M. A new method for predicting sorption isotherms at different temperatures: extension to the GAB model. Journal of Food Engineering, v. 118, p. 247–255, 2013.

Telis, V. R. N.; Martínez-Navarrete, N. Collapse and color changes in grapefuit juice poder as affected by water activity, glass transition, and addition of carbohydrate polymers. Food Biophysics, v. 4, p. 83-93, 2009.

Tonon, R. V.; Grosso, C. R. F.; Hubinger, M.D. Influence of emulsion composition and inlet air temperature on the microencapsulation of flaxseed oil by spray drying. Food Research International, v. 44, p. 282-289, 2011.

CONCLUSÃO GERAL

O ponto isoelétrico do isolado proteico de soja foi observado no pH 4,6 e em soluções de pH mais baixos que esse valor foi verificada a interação atrativa do isolado proteico de soja e da pectina de alta metoxilação por meio da observação de complexos formados. O pH de 3,5 foi estabelecido para produção das emulsões em função da interação observada entre os biopolímeros.

A caracterização do óleo de buriti atestou sua alta qualidade, revelando altos teores de carotenoides, tocoferois e ácidos graxos monoinsaturados.

Por meio do planejamento experimental DCCR, foi possível obter uma emulsão em condições otimizadas, estável por pelo menos 7 dias, com tamanho de gotas reduzido, condutividade elétrica baixa e alto módulo de cargas negativas. Essa emulsão apresentou comportamento reológico do tipo pseudoplástico, porém, em condições de baixa deformação, o seu espectro mecânico apresentou comportamento viscoelástico característico de um gel fraco.

Além disso, foi possível observar a interação do isolado proteico de soja com o óleo de buriti formando as gotículas dispersas de óleo e a interação da pectina de alta metoxilação com o isolado proteico de soja, formando a dupla camada na interface entre a fase dispersa e a fase contínua. Observou-se um excesso de pectina disperso na fase contínua, contribuindo para a estabilidade do sistema.

Microcápsulas de óleo de buriti com resultados satisfatórios para rendimento e retenção de compostos bioativos foram produzidas por meio da secagem em spray dryer da emulsão otimizada com adição do adjuvante de secagem, maltodextrina. As amostras de microcápsulas produzidas a partir da adição de diferentes teores de maltodextrina apresentaram diferenças significativas ($p \leq 0,05$) entre si com relação a cor, rendimento de encapsulação, eficiência da encapsulação e da retenção de

carotenoides e eficiência da encapsulação e da retenção de óleo. A amostra contendo maior teor de maltodextrina apresentou coloração menos intensa, porém, em contrapartida, apresentou maior rendimento, eficiência de encapsulação e retenção dos compostos bioativos.

As temperaturas de transição vítrea e de relaxação das microcápsulas foram dependentes da atividade de água. A temperatura de relaxação aumentou com a frequência e diminuiu com a atividade de água. Além disso, a relaxação mecânica ocorreu pelo menos 30 °C acima da temperatura de transição vítrea.

Diante do exposto, acredita-se ter atingido o objetivo de produzir e caracterizar emulsões e microcápsulas de óleo de buriti ricas em carotenoides para aplicação em enriquecimento de alimentos.

SUGESTÕES PARA TRABALHOS FUTUROS

Para dar continuidade ao tema estudado e complementar o trabalho realizado no desenvolvimento desse projeto são sugeridas as seguintes abordagens:

- Estudo da estabilidade dos carotenoides presentes nas microcápsulas de óleo de buriti ao longo do tempo e em diferentes temperaturas de armazenamento e posterior correlação com as temperaturas de transição vítrea e de relaxamento.

- Estudo da influência da pectina no processo de secagem de emulsões de óleo de buriti e obtenção de microcápsulas de óleo de buriti.

- Aplicação das emulsões e microcápsulas de óleo de buriti no desenvolvimento de molho para saladas, creme vegetal e bolo de chocolate enriquecidos em carotenoides.

unesp

UNIVERSIDADE ESTADUAL PAULISTA
"JÚLIO DE MESQUITA FILHO"
Campus de São José do Rio Preto

TERMO DE REPRODUÇÃO XEROGRÁFICA

Autorizo a reprodução xerográfica do presente Trabalho de Conclusão, na íntegra ou em partes, para fins de pesquisa.

São José do Rio Preto, 23 / 04 / 2018

Miriam Luisa Faria Freitas

Assinatura do autor